

*Final Report*

USE OF AGGREGATE IMAGE MEASUREMENT SYSTEM (AIMS) TO  
EVALUATE AGGREGATE POLISHING IN FRICTION SURFACES

UF Project No.: 00092545

Contract No.: BDK75 977-44

*Submitted to:*

Florida Department of Transportation  
605 Suwannee Street  
Tallahassee, FL, 32399



Dr. Reynaldo Roque, P.E.  
Abolfazl Ravanshad  
George Lopp

Department of Civil and Coastal Engineering  
College of Engineering  
365 Weil Hall, P.O. Box 116580  
Gainesville, FL, 32611-6580  
Tel: (352) 392-9537 extension 1458  
Fax: (352) 392-3394

**August 2013**

## DISCLAIMER

The opinions, findings and conclusions expressed in this publication are those of the authors and not necessarily those of the Florida Department of Transportation. This report does not constitute a standard, specification, or regulation. This report was prepared in cooperation with the State of Florida Department of Transportation.

# SI\* (MODERN METRIC) CONVERSION FACTORS

## APPROXIMATE CONVERSIONS TO SI UNITS

## APPROXIMATE CONVERSIONS FROM SI UNITS

Symbol	When You Know	Multiply By	To Find	Symbol	When You Know	Multiply By	To Find	Symbol
<b>LENGTH</b>								
in	inches	25.4	millimeters	mm	millimeters	0.039	inches	in
ft	feet	0.305	meters	m	meters	3.28	feet	ft
yd	yards	0.914	meters	m	meters	1.09	yards	yd
mi	miles	1.61	kilometers	km	kilometers	0.621	miles	mi
<b>AREA</b>								
in <sup>2</sup>	square inches	645.2	square millimeters	mm <sup>2</sup>	square millimeters	0.0016	square inches	in <sup>2</sup>
ft <sup>2</sup>	square feet	0.093	square meters	m <sup>2</sup>	square meters	10.764	square feet	ft <sup>2</sup>
yd <sup>2</sup>	square yards	0.836	square meters	m <sup>2</sup>	square meters	1.195	square yards	yd <sup>2</sup>
ac	acres	0.405	hectares	ha	hectares	2.47	acres	ac
mi <sup>2</sup>	square miles	2.59	square kilometers	km <sup>2</sup>	square kilometers	0.386	square miles	mi <sup>2</sup>
<b>VOLUME</b>								
fl oz	fluid ounces	29.57	milliliters	ml	milliliters	0.034	fluid ounces	fl oz
gal	gallons	3.785	liters	l	liters	0.264	gallons	gal
ft <sup>3</sup>	cubic feet	0.028	cubic meters	m <sup>3</sup>	cubic meters	35.71	cubic feet	ft <sup>3</sup>
yd <sup>3</sup>	cubic yards	0.765	cubic meters	m <sup>3</sup>	cubic meters	1.307	cubic yards	yd <sup>3</sup>
NOTE: Volumes greater than 1000 l shall be shown in m <sup>3</sup> .								
<b>MASS</b>								
oz	ounces	28.35	grams	g	grams	0.035	ounces	oz
lb	pounds	0.454	kilograms	kg	kilograms	2.202	pounds	lb
T	short tons (2000 lb)	0.907	megagrams	Mg	megagrams	1.103	short tons (2000 lb)	T
<b>TEMPERATURE (exact)</b>								
°F	Fahrenheit temperature	5(F-32)/9 or (F-32)/1.8	Celcius temperature	°C	Celcius temperature	1.8C + 32	Fahrenheit temperature	°F
<b>ILLUMINATION</b>								
fc	foot-candles	10.76	lux	lx	lux	0.0929	foot-candles	fc
fl	foot-Lamberts	3.426	candela/m <sup>2</sup>	cd/m <sup>2</sup>	candela/m <sup>2</sup>	0.2919	foot-Lamberts	fl
<b>FORCE and PRESSURE or STRESS</b>								
lbf	poundforce	4.45	newtons	N	newtons	0.225	poundforce	lbf
psi	poundforce per square inch	6.89	kilopascals	kPa	kilopascals	0.145	poundforce per square inch	psi

\* SI is the symbol for the International System of Units. Appropriate rounding should be made to comply with Section 4 of ASTM E380.

(Revised August 1992)

1. Report No.		2. Government Accession No.		3. Recipient's Catalog No.	
4. Title and Subtitle  Use of Aggregate Image Measurement System (AIMS) to Evaluate Aggregate Polishing in Friction Surfaces				5. Report Date  June 2013	
				6. Performing Organization Code  00092545	
7. Author(s)  Reynaldo Roque, Abolfazl Ravanshad, and George Lopp				8. Performing Organization Report No.	
9. Performing Organization Name and Address University of Florida Department of Civil and Coastal Engineering 365 Weil Hall P.O. Box 116580 Gainesville, FL 32611-6580				10. Work Unit No. (TRAIS)	
				11. Contract or Grant No.  BDK75 977-44	
12. Sponsoring Agency Name and Address Florida Department of Transportation Research Management Center 605 Suwannee Street, MS 30 Tallahassee, FL 32399				13. Type of Report and Period Covered  Final 04/18/11-08/31/13	
				14. Sponsoring Agency Code	
15. Supplementary Notes					
16. Abstract  This study was conducted to identify and evaluate Aggregate Image Measurement System (AIMS) capability in the pre-evaluation of aggregates for use in friction course. For purposes of this study, frictional characteristics of different aggregate types were measured and analyzed using a combination of AIMS and Micro-Deval. The unique aspect of this project was using AIMS to measure the microtexture of aggregates after several years in road service. The researchers obtained field cores from time-stamped test sections constructed using the aggregates selected for this study. The researchers then evaluated the microtexture and macrotexture of core surfaces using a surface scanning feature available in AIMS. Individual aggregate particles were removed from the surface layer and evaluated using AIMS. The researchers used these data, along with several years of field friction numbers extracted from the FDOT database, to determine the influence of aggregate properties on pavement friction performance in the field. Selecting road sections with open-graded friction course minimized the effects of mix design and gradation variables. The results of the study indicated that texture index, as measured by AIMS, was highly affected by color variation and cannot be used reliably to evaluate aggregate surface microtexture. Furthermore, using AIMS to measure roadway macrotexture from pavement cores did not appear to be a good alternative to field measurement. The researchers found no statistically significant relationship between pavement friction performance and texture measurement using AIMS on virgin aggregates or field cores.					
17. Key Word  Aggregate, Image, Micro-Deval, Friction, Polish, Skid Resistance, Pre-evaluation, Pavement texture, AIMS, Color variation			18. Distribution Statement  No restrictions. This document is available to the public through the National Technical Information Service, Springfield, VA, 22161.		
19. Security Classif. (of this report)  Unclassified		20. Security Classif. (of this page)  Unclassified		21. No. of Pages  104	22. Price

## ACKNOWLEDGMENTS

The authors would like to acknowledge and thank the Florida Department of Transportation (FDOT) for providing technical and financial support, as well as materials for this project. Special thanks go to project manager John Shoucair, as well as Mark Gregory for all of his hard work and assistance in this project. In addition, a thank you to the engineers of the Pavement Evaluation Section of the State Materials Office (SMO) for contributing their experience throughout the course of this work. Their efforts are sincerely appreciated and clearly made a positive impact on the quality of the research.

## EXECUTIVE SUMMARY

This study was conducted to identify and evaluate Aggregate Image Measurement System (AIMS) capability in the pre-evaluation of aggregates for use in friction course. For purposes of this study, frictional characteristics of different aggregate types were measured and analyzed using a combination of AIMS and Micro-Deval. The Micro-Deval polishing device was used only for polishing aggregates at different levels in a non-standard procedure to evaluate the polishing behavior of a broad range of Florida aggregates. The unique aspect of this project was using AIMS to measure the microtexture of aggregates after several years in road service. The researchers obtained field cores from time-stamped test sections constructed using the aggregates selected for this study. The researchers then evaluated the microtexture and macrotexture of core surfaces using a surface scanning feature available in AIMS. Individual aggregate particles were removed from the surface layer and evaluated using AIMS. The researchers used these data, along with several years of field friction numbers extracted from the FDOT database, to determine the influence of aggregate properties on pavement friction performance in the field. Selecting road sections with open-graded friction course minimized the effects of mix design and gradation variables.

The researchers found that texture index, as measured by AIMS, is highly affected by color variation and cannot be used reliably to evaluate aggregate surface texture. Although AIMS appears to capture the effects of conditioning with Micro-Deval for both granitic and limestone aggregates, the color variation in the aggregate surfaces observed in this study had an overwhelming effect on the texture index measured by AIMS. Furthermore, regardless of which aggregate type was subjected to polishing, the relative change in texture index did not distinguish between different aggregate types.

In addition, skid resistance is clearly affected by pavement texture at all length scales, ranging from micro- to macro-scale. AIMS can measure texture in only a few length scales, which restricts the amount of possible information which can be collected from aggregate surface.

Analyzing the correlation between macrottexture measurements using AIMS in the laboratory, and macrottexture data available in FDOT database measured in the field using Circular Texture Meter (CTMeter) revealed that using AIMS to measure roadway macrottexture from pavement cores did not appear to be a good alternative to field measurement.

The researchers conducted numerous measurements and comprehensive statistical analysis on the collected data, but found no statistically significant relationships between pavement friction performance and pavement micro- and/or macrottexture measurement using AIMS on virgin aggregates or field cores.

The researchers used the extensive evaluations performed in this study to recommend further evaluation of the physical meaning of texture index, as well as the development of roughness references using surface profilers and available topographic data analysis techniques to estimate the effect of color variation. The researchers also suggested to further development of a strong correlation between the imaging technique results and topographic analytical models, and recommended that Micro-Deval performance be further evaluated as an accelerated aggregate polishing technique.

## TABLE OF CONTENTS

	<u>page</u>
DISCLAIMER .....	ii
SI (MODERN METRIC) CONVERSION FACTORS.....	iii
TECHNICAL REPORT DOCUMENTATION PAGE.....	iv
ACKNOWLEDGMENTS .....	v
EXECUTIVE SUMMARY .....	vi
LIST OF TABLES .....	x
LIST OF FIGURES .....	xi
CHAPTERS	
1 INTRODUCTION .....	1
1.1 Background.....	1
1.2 Scope.....	2
1.3 Objectives .....	2
1.4 Research Approach.....	3
1.5 Report Organization.....	4
2 LITERATURE REVIEW .....	5
2.1 Introduction.....	5
2.2 Friction Definition .....	5
2.3 Pavement Surface Texture.....	6
2.4 Friction Mechanism .....	9
2.5 Friction Measurement Methods.....	11
2.6 Texture Measurement Methods .....	14
2.7 Pre-evaluation of Aggregates for Application in Friction Course.....	18
3 MATERIALS AND TESTING	
3.1 Introduction.....	22
3.2 Aggregate Sources .....	22
3.3 Field Sections.....	25
3.4 Testing Methods .....	28
3.4.1 Micro-Deval Test.....	30
3.4.2 Aggregate Imaging Measurement System (AIMS).....	33

4	RESULTS AND DATA ANALYSIS .....	38
4.1	Introduction.....	38
4.2	Polishing Characteristics of Virgin Aggregates .....	38
4.3	Core Analysis.....	43
4.3.1	Macrotexture Measurement.....	43
4.3.2	Microtexture Measurement .....	48
4.4	Skid Resistance and its Relationship to Aggregate and Pavement Texture .....	54
5	CLOSURE .....	59
5.1	Summary and Findings .....	59
5.2	Conclusions.....	60
5.3	Recommendations and Future Work .....	61
	LIST OF REFERENCES .....	62
APPENDICES		
A	TEXTURE INDEX DISTRIBUTION OF VIRGIN AGGREGATES BEFORE AND AFTER POLISHING.....	71
B	MEASURED PROFILES OF CORES .....	81
C	TEXTURE INDEX DISTRIBUTION OF LABORATORY POLISHED AGGREGATES, SURFACE SCAN OF CORES, AND REMOVED AGGREGATES FROM CORES .....	87

## LIST OF TABLES

<u>Table</u>	<u>page</u>
Table 2.1 Factors affecting pavement friction .....	6
Table 2.2 Factors affecting pavement microtexture and macrotexture.....	9
Table 2.3 Field friction measurement devices .....	12
Table 3.1 Coarse aggregates physical requirements to be used in asphalt concrete .....	23
Table 3.2 Common types of friction course in Florida.....	24
Table 3.3 Aggregate types used in this study .....	25
Table 3.4 Selected road sections for this study.....	26
Table 3.5 FC-5 gradation design range.....	27
Table 3.6 Preparation of Micro-Deval samples based on standard (AASHTO T 327-09)	31
Table 3.7 Preparation of Micro-Deval samples in this project .....	32
Table 4.1 Average texture index and angularity index before and after polishing.....	40
Table 4.2 Average MPD values measured by AIMS.....	45
Table 4.3 Average RMS values measured by AIMS .....	47
Table 4.4 Average texture index values obtained from core surface analysis.....	49
Table 4.5 Average texture index values of individual aggregates obtained from cores ....	51
Table 4.6 Traffic data for all road sections .....	56

## LIST OF FIGURES

<u>Figure</u>	<u>page</u>
Figure 2.1 Pavement surface texture levels and the tire-pavement interactions affected by each level .....	8
Figure 2.2 Adhesion and hysteresis components .....	10
Figure 2.3 Generalized pavement friction model .....	13
Figure 2.4 Operating scales of different topographic measurement techniques .....	16
Figure 3.1 FDOT-approved coarse aggregate sources.....	24
Figure 3.2 Coring from Site No. 10 .....	28
Figure 3.3 Micro-Deval apparatus .....	30
Figure 3.4 Aggregate and steel balls interaction mechanism in Micro-Deval apparatus ..	30
Figure 3.5 Aggregate Imaging Measurement System: (a) AIMS1 (b) AIMS2 .....	34
Figure 3.6 Core scanning directions .....	36
Figure 3.7 Machine interface window .....	37
Figure 4.1 LA abrasion test results of studying aggregates .....	39
Figure 4.2 Change of texture index as a function of polishing time in the Micro-Deval ..	41
Figure 4.3 Comparison of aggregate types based on their texture index before polishing in Micro-Deval (BMD), and after polishing in Micro-Deval (AMD) at different polishing time.....	42
Figure 4.4 Comparison of aggregate types based on their angularity index before polishing in Micro-Deval (BMD), and after polishing in Micro-Deval (AMD) at different polishing time.....	42
Figure 4.5 Measured and normalized core surface profiles .....	44
Figure 4.6 Mean profile depth calculations (ASTM E1845-09).....	45
Figure 4.7 AIMS MPD for different road sections at different segment lengths .....	46
Figure 4.8 AIMS and CTMeter MPD values for five sections .....	46
Figure 4.9 Studying road sections sorted based on AIMS RMS value .....	47

Figure 4.10 Captured images from a core at five magnification levels .....	48
Figure 4.11 Distribution of texture index for core 5-4-A (Site No. 5, sample 4 and direction A) .....	50
Figure 4.12 average texture index values obtained from virgin aggregates and field cores at 12.6X magnification level .....	52
Figure 4.13 granitic aggregate (GA553) images and corresponding texture index values after 180 minutes polishing .....	53
Figure 4.14 limestone aggregate (87339) images and corresponding texture index values after 180 minutes polishing .....	54
Figure 4.15 Texture index values of three individual aggregates obtained from Site No. 6 constructed using limestone aggregate (87339) .....	54
Figure 4.16 Friction number variations for all road sections.....	55
Figure 4.17 Friction number at a specific traffic level.....	57
Figure 4.18 The relationship between friction number and macrotexture statistical parameters .....	58
Figure A.1 Texture distribution of 87090 before and after polishing (#4) .....	72
Figure A.2 Texture distribution of 87090 before and after polishing (#3/8) .....	72
Figure A.3 Texture distribution of 87145 before and after polishing (#4) .....	73
Figure A.4 Texture distribution of 87145 before and after polishing (#3/8) .....	73
Figure A.5 Texture distribution of 87339 before and after polishing (#4) .....	74
Figure A.6 Texture distribution of 87339 before and after polishing (#3/8) .....	74
Figure A.7 Texture distribution of 87648 before and after polishing (#4) .....	75
Figure A.8 Texture distribution of 87648 before and after polishing (#3/8) .....	75
Figure A.9 Texture distribution of HN717 before and after polishing (#4) .....	76
Figure A.10 Texture distribution of HN717 before and after polishing (#3/8) .....	76
Figure A.11 Texture distribution of 70693 before and after polishing (#4) .....	77
Figure A.12 Texture distribution of 70693 before and after polishing (#3/8) .....	77
Figure A.13 Texture distribution of NS315 before and after polishing (#4) .....	78

Figure A.14 Texture distribution of NS315 before and after polishing (#3/8).....	78
Figure A.15 Texture distribution of GA553 before and after polishing (#4) .....	79
Figure A.16 Texture distribution of GA553 before and after polishing (#3/8) .....	79
Figure A.17 Texture distribution of GA383 before and after polishing (#4) .....	80
Figure A.18 Texture distribution of GA383 before and after polishing (#3/8) .....	80
Figure B.1 Profiles measured from three cores of Site No.1 at four directions.....	82
Figure B.2 Profiles measured from three cores of Site No.2 at four directions.....	82
Figure B.3 Profiles measured from three cores of Site No.3 at four directions.....	83
Figure B.4 Profiles measured from three cores of Site No.4 at four directions.....	83
Figure B.5 Profiles measured from three cores of Site No.5 at four directions.....	84
Figure B.6 Profiles measured from three cores of Site No.6 at four directions.....	84
Figure B.7 Profiles measured from three cores of Site No.7 at four directions.....	85
Figure B.8 Profiles measured from three cores of Site No.8 at four directions.....	85
Figure B.9 Profiles measured from three cores of Site No.9 at four directions.....	86
Figure B.10 Profiles measured from three cores of Site No.10 at four directions.....	86
Figure C.1 Site No.1 and limestone aggregate 87145 .....	88
Figure C.2 Sites No.2 and No.3 and granitic aggregate GA553.....	88
Figure C.3 Sites No.4 and No.6 and limestone aggregate 87339 .....	89
Figure C.4 Site No.5 and granitic aggregate GA383 .....	89
Figure C.5 Sites No.7 and No.9 and limestone aggregate 87090 .....	90
Figure C.6 Site No.8 and Wackestone aggregate 70693 .....	90
Figure C.7 Site No.10 and granitic aggregate NS315.....	91

## CHAPTER 1 INTRODUCTION

### **1.1 Background**

Friction resistance is one of the most critical performance parameters for asphalt pavements as it has a great effect on the safety of the traveling public. Many researchers around the world have reported a strong relationship between pavement friction and rate of crashes (Hall et al. 2006; Miller and Johnson, 1973; Rizenbergs et al., 1972; McCullough and Hankin, 1966; Wallman and Astron, 2001, Gandhi et al., 1991).

Pavement skid resistance is a function of different factors including the microtexture and macrotexture of the pavement surface. Microtexture, which is highly related to the surface characteristics and mineralogy of aggregates, provides a rough surface that disrupts the continuity of water film and produces frictional resistance between the tire and pavement by creating intermolecular bonds. Macrotexture, which is more affected by aggregate gradation and mix design, improves wet frictional resistance, particularly at high speeds, by providing surface drainage (Hanson and Prowell, 2004; Kowalski, 2007). The literature review shows that aggregate characteristics have a great effect on the frictional properties of flexible pavements.

Finding a direct specification for the selection and use of aggregates to ensure satisfactory frictional performance has been a focus for many researchers and transportation agencies. Currently, historical background of the aggregate performance or construction of test sections forms the basis for aggregate selection for use in asphalt mixtures (West et al., 2001; Goodman et al., 2006). However, it is well known that the existing sources of high quality aggregates are being rapidly depleted, and there will be a great need for new acceptable sources that can ensure

safety. Furthermore, evaluation by means of field test sections requires several years and is costly.

## **1.2 Scope**

The researchers for this study hypothesize that pavement friction performance can be improved by selection of polish-resistant aggregates with certain shape characteristics (Masad et al., 2009). Aggregates must be selected using characteristics that can be obtained from relatively short-term laboratory tests and based on ability to provide an acceptable level of surface friction throughout the pavement service life. Consequently, there is a need for a more effective and expeditious testing protocol able to correlate the measured frictional characteristics of aggregates to their long-term frictional performance in the field.

Aggregate Image Measurement System (AIMS) is a relatively new tool with the capability of providing aggregate shape properties of both fine and coarse aggregates including form, angularity, and surface texture. It is an integrated hardware/software system that provides these aggregate properties in a manner that is operator-independent (Bathina, 2005). Core surface analysis is a relatively new feature of AIMS, which is used for measuring microtexture and macrotexture at the core surface.

The Florida Department of Transportation (FDOT) sought to identify an efficient protocol using AIMS, along with other laboratory tools that can reliably pre-evaluate the suitability of aggregates for use in pavement friction course. In order to achieve this goal, a relationship between AIMS measurements and field friction performance must be established.

## **1.3 Objectives**

The primary objective of this study is to investigate AIMS and its role in the aggregate selection and pre-evaluation processes by evaluating aggregates with different characteristics and

by studying frictional performance of mixtures constructed using these aggregate types. The following steps were used to achieve the objectives:

- Identify different aggregate geologies from sources currently approved or seeking approval for use in FDOT's friction course pavement.
- Direct the sampling of all identified aggregate sources for selected laboratory testing.
- Coordinate with the FDOT State Materials Office's Pavement Material Systems to select FDOT road sections suitable for coring and collect desired cores.
- Establish a laboratory polishing protocol to simulate accelerated field polishing of sampled aggregates.
- Use AIMS to measure aggregate surface microtexture of all sampled aggregates before and after polishing.
- Measure core surface microtexture and macrotexture using AIMS.
- Establish a protocol for obtaining aggregate samples from cores for aggregate microtexture analysis in AIMS.
- Measure microtexture of removed aggregates from cores using AIMS.
- Determine a laboratory factor or function that considers the polishing of aggregates and correlates AIMS data with frictional performance in the field.

#### **1.4 Research Approach**

The overall approach to this project will involve identification of accelerated aggregate polishing procedures, and microtexture measurement protocols using AIMS that can be related to the aggregate's measured long-term frictional performance in the field. This goal will be accomplished by subjecting a broad range of Florida aggregates to different levels of accelerated laboratory polishing. The microtexture reduction measured by AIMS will then be compared to

the measured frictional performance and aggregate microtexture (from field cores) of pavements produced with aggregates from the same geologies. In addition, macrotexture measurements from AIMS (using field cores) will be evaluated to isolate the effect of aggregate microtexture on frictional performance.

### **1.5 Report Organization**

Chapter 2 presents a summary of literature review. Chapter 3 explains the materials, testing equipment, and methods used in this study. Chapter 4 includes the results and discussion, and Chapter 5 presents the conclusions and recommendations of this study. Appendix A depicts the texture index distribution of virgin aggregates before and after polishing in laboratory. Appendix B presents scan line profiles of all measured cores in this study, and Appendix C depicts distribution of texture index measured by AIMS from polished virgin aggregates, scanning core surfaces, and aggregates removed from cores, all at a constant magnification level (12.6X).

## CHAPTER 2 LITERATURE REVIEW

### **2.1 Introduction**

Traffic safety and adequate skid resistance have long been a concern for public officials responsible for the safety of the traveling public. Researchers have made numerous to characterize friction in asphalt concrete pavements, resulting in considerable progress in this area. However, due to the numerous factors involved in tire-pavement interaction process, the prediction of friction performance in asphalt concrete pavements has not been realistically addressed. This chapter presents a summary of major findings and research studies on pavement friction characterization performed to date. This chapter will define, explain the mechanism of, and address the major factors involved in friction and skid resistance. It will also introduce the field and laboratory methods of friction and pavement texture measurement and focus on image processing application. Finally, this chapter will present a review on the role of aggregate characteristics in pavement friction performance.

### **2.2 Friction Definition**

Pavement friction is defined as a resistant force generated by the relative motion between tire and pavement surface when the tire rolls and slides over the pavement surface (Hall et al., 2006). This force plays a major role in controlling vehicle direction and speed and is therefore a key factor in providing traffic safety (Kokkalis, 1998; Hall et al., 2006; Noyce et al. 2005; Li et al., 2005).

Factors affecting tire-pavement friction are numerous (Table 2.1), and the amount of developed friction depends on a complex interaction of these factors, notably pavement texture, tire condition, the presence of water and vehicle speed. Road surface material properties are another key parameter (Kokkalis, 1998; Woodside and Woodward, 2002).

Table 2.1 Factors affecting pavement friction (Hall et al., 2006; Wallman and Astron, 2001; Kokkalis, 1998)

Road Characteristics	Vehicle Operating Parameters	Tire Properties	Environment
Type of surface Surface texture (microtexture, macrotexture) Mix design Roadway geometry Material properties (mineralogy, hardness, density)	Vehicle type Suspension system Breaking system Vehicle speed Load magnitude and distribution Driving maneuver	Tire type and condition Tread pattern and depth Inflation pressure Hardness and wear Temperature Specific heat	Climate (wind, temperature, rainfall, snow, ice) Surface contamination (dirt, mud, debris, salt, sand)

It is impossible to define an equation or identify a correlation between all of these factors in order to predict skid resistance in all possible conditions (Kokkalis, 1998). However, many research groups specializing in areas such as pavement, tribology, and mineralogy continue to investigate the problem of characterizing tire-pavement interaction. The term of skidding resistance is used to show the road contribution to friction which typically refers to wet conditions as the presence of water acts as a lubricant, while most HMA surfaces have an adequate level of skid resistance in dry condition (Woodside and Woodward, 2002). The present paper mainly discusses the contribution of pavement surface to skid resistance development.

### 2.3 Pavement Surface Texture

Pavement surface characteristics directly affect driver safety and comfort. In order to satisfy the driving public, pavement surfaces should provide adequate friction, good ride quality, and low levels of noise (Flintsch et al., 2003). Texture is the main feature of pavement surface which

controls most of the tire-pavement interactions such as wet friction, noise, splash and spray, rolling resistance, and tire wear (Henry, 2000; Ergun et al., 2005).

Pavement surface texture can be affected by asperities in pavement surface ranging from micro-scale irregularities in an individual aggregate to a span of several feet of unevenness in a finished pavement project. Road engineers have categorized pavement texture into four domains: microtexture, macrotexture, megatexture, and roughness (unevenness) (Hall et al., 2006; Kokkalis et al., 2002; Flintsch et al., 2003). These domains are based on wavelength ( $\lambda$ ) and peak-to-peak amplitude (A) of texture components. The effects of two levels of texture—microtexture and macrotexture—are dominant in pavement skid resistance (Henry, 2000).

Microtexture was classified in 1987 by the Permanent International Association of Road Congresses (PIARC) as irregularities within wavelengths of less than 0.5 mm ( $\lambda < 0.5$  mm) and peak-to-peak amplitudes of 1 to 500 micrometers ( $A = 1$  to 500  $\mu\text{m}$ ). Macrotexture is defined as irregularities within wavelengths of 0.5 to 50 mm ( $0.5$  mm  $< \lambda < 50$  mm) and peak-to-peak amplitudes of 0.1 to 20 millimeter ( $A = 0.1$  to 20 mm) (Henry, 2000; Hall et al., 2006).

According to the literature, pavement surface is generally considered harsh if it has an average microtexture of more than 0.05 mm, and is considered rough if has an average macrotexture of more than 1.5 mm (Kokkalis et al., 2002). Figure 2.1 illustrates pavement surface texture classifications based on the wavelength of texture elements and the tire-pavement interactions affected by each wavelength range (Henry, 2000; Hall et al., 2006). It should be noted that both the amplitude and the wavelength parameters are important in terms of friction force development (Persson, 2001).

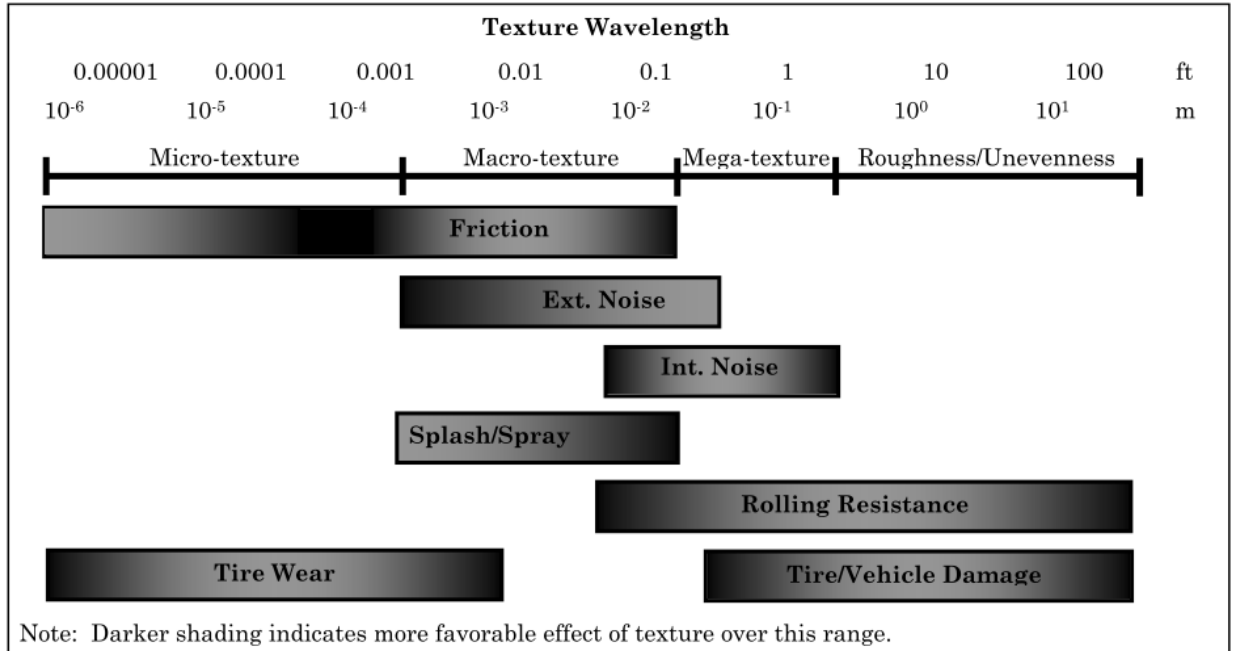


Figure 2.1 Pavement surface texture levels and the tire-pavement interactions affected by each level (Henry, 2000; Hall et al., 2006)

Pavement microtexture is mainly a function of aggregate mineralogy and may be an indicator of pavement surface or aggregate polishing degree (Kokkalis et al., 2002; Hall et al., 2006). Microtexture varies from harsh state in newly paved surfaces to polished state in surfaces under the effects of traffic and weathering. Skid resistance at any speed range is highly affected by microtexture (Kokkalis et al., 2002; Ergun et al., 2005). Aggregates with desirable frictional characteristics can control microtexture (Noyce et al., 2005).

Pavement macrotexture is mainly attributed to the coarseness of road surfaces and its magnitude depends on several mixture properties such as aggregate gradation, aggregate size, shape characteristics, distribution of coarse aggregates, and construction and finishing techniques (Noyce et al., 2005; Hall et al., 2006). Macrotexture plays a major role in water drainage in the tire contact area, rubber tire deformation, the coefficient of friction at higher speeds, and the friction-speed gradient. Inadequate macrotexture may result in reduced wet skid resistance, especially at higher speeds (Dahir, 1979; Kokkalis et al., 2002; Ergun et al., 2005).

Table 2.2 provides a summary of the factors affecting asphalt pavement microtexture and macrotexture. Higher mix air content allows for more water drainage (which increases friction) and increased air drainage (which reduces noise). The content, viscosity, and aging properties of mix binder can affect macrotexture in terms of bleeding and raveling (Hall et al., 2006). All of these factors should be considered during the design process.

Table 2.2 Factors affecting pavement microtexture and macrotexture (Hall et al., 2006; Sandberg and Ejsmont, 2002; Henry, 2000; Rado, 1994; PIARC, 1995; AASHTO, 1976)

Pavement Surface Type	Factor	Microtexture	Macrotexture
Asphalt	Maximum aggregate dimensions		✓
	Coarse aggregate types	✓	✓
	Fine aggregate types		✓
	Mix gradation		✓
	Mix air content		✓
	Mix binder		✓

## 2.4 Friction Mechanism

In order to understand the skid resistance phenomenon, the mechanism of tire-pavement interaction must be considered alongside surface texture analysis (Kokkalis, 1998). The analysis of rubber materials sliding against a rigid rough surface is typically modeled on information such as viscoelastic property of the rubber, surface roughness statistics, sliding speed, contact pressure and temperature (Westermann 2004). This area of research is related to Tribology, a branch of science and engineering which studies contact mechanics of interacting surfaces in relative motion by applying the principles of friction, lubrication, and wear.

Tire-pavement friction is commonly characterized by two major components: adhesion and hysteresis (Figure 2.2). The contribution of each component to wet skid resistance depends on many factors such as sliding speed, properties of surfaces, and temperature.

Adhesion is associated with the intermolecular bonding formed between rubber and aggregate surfaces, a bond that can only be broken by energy (Kokkalis, 1998; Klüppel et al., 2000). Adhesion is important to tire-pavement interaction on clean, dry, smooth surfaces (Persson, 2000; Klüppel et al., 2000). Hysteresis results from energy dissipation via cyclic deformation of tire rubber when slides on surface asperities. At all length scales, hysteresis has a greater effect on friction force development than adhesion has on tire-pavement interaction (Persson, 2000; Choubane, 2004; Noyce et al., 2005). In pavements and in terms of texture classification, hysteresis is mainly induced by aggregate microtexture and mixture macrotexture (Villani, 2011).

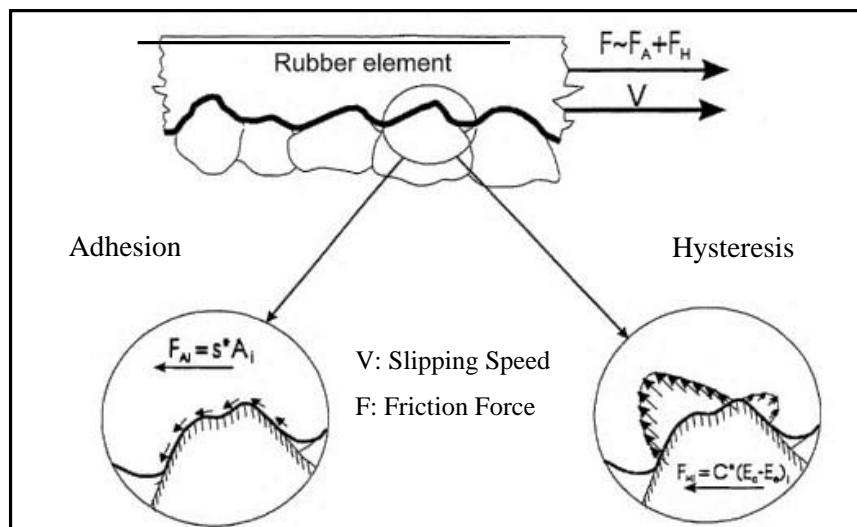


Figure 2.2 Adhesion and hysteresis components (Choubane et al., 2004)

Researchers such as Greenwood/Williamson, Kummer, Moore, Yandell, Grosch, Persson, Heinrich/Klüppel, and many others have made extensive efforts to qualitatively and quantitatively model these two skid resistance components and relate friction to surface roughness. Many of the advanced analytical models in this area are based on the application of fractal and self-affinity concepts to characterize aggregate surface roughness over a broad range

of length scales. It has been revealed that fractured surface of many materials such as aggregate can be described as self-affine surfaces over a wide range of roughness (Persson, 2001).

## **2.5 Friction Measurement Methods**

Many pavement engineers have been engaged in finding methods to measure friction in order to reduce the risk of traffic crashes. At present, a variety of friction measurement devices are used around the world to evaluate pavement friction performance. While these devices are not complicated, it is difficult to control the parameters that affect the friction forces that they measure (Wallman and Astron, 2001).

Pavement friction in the field can be measured using four types of test equipment: locked wheel (100% slip), constant slip (normally 10-20% slip), side force, and variable slip (0-100% slip). Slip is defined as the slip speed to operating speed ratio. The friction force generated in the wheel hub directly after braking to locked wheels depends on this parameter, and the maximum friction force is reached at the slip rate of 7-20% (Permanent International Association of Road Congresses (PIARC), 1995; Wallman and Astron, 2001; and FHWA 2010).

Each type of testing approach is used to estimate a specific aspect of friction performance. The locked wheel method is used to model the condition of braking without anti-lock brakes, and the side force method is used to estimate the vehicle's ability to maintain control on curves. The fixed slip and variable slip methods are related to braking conditions with anti-lock brakes (Wallman and Astron, 2001; and FHWA 2010). Table 2.3 summarizes some available testing equipment developed for each measuring approach. A comprehensive summary of these testing devices can be found in NCHRP report 291 (Henry, 2000). Some devices are more popular than others and are used by several countries (Wallman and Astron, 2001).

Table 2.3 Field friction measurement devices

Locked Wheel	Side Force	Fixed Slip	Variable Slip
Skid Trailer (ASTM E 274)	SCRIM	Runway Friction Tester	Norsemeter SALTAR
Diagonal Braked Vehicle	MuMeter	Griptester	IMAG
Japanese Skid Tester	Odoliograph	Saab Friction Tester	
LCPC Adhera	Stradograph	Portable Friction tester	
Polish SRT-3		DWW trailer	
Skiddometer BV-8		Skiddometer BV-11	

The locked wheel skid trailer (ASTM E 274) is the most common device used by U.S. state highway agencies (Luo, 2003). This equipment includes a truck containing a large water tank and a trailer with a locking mechanism on one wheel (Davis, 2001). Variables such as the testing speed, test tire, pavement texture, age of pavement in service, and temperature of the contacting surfaces can influence wet skid resistance measurements in the field.

The locked wheel test can be conducted at any speed, and while standard types of tires including ribbed, smooth, or patterned can be used, the ribbed tire (ASTM E 501) is the most common test tire (Wallman and Astron, 2001; Davis, 2001).

Pavement surface texture changes over time under prevailing traffic and weathering conditions that could be detrimental or beneficial to skid resistance (Dahir, 1979; Flintsch et al., 2005). The physical and environmental factors of weather such as freezing and thawing, wetting and drying, and oxidation of aggregates can influence texture (Dahir, 1979). Traffic also affects surface texture by applying various vertical and horizontal stresses that results in abrasions, crushing, and breaking of aggregates. Compaction and embedment of aggregates caused by traffic can reduce macrotexture in pavement surface (Kokkalis et al., 2002).

Generally, most road surfaces experience peak skid resistance after a few weeks of traffic wears asphalt binder from aggregate surfaces (Chelliah et al., 2003; Masad et al., 2009). Under constant traffic conditions with no structural deterioration, the skid resistance loss rate progressively decreases, and then stabilizes at a lower level. Based on empirical observations, this equilibrium state usually occurs after 1 to 5 million passenger vehicle passes or two years (Diringer et al., 1990; Chelliah et al., 2003).

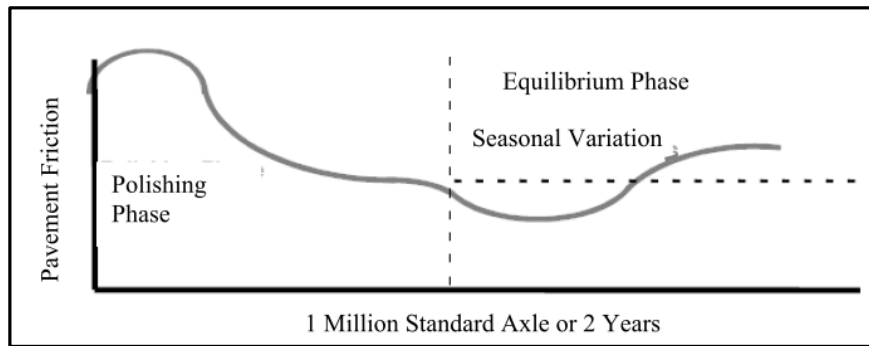


Figure 2.3 Generalized pavement friction model (Chelliah et al., 2003; Diringer et al., 1990; Masad et al., 2009).

Friction measured by skid trailer can fluctuate with seasonal variation. The lowest level of skid resistance occurs in the summer months due to the accumulation of a higher amount of small particles and debris (Wallman and Astron, 2001; Chelliah et al., 2003; Masad et al., 2009). Pavement temperatures also can have a large effect on pavement friction in correspondence to speed (Flintsch et al., 2005). Some researchers observed an approximate reduction of 30% in skid resistance between a winter peak and summer minimum (Transit New Zealand (TNZ), 2002; Masad et al., 2009).

Other testing equipment and methods for friction measurement can be categorized as portable and laboratory testing devices, such as the Dynamic Friction Tester (DFT), pendulum devices including the British Pendulum Tester (BPT), the North Carolina State University Variable Speed Friction Tester, the Michigan Laboratory Friction Tester, the Pennsylvania

Transportation Institute Friction Tester, and the Wehner/Schulze Friction Device. The BPT and the DFT are the most commonly used devices in this category.

The BPT (ASTM E 303) has been accepted worldwide and is one of the simplest and least expensive testing devices developed to measure low speed (about 10 km/h) friction in pavements (Giles et al., 1964; Saito et al., 1996). However, researchers have experienced on many occasions that BPT measurements could be affected by pavement surface macrotexture and parameters such as surface contact area and aggregate gap width, which can result in unreliable friction measurement results (Purushothaman et al. 1988, Fwa et al. 2003, Lee et al. 2005).

The DFT (ASTM E 1911) is a disc-rotating tester that measures friction force between a surface and three rubber pads attached to the disc. The disc rotates horizontally at a linear speed of 20-80 km/h under a constant load. It touches the surface at different speeds, allowing the DFT to measure skid resistance at any speed in this range (Saito et al., 1996).

## **2.6 Texture Measurement Methods**

Roughness characterization and pavement texture measurement has made significant progress over the past few decades. During this period, researchers have developed a broad range of testing methods from simple indirect evaluation techniques to high-tech direct measurements that can be conducted in the field or in the laboratory. Some of these testing methods are in very limited use and can only be found in a few specific sources. Some practical techniques and devices for capturing microtexture and macrotexture are available.

There are several methods for measuring macrotexture including volumetric methods and profile tracers. Volumetric methods include the Sand Patch Method (ASTM E 965), the grease patch method, and the Silly Putty method. In each of these methods, a known volume of material spreads over the surface and the average macrotexture depth is determined by dividing the

known volume of the material by the covered area (Ergun et al., 2005; Jayawickrama et al., 1996). These methods have the advantage of simplicity and low operation cost, but have some disadvantages, including lane closure requirements, repeatability constraints, and labor-intensive activity (Hall et al., 2006).

Another volumetric method for pavement macrotexture characterization is the Outflow Meter Test (OFT) (Henry, 2000). This method uses the relative rate of water drainage through surface texture and mixture voids to estimate macrotexture (Moore, 1966; Hall et al., 2006). However, it has been shown that there is a poor correlation between OFT output (outflow time) and other texture measurement parameters like Mean Profile Depth (MPD) or Mean Texture Depth (MTD) (Hall et al., 2006).

Significant advances in optics and laser technology have led to the development of non-contact surface profiling techniques to characterize macrotexture, even at highway speed. Examples of optic profile tracer devices include Mini-Texture-Meter and Selcom Laser System.

Circular Texture Meter (CTMeter) is one of the most common laser-based devices for measuring the MPD of a pavement at a static location in the laboratory as well as in the field (Abe et al., 2000; Noyce et al., 2005). CTMeter measures the 892 mm circular profile of the pavement surface matching the measurement path of the DFT (Hall et al., 2006). According to the literature, MPD measured by CTMeter has a strong correlation with parameters obtained from volumetric methods such as MTD and outflow time, except for when measuring highly porous surfaces (Noyce et al., 2005).

Pavement surface microtexture cannot be measured directly in the field at highway speed. Therefore, many field-testing methods estimate microtexture indirectly. As discussed above, microtexture is more responsible for friction at lower speeds. Microtexture in the field is

typically estimated using low speed friction measurement devices such as the BPT, the DFT, or the locked wheel skid trailer (running at low speed) (Henry, 2000; Flintsch et al., 2003). These testing methods capture microtexture effects by indirectly measuring the influence on measured friction.

In order to have enough information for friction characterization, it is important to directly measure microtexture and acquire topographic data covering the full range of target scales. Progress in optic device technology has made it possible to measure microtexture directly. Electron microscopy, stereo photography, interferometry, structured light, and Scanning Laser Position Sensor (SLPS) are data acquisition techniques based on optic device application. Figure 2.4 represents some available topographic data acquisition techniques operating near the target scales available for use in pavement (Johnsen, 1997).

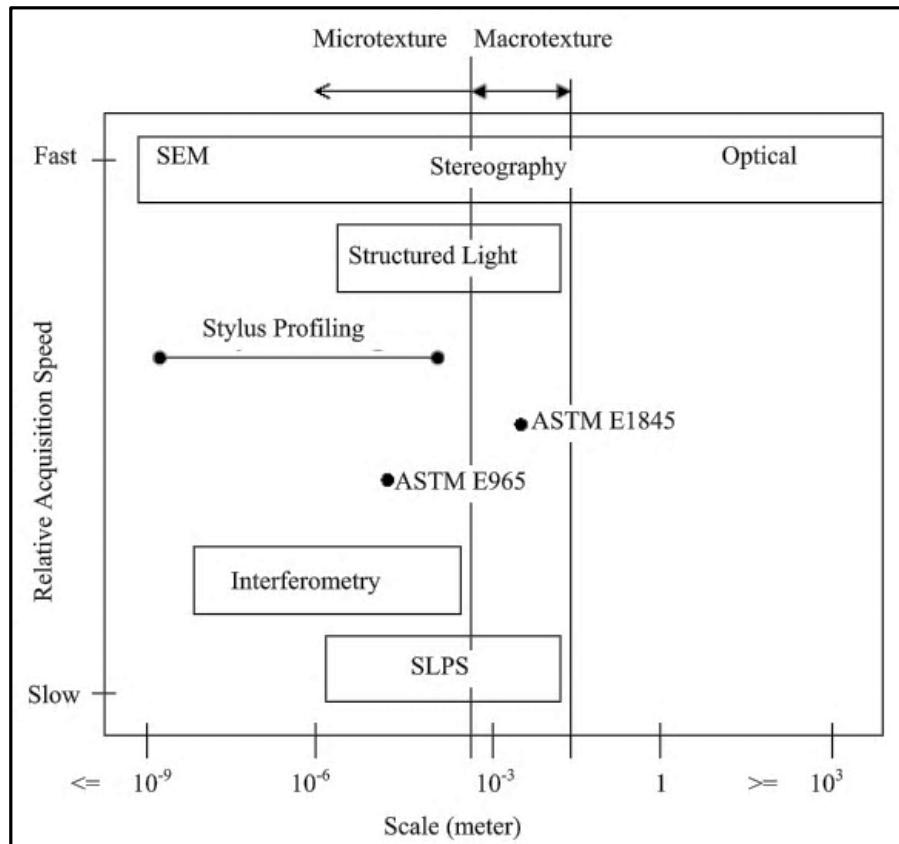


Figure 2.4 Operating scales of different topographic measurement techniques (Johnsen, 1997).

In this figure, stylus profiling technique—a direct contact measurement method—has been compared with optic devices. However, 3-D acquisition techniques are more favorable than 2D methods such as stylus as they contain topographic information for characterization in both 2-D and 3-D analysis methods (Johnsen, 1997). Interferometry and the stylus profiling techniques cover a portion of the target scales for determining pavement texture and are useful for studying topographic data with isotropic features if the acquisition scale supports data analysis (Johnsen et al., 1994; Johnsen, 1997). The SLPS was specifically designed for topographic measurement of pavement surfaces. This device is highly portable and can be easily utilized for in situ measurement (Johnsen, 1997). Structured light and the SLPS techniques cover the full range of target scales; however, preliminary analysis of topographic data acquired with structured light showed limited elevation range in measurement of large-scale pavement surface features (Johnsen, 1997).

Image-based techniques are classified as direct characterization methods of microtexture. Over the last two decades, researches have used varying methods of capturing 2D and 3D images from pavement and aggregate surfaces, and have implemented different digital scanning systems and computer algorithms to analyze these images (Johnsen, 1997). Texture analysis is commonly performed using black and white or gray scale images. Using black and white images has disadvantages such as high-resolution image requirement and loss of texture details (Al-Rousan et al., 2007). The majority of these methods assume that gray level variations are representative of local relief variations; however, this variation can be attributed to color variation, roughness, or both (Khoudeir, 2004). Masad et al. (2001) developed a computer-controlled device called Aggregate Imaging System (AIMS) to capture aggregate shape characteristics including form, angularity, and surface texture, and introduced Texture Index as a representation of microtexture.

The researchers theorized that, by using multi-scale resolution wavelet transformation, AIMS could capture true texture and distinguish between variations in gray intensities due to variations in relief and other factors (Fletcher et al., 2002). By applying the Fourier transform-based morphological analysis method, Wang et al. (2005) attempted to characterize the shape, angularity and texture of aggregates using 2D images captured from aggregate surfaces.

First proposed by Woodham (1980), stereo photography is a widely used shape recovery technique for reconstructing the 3D texture of pavement surface from 2D images (Gendy et al., 2007). This technique requires special focusing tools, and is based on a pair of images, each taken from a specific angle of the inspected surface (Johnsen 1997). Despite successful application of this technique to recover surface texture, limitations include need for high illumination intensity in dark surfaces such as asphalt pavement, the effects of equipment on precision, and the effect of material color, ambient environment, and lighting direction and type (Gendy et al., 2007). Gendy et al. (2011) reported that stereo photography and other image-based techniques could be successfully applied to recover pavement surface topography.

### **2.7 Pre-evaluation of Aggregates for Application in Friction Course**

The polishing of aggregates characteristics has long been considered a useful method in providing an acceptable level of skid resistance (Kokkalis and Panagouli, 1999). Clearly, aggregates must be durable and abrasion resistant to prevent crushing, degradation, and disintegration during storage, transportation, construction, and traffic loadings stresses (Wu et al. 1998). Aggregate must be hard and tough in order to be wear-resistant, and must possess and retain sharp asperities to be polish-resistant, the latter of which occurs due to irregular crystal fracture, or differential hardness of the constituent minerals (Dahir, 1979).

Particle size, shape, gradation, and mineralogy are important properties for improving surface aggregate resistance to wear and polishing resistance. Studies indicate that, in bituminous mixtures, the role of coarse aggregate type is more dominant in determining skid resistance than other mix constituents such as asphalt content, fine aggregate type, and coarse aggregate grading (Crouch, 1996).

Aggregates in the asphalt mixture are polished differently based upon their mineralogy. Aggregates have varying ability to withstand the polishing action of traffic and maintain microtexture; therefore, different aggregates have different polishing rates (McDaniel et al., 2003; Kowalski, 2007). For example, limestone is the most susceptible to polishing, which produces the lowest skid resistance, and is the main cause of pavement slipperiness (Csathy et al., 1968). Other groups—such as basalt, granite, and quartzite—have intermediate resistance against polishing (Bloem, 1971). Kokkalis and Panagouli (1999) posited that aggregates composed of hard and soft minerals have higher skid resistance than aggregates consisting predominantly of minerals of the same hardness.

The polishing behavior of aggregates can be evaluated through laboratory test procedures (Noyce et al., 2005). Several researchers attempted to develop laboratory test methods to pre-evaluate aggregates and relate aggregate properties to skid resistance; however, there is little agreement on which engineering properties of an aggregate should be considered in order to provide adequate frictional resistance at various traffic levels (Crouch, 1996; Masad et al., 2009). Diringer et al. (1990) developed an exponential model to estimate the empirical relationship between aggregate microtexture and cumulative polishing using the British Pendulum Tester and the British Polishing Wheel (BPW). The researchers then attempted to identify a relationship between minimum polish value and long-term minimum skid resistance to establish an

acceptable limit for prequalification of aggregates. Masad et al. (2009) of University of Texas A&M used Micro-Deval and AIMS to capture aggregate polishing characteristics and attempted to relate these properties to field and laboratory friction performance by considering the effect of traffic and mix gradation.

Polishing techniques are part of any aggregate classification system that evaluates an aggregate for pavement surface application (Masad et al., 2009). Researchers have conducted the accelerated polishing of aggregates and HMA specimens using different equipment types and methods over the years (Wallman and Astron, 2001). Laboratory-scale accelerated polishing devices can be classified into three groups: aggregate sample polishing, HMA specimen polishing, and those capable of polishing either aggregate samples or HMA specimens. Devices that polish aggregate samples include BPW, Michigan Indoor Wear Track, and the Micro-Deval. The National Center for Asphalt Technology (NCAT) laboratory-scale accelerated polishing device has been designed to polish HMA specimens. The third group includes the NCSU Wear and Polishing Machine, the Wehner/Schulze Polishing Machine, and the Penn State Reciprocating Polishing Machine. McDaniel and Coree (2003) present some of these techniques, their advantages, and their disadvantages in more detail.

Other laboratory tests and methods for classifying and pre-evaluating aggregates include evaluating aggregates durability and soundness. In addition to toughness and abrasion resistance, aggregates must be resistant to breakdown or disintegration when subjected to wetting and drying and/or freezing and thawing. This category includes laboratory tests such as Sodium and Magnesium Sulfate Soundness (AASHTO T 104), Freezing and Thawing Soundness (AASHTO T 103), Aggregate Durability Index (AASHTO T 210), and Canadian Freeze-Thaw Test (Wu et al., 1998).

In addition to the laboratory tests, FDOT uses skid field testing to evaluate candidate aggregates for use in pavement surface courses. After a candidate aggregate meets the laboratory test requirements, a trial pavement section is constructed using the candidate aggregate. The locked wheel trailer testing method is then conducted on the trial section to evaluate its friction performance. No minimum traffic volume is required for approval of the trial section. If the test results are satisfactory, a test section with a minimum speed limit of 50 mph and a minimum average daily traffic of 14,000 is constructed using the candidate aggregate. At the same time, a control section meeting the test section criteria and adjoining the test section is constructed with an already-approved aggregate. Friction tests are then performed on the test section immediately after construction at monthly intervals for 2 months and at intervals of 2 months thereafter until the accumulated traffic reaches 6 million vehicles or until the skid numbers stabilize. Frictional tests are conducted on the test and control sections at 40 mph in accordance with ASTM E 274 using both ribbed and blank test tires (Jayawickrama, 1996). If necessary, additional testing is done at a speed of 60 mph. Candidate aggregates are approved for use in highway projects only if the test section exhibits friction numbers above 30 and compares favorably with the control section (Jayawickrama, 1996). Obviously, this process is laborious, expensive, and time consuming, and justifies the need for finding a new laboratory method for pre-evaluation of aggregates.

## CHAPTER 3 MATERIALS AND TESTING

### **3.1 Introduction**

As discussed in Chapter 2, ensuring an acceptable level of friction performance through pre-evaluation of new aggregate sources for pavement surface application has been a challenge for many years. Therefore, there is a great need for a relatively short-term laboratory test to characterize aggregate properties and relate these properties to pavement surface performance. This chapter briefly explains the aggregate sources selected for this study and the laboratory measurements conducted to evaluate texture and polishing resistance on virgin aggregates. It also describes the coring and texture measurement of field cores obtained from road sections with a known construction history, traffic conditions, and a skid resistance record. A broad range of Florida aggregates were collected and cores were taken from roads with the same aggregate types.

### **3.2 Aggregate Sources**

As mentioned in Chapter 2, pavement skid and wear resistance is highly dependent on aggregate characteristics. In asphalt pavement surfaces, coarse aggregates are mostly responsible for providing friction, and, therefore, their characteristics are important in terms of pavement performance characterization. This paper deals only with the evaluation of coarse aggregate frictional properties.

Current procedure in pre-evaluation of aggregates in Florida was discussed in the previous chapter. According to the current standards, coarse aggregates must meet chemical and physical

requirements in laboratory tests to be accepted as an aggregate source for use in asphalt concrete. These approved aggregates can then be employed in friction courses if they exhibit satisfactory friction resistance in test sections. Table 3.1 summarizes the required physical properties for coarse aggregates in Florida.

Table 3.1 Coarse aggregates physical requirements to be used in asphalt concrete

Test	Requirement
Los Angeles Abrasion (FM 1-T 096)	maximum loss 45%
Soundness (Sodium Sulfate)	maximum loss 12%
Flat or elongated pieces	maximum 10%

Due to the low polishing resistance of many native Florida limestone aggregates, friction courses are required on the majority of state roadways to provide safety. Some aggregates in Florida friction courses are oolitic limestones from southeast Florida. Figure 3.1 shows the geographical location of coarse aggregate sources in Florida. It should be noted that, due to a limited supply of in-state, high-quality coarse aggregate sources, the FDOT imports some out-of-state aggregates such as GA383.

Depending on highway serviceability level, two types of friction courses are usually employed in the state of Florida: 1) open-graded friction courses, and 2) dense-graded friction courses. Table 3.2 summarizes the general characteristics of these friction surfaces and denotes that open-graded FC-5 mixtures must contain 100% accepted coarse aggregates. Open-graded friction courses are used in high-speed, multi-lane facilities to provide a higher level of macrotexture and dense-graded friction courses are used in all other state-owned facilities (Choubane, 2002).

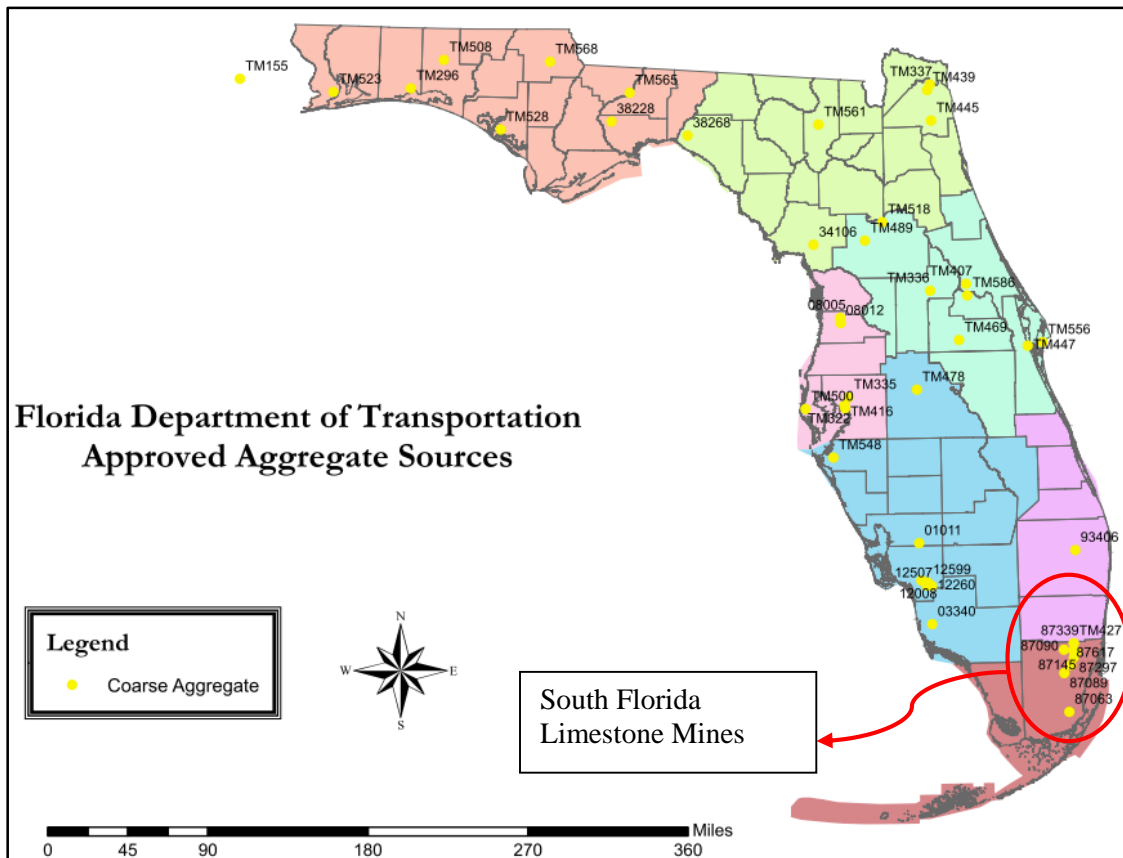


Figure 3.1 FDOT-approved coarse aggregate sources

Table 3.2 Common types of friction course in Florida

Open -graded friction course	Dense-graded friction course
Required on high speed multi-lane facilities. <ul style="list-style-type: none"> <li>Design Speed <math>\geq</math> 50 mph</li> </ul>	Required on all jobs with: <ul style="list-style-type: none"> <li>Design Speed <math>\geq</math> 35 mph, except rural 2-lane roads with 5-yr projected AADT of <math>\leq</math> 3,000</li> </ul>
FC-5 (3/4" to 7/8" thick)	FC-9.5 (1" thick) FC-12.5 (1 1/2" thick)
100% friction approved aggregate (No RAP) <ul style="list-style-type: none"> <li>Granite aggregate requires hydrated lime</li> </ul>	100% Oolitic limestone or 60% granite <ul style="list-style-type: none"> <li>If granite, then can contain 20% RAP, otherwise no RAP</li> </ul>
ARB-12 or PG76-22 depending on traffic level	ARB-5 or PG 76-22 depending on traffic level

After several meetings and conference calls with the FDOT office, nine different aggregate sources were selected for evaluation in this study (Table 3.3). Each aggregate type has been used in friction courses in Florida, except for HN717 which is not approved for friction course. Samples of the aggregate types were collected by FDOT State Materials Office (SMO) personnel over the entire state and then properly stored by the University of Florida.

Table 3.3 Aggregate types used in this study

Source Number	Material Type	Material Source	Aggregate ID	Application Status
1	Oolitic Limestone	Cemex	87090	Approved
2	Oolitic Limestone	Titan America, LLC	87145	Approved
3	Oolitic Limestone	White Rock Quarries	87339	Approved
4	Oolitic Limestone	SDI Quarry	87648	Approved
5	Granitic	Martin Marietta Materials	GA383	Approved
6	Granitic	Junction City Mining	GA553	Approved
7	Granitic	Martin Marietta Materials	NS315	Approved
8	Siliceous Wackestone	Hubbard Materials Co.	70693	Approved
9	Granitic	Honduran Aggregate	HN717	Unapproved

### 3.3 Field Sections

The main objective of this study was to evaluate the success of predicting aggregate type friction performance in the field, based on laboratory tests on virgin aggregates. Selection of field sections for friction performance evaluation is covered here.

Florida has a large road network, including varying road types, such as farm-to-market roads, interstates, state highways, and U.S. highways. The research team, in coordination with SMO Pavement Material Systems personnel, selected ten road sections suitable for evaluation and coring based on different parameters, including aggregate type, availability of skid data, road

classification, mixture type, availability of traffic data, and availability of construction history. These sections were located in different FDOT districts and the initial road sections were selected because they had the same aggregate type as those selected for aggregate study. It should be noted that both SDI Quarry (87648) and Honduran aggregates (HN717) were included for laboratory evaluation only, since there is a little or no construction history for these aggregates, therefore, friction performance of only seven of the nine aggregate types were evaluated in the field. For some aggregate types, multiple sections were selected for evaluating the effect of time and traffic on pavement texture. Table 3.4 summarizes the ten project locations identified for coring, along with the seven aggregate types used in their construction. The pavements used in these sections were between two and eleven years old.

Table 3.4 Selected road sections for this study

Site Number	County	Project ID	Straight Line MP	Lane Tested	Surface	Age	Aggregate type	Aggregate ID
1	Bradford	28010000	3.007 to 3.575	SBTL	FC-5	11	Limestone	87145
2	Alachua	26060000	0.000 to 1.254	NBTL	FC-5	7	Granite	GA553
3	Columbia	29180000	19.000 to 27.380	NBTL	FC-5M	7	Granite	GA553
4	Polk	16030000	3.055 to 5.415	NBTL	FC-5	8	Limestone	87339
5	Polk	16180000	2.890 to 6.334	NBTL	FC-5	4	Granite	GA383
6	Lee	12075000	27.273 to 34.138	NBTL	FC-5	7	Limestone	87339
7	Flagler	73010000	10.890 to 23.673	SBTL	FC-5M	5	Limestone	87090
8	Orange	75020000	7.169 to 7.298	SBTL	FC-5	<2	Wackestone	70693
9	Alachua	26050000	12.145 to 12.540	NBTL	FC-5	9	Limestone	87090
10	Alachua	26050000	14.380 to 15.285	NBTL	FC-5	9	Granite	NS315

Mix type was limited in this study to open-graded friction courses (FC-5 or FC-5M) in order to remove the effect of mix variables on skid performance analysis. Furthermore, open-graded friction course is constructed using 100% approved aggregates (no blended aggregates) and employed on high-speed, multi-lane facilities for which friction performance prediction is more critical. Gradation analysis of FC-5 mixtures reveals that around 50% of materials passed the 9.5 mm sieve and were retained on the 4.75 mm sieve, while around 20% of aggregates passed the 12.5 mm sieve and were retained on the 9.5 mm sieve (Table 3.5). Therefore, these two aggregate sizes were identified as two representative sizes for laboratory testing based on gradation analysis of typical open-graded friction courses in Florida.

Table 3.5 FC-5 gradation design range

3/4 inch	1/2 inch	3/8 inch	No. 4	No.8	No. 16	No.30	No.50	No.100	No.200
100	85-100	55-75	15-25	5-10	--	--	--	--	4-5

Five cores were taken every ten feet from the outside wheel path of the outer lane. Although skid testing is performed on the inside wheel path of the outer lane, considering the safety issues, it was reasonably assumed that both wheel paths experience the same polishing action. The most polishing action occurs in the outer lane because of high truck traffic in this lane. These cores were transferred to the laboratory and prepared for testing. The FDOT scheduled the maintenance of traffic. Figure 3.2 shows coring operation in Site No. 10.



Figure 3.2 Coring from Site No. 10

### 3.4 Testing Methods

As discussed above, it is well known that the existing sources of high quality aggregates are being rapidly depleted, and there is need for new acceptable aggregate sources that can ensure safety. For acceptance purposes, it must be determined whether new aggregate sources can provide an acceptable level of surface friction throughout the pavement service life. This determination should be based on aggregate characteristics that can be obtained from relatively short-term laboratory tests. In an attempt to find a solution, Masad (2009) and his colleagues at the Texas A&M University developed and used the AIMS to characterize aggregate polishing behavior, and establish its relationship to field skid resistance by considering variables such as traffic, mix gradation, and mix polishing resistance. In a similar effort, the FDOT seeks to identify an efficient protocol using AIMS along with other tools that can reliably pre-evaluate aggregates for pavement friction course application. In order to achieve this goal, a relation between AIMS measurements and field friction performance must be established.

Assuming that asphalt mixture friction performance is mainly a function of coarse aggregate frictional characteristics, virgin aggregate polishing resistance must be characterized. Among different testing methods and devices introduced in Chapter 2 for performing accelerated aggregate polishing, two of the most common are the British Wheel and Micro-Deval methods. The British Wheel method (AASHTO T 279) relies on preparing coupons of aggregate glued to a plate, and polishing these coupons using a wheel and abrasion material. This method is time consuming, as it takes nine hours to complete, in addition to the time and care involved in preparing the coupons. The coupons were designed for evaluation with the British Pendulum Tester—which does not provide a direct measure of microtexture—and are not readily suitable for microtexture measurements with AIMS.

The Micro-Deval method (AASHTO T 327) polishes aggregates through interaction among aggregates and between aggregates and steel balls when water is present. The post-polishing surface texture can be controlled through polishing time and number of revolutions. The test involves considerably less preparation and conditioning time and produces specimens that are readily suitable for microtexture measurements with AIMS. This test has been successfully used in combination with AIMS in the past as well. The Micro-Deval device but a modified version of the standard method used to polish virgin aggregates in the laboratory. The next section will present more details about this device and the applied method.

Relative resistance of aggregates to polishing is determined with AIMS by measuring microtexture before and after accelerated polishing in the laboratory. This method uses Micro-Deval to obtain changes in microtexture as a function of polishing time. This data is then used for analyzing the friction data obtained from FDOT databases and texture measurements conducted on field cores using AIMS for pavements produced with the same aggregate type. In

the current study, application of AIMS in evaluation of field cores comprises three procedures: a) microtexture measurement of core surfaces, b) macrotexture measurement of core surfaces, and c) microtexture measurement of coarse aggregates removed from core surfaces. This device and measurement technique will be explained later in this chapter.

### 3.4.1 Micro-Deval Test

Micro-Deval is a quick, reliable, and precise test that uses simple equipment, has good reproducibility of results both within and between laboratories, and has demonstrated correlation to field performance (Lang et al., 2007). This test is used to evaluate aggregate abrasion resistance and durability for use in pavements (Rogers et al., 2003). In Micro-Deval apparatus (Figure 3.3), aggregates interact with each other and with steel balls and water in a rotating steel container (Figure 3.4).



Figure 3.3 Micro-Deval apparatus



Figure 3.4 Aggregate and steel balls interaction mechanism in Micro-Deval apparatus (Masad et al., 2009)

This test was developed originally in France in the 1960s and has since been accepted as the European Union standard (Hanna et al., 2003; Rogers et al., 2003). In North America, the Micro-Deval test was first studied in Quebec in the 1980s, and the Ontario Ministry of Transportation conducted extensive research throughout the 1990s to refine and characterize the test (Lang et al., 2006). AASHTO adopted Micro-Deval as a standard test (AASHTO T327) in a 2005 report entitled Standard Test Method for Resistance of Coarse Aggregate to Degradation by Abrasion in the Micro-Deval Apparatus. Although many researchers and transportation agencies have reported good correlation between Micro-Deval and field performance, NCAT research revealed that these results are true for some but not all mineralogical aggregate types (Cooley and James, 2003; Lang et al., 2007).

In standard testing procedure, 1,500 grams of an aggregate sample in the range of 4.75 mm to 16 mm are washed and soaked in water for at least one hour prior to the test. The prepared aggregate sample is then placed in a steel container and loaded with 5,000 grams of steel balls and 2,000 ml of tap water. This material is subjected to 9,600 to 12,000 revolutions, and the sample weight loss (weight of aggregate that passed a #16 sieve size) is calculated and reported (Masad et al., 2009; Rangaraju et al., 2008).

According to AASHTO standard testing methods, in cases where the nominal maximum size of coarse aggregate is 12.5 mm or less, gradation and mass of the Micro-Deval sample must be as depicted in Table 3.6.

Table 3.6 Preparation of Micro-Deval samples based on standard (AASHTO T 327-09)

Passing	Retained	Mass
12.5 mm	9.5 mm	750 gr
9.5 mm	6.3 mm	375 gr
6.3 mm	4.75 mm	375 gr

Gradation analysis revealed that the open-graded friction course selected for this project is in this category; however, in this study, the Micro-Deval apparatus was used in a non-standard procedure. The 6.3 mm sieve—not a standard SUPERPAVE sieve—was removed from sample preparation and instead, the researchers used Table 3.7 for sample fabrication.

Table 3.7 Preparation of Micro-Deval samples in this project

Passing	Retained	Mass
12.5 mm	9.5 mm	750 gr
9.5 mm	4.75 mm	750 gr

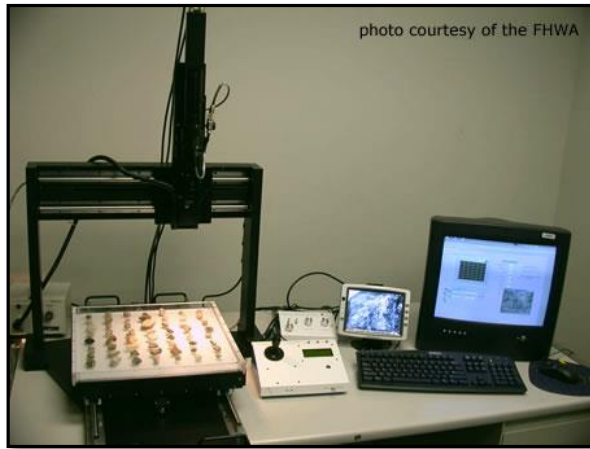
In spite of its removal in sample fabrication, this sieve was used after polishing to exclude polished or broken aggregates that fell from the upper sieve, as it is assumed that polishing action in Micro-Deval is dependent to the size of aggregates. This gradation of Micro-Deval sample is consistent with the selected representative sizes discussed earlier. In this project, Micro-Deval was used for polishing simulation only and weight loss was not measured.

The 1,500-gram Micro-Deval specimens were prepared according to Table 3.7 and subjected to polishing using the Micro-Deval apparatus. Samples were subjected to polishing intervals of 50, 105, and 180 minutes to evaluate the change in aggregate texture. These polishing intervals were selected based on work by Masad et al. (2009). Moreover, multiple aggregate samples used at different intervals rather than using a single test sample for all intervals. After polishing, aggregate samples were sieved, washed, and several 50-particle samples were selected through quartering. These samples were run in the AIMS unit to capture the change in texture versus polishing time.

### 3.4.2 Aggregate Imaging Measurement System (AIMS)

In the past decade, application of digital image processing to capture aggregate shape properties has been of interest to many researchers such as Masad, Khoudeir, Wang, and Elunai. AIMS—the focus of this project—is an automated aggregate imaging system that uses a scanning system and digital image processing to characterize aggregate shape characteristics including the angularity, form, and texture of coarse aggregates, as well as the form and angularity of fine aggregates (Masad et al., 2009). Masad (2003) and his colleagues at the University of Texas A&M designed the system to capture images with varying resolutions, fields of view, and lighting schemes. It is an integrated system composed of image acquisition hardware and computer software to run the system and analyze data (Pine Manual, 2010).

There are two versions of AIMS: 1) the prototype version, AIMS 1, and 2) the commercial version, AIMS 2 (Figure 3.5). The updated version has new hardware and was designed to provide manufacturability and convenience. AIMS 1 required the operator to place each coarse particle in accurate table positions at specific grid points, while AIMS 2 turntable trays simplify the material loading by providing grooves in the tray where the operator should place the particles. Current simplification efforts are attempting to eliminate the effect of ambient laboratory lighting through use of a black chamber; however, updating equipment in both lighting and camera performance resulted in texture output differences compared to AIMS 1 (Gates et al., 2011). In order to maintain the AIMS 1 texture scale, researchers applied a shift factor to the AIMS 2 data to address this scale shift; however, this normalization is questionable.



(a)



(b)

Figure 3.5 Aggregate Imaging Measurement System: (a) AIMS1 (b) AIMS2

For this method, a digital camera with a predefined zoom level is used to capture digital images of the aggregates. AIMS equipment is equipped with back-lighting and top-lighting units, the latter of which is used to capture gray images. Three measures of aggregate shape properties—Texture Index, Angularity Index, and Sphericity Index—are calculated based on these 2-D aggregate images (Masad et al., 2009).

In general, texture—the only aggregate shape characteristic of interest in this study—involves aggregate microtexture and mixture macrotexture. AIMS Texture Index, is calculated by application of Wavelet transformation on surface images. Wavelet theory offers a mathematical framework for multi-scale image texture analysis (Fletcher et al., 2002). Texture Index ranges from 0 to 1,000 with a smooth polished surface approaching a value of 0. Al-Rousan (2004) presented more details regarding analysis procedures.

AIMS 2 has the capability to scan the surface of pavement cores and characterize core surface at both the micro- and macro-texture levels. These scans include surface texture image analysis at several magnification levels, as well as a measuring height profile of the surface (Pine Manual, 2010). Masad and his colleagues have conducted the majority of AIMS application

research and have used AIMS in several projects. The researchers found that this test method is highly repeatable and reproducible. In an interlaboratory study (2011) involving 32 laboratories, Masad et al. demonstrated that AIMS 2 can provide objective and reproducible shape characterization of aggregates.

Specimen preparation for running AIMS includes three tasks:

**Virgin aggregates:** Research has identified representative aggregate sizes for microtexture measurement. Texture Index is sensitive to surface dust, so aggregates were washed using water and air-dried before testing. All aggregate samples were sieved and washed, and several 50-particle samples in the range of representative sizes selected by quartering, were run through the AIMS unit. It should be noted that each sample was tested three times and aggregates were repositioned for each test.

**Cores:** A slice measuring less than 35 mm—the maximum thickness in operation range of AIMS for scanning core surface—was obtained from the surface of a core. The researchers for this study found it more beneficial to use cores of 30 mm or less for evaluation with AIMS. Care was taken to keep the cutting face parallel to the pavement surface in order to reduce the effect of a non-level specimen on macrotexture measurement. Clay supports were used to level the specimen as much as possible prior to measurement; however, AIMS software has an option to make this adjustment automatically for measured data using a height normalization technique.

Core surfaces were washed and cleaned using brushes to remove contamination. Each core was rotated and scanned along each of four intersecting scan lines (Figure 3.6). The system scans the surface of the specimen five times and each scan capture images at different magnifications covering the entire core diameter. The first scan is at maximum magnification, when the height of the specimen is recorded at each image location in addition to the texture image. Each

magnification has a progressively larger field of view, which results in fewer images for each complete diameter scan than the previous scan. The number of texture images can be changed by changing the span and measurement interval. At the maximum magnification level (15.8X), 68 images obtained for 2 mm interval over a span of 136 mm for a 150 mm diameter core.

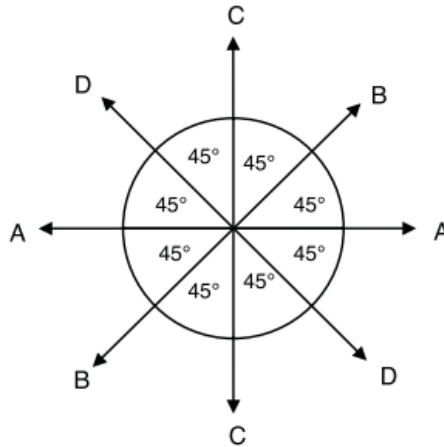


Figure 3.6 Core scanning directions

**Aggregates removed from cores:** Since only the top (exposed) aggregate surface in field pavements experiences polishing, it was very important to obtain aggregate from cores in such a way that the exposed surface was used for microtexture measurement in AIMS. The core slice was heated to a temperature that allowed the aggregate to be easily separated from the mixture. Aggregates in the range of representative sizes were removed from the core surface for microtexture measurement. The polished face of the removed aggregates was cleaned of dust, and these particles were marked according to their surface orientation. AIMS measurement on these particles was performed individually by manually operating the image acquisition hardware within the Machine Interface Window, which provides control of the various hardware functions and real-time camera images (Figure 3.7). Every setting was kept similar to the automated measurement and texture index was calculated using wavelet coefficients extracted from the data file. Clay supports were used for placing polished aggregate surfaces under the

camera in their original core position. This procedure made it possible to capture the polished aggregate surface that has been in contact with tire. Fifty particles were selected from three cores of each section and two cores were saved for future analysis.

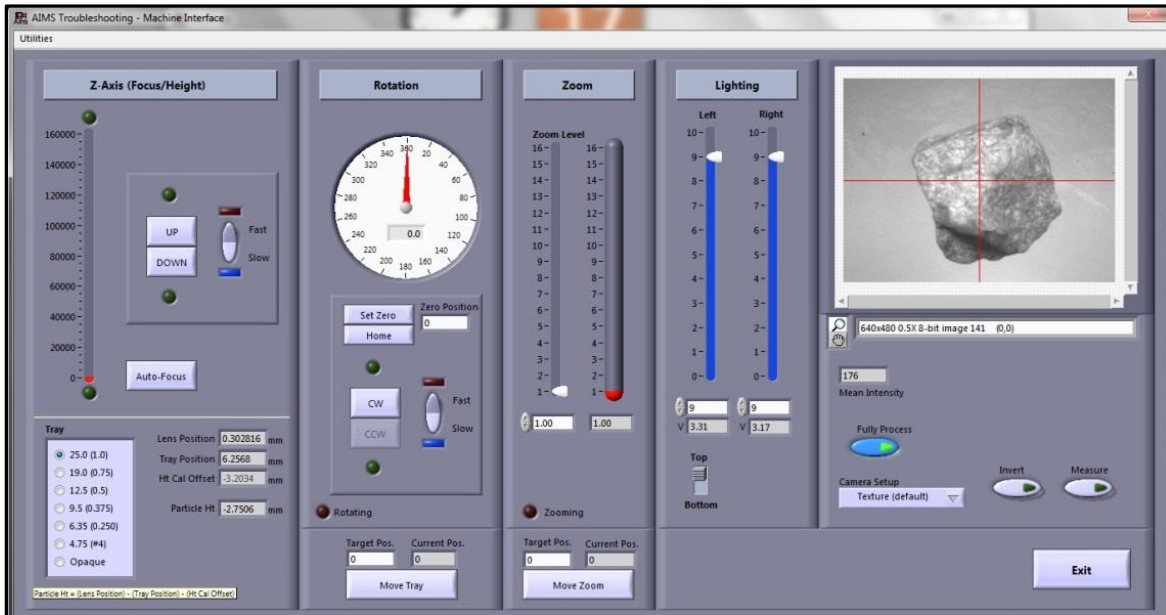


Figure 3.7 Machine interface window

## CHAPTER 4 RESULTS AND DATA ANALYSIS

### **4.1 Introduction**

Chapter 4 discusses AIMS measurement test results conducted on virgin and laboratory polished aggregates, core surfaces, and aggregates removed from cores. This chapter also analyzes skid resistance data for selected road sections to evaluate field friction performance. Finally, it analyzes aggregate characteristics measured by AIMS, along with the core measurements used to evaluate the potential relationships between these properties and skid resistance characteristics in the field.

### **4.2 Polishing Characteristics of Virgin Aggregates**

As previously discussed, the properties of aggregates, particularly coarse aggregates, greatly influence pavement skid resistance. Aggregates have different textures and polishing resistances due to varying mineralogy, formation, and crushing processes. Seven of the nine aggregate sources selected for evaluation in this study have been used in friction course in Florida.

Figure 4.1 depicts the average weight loss percentages in the Los Angeles abrasion test—conducted in the original mines of selected aggregates—which provides a relative indication of aggregate toughness during transport and handling. As expected, limestone aggregates exhibited significantly higher weight loss or lower abrasion resistance than other aggregates in this study.

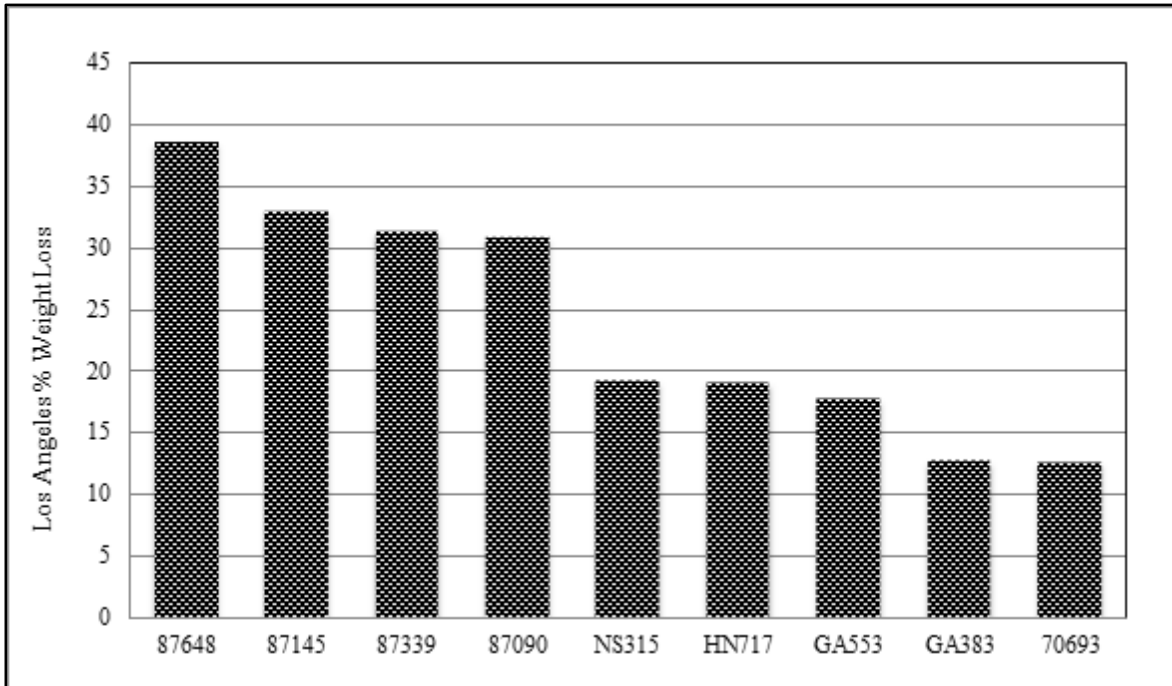


Figure 4.1 LA abrasion test results of aggregates study

The researchers for this study performed a total of 216 AIMS tests on virgin and laboratory polished aggregate samples (each sample included 50 particles) for two ranges of representative aggregate sizes, and each size measured at a different magnification level. The texture index results presented herein represent the average values obtained from the two size ranges and magnification levels. Table 4.1 presents a summary of the texture index and angularity index before and after polishing in Micro-Deval. Figures A.1 to A.18 in Appendix A also show the texture distribution for each size range of the nine aggregate types measured using AIMS. As discussed in Chapter 3, each sample was run three times to gain a true statistical representative, and aggregates were repositioned each time.

Table 4.1 Average texture index and angularity index before and after polishing

<b>Texture Index</b>									
	<b>GA383</b>	<b>GA553</b>	<b>70693</b>	<b>NS315</b>	<b>HN717</b>	<b>87339</b>	<b>87648</b>	<b>87090</b>	<b>87145</b>
0	605.9	518.8	457.0	340.3	306.1	178.3	160.5	135.7	147.6
50 min	582.5	576.6	410.2	298.1	285.2	145.0	147.2	134.3	124.3
105 min	579.6	534.2	330.5	288.6	242.5	147.4	125.8	131.1	118.0
180 min	538.4	510.0	318.6	280.4	247.5	143.5	117.5	114.1	111.4
Loss	67.5	8.8	138.4	59.9	58.6	34.8	43.0	21.6	36.3
Loss (%)	11.1	1.7	30.3	17.6	19.1	19.5	26.8	15.9	24.6
<b>Angularity Index</b>									
	<b>NS315</b>	<b>70693</b>	<b>GA383</b>	<b>GA553</b>	<b>HN717</b>	<b>87648</b>	<b>87090</b>	<b>87339</b>	<b>87145</b>
0	2931.7	2852.3	2754.2	2761.9	2478.1	2950.8	3149.0	3182.2	2991.0
50 min	2623.0	2628.6	2540.8	2372.7	1779.5	2137.6	2158.4	1911.2	2065.6
105 min	2549.6	2278.7	2272.6	2147.7	1552.3	1849.4	1948.1	1913.9	1919.8
180 min	2451.0	2355.3	2301.8	1993.4	1710.3	1660.5	1532.3	1485.1	1461.1
Loss	480.8	497.0	452.4	768.5	767.9	1290.3	1616.7	1697.1	1529.9
Loss (%)	16.4	17.4	16.4	27.8	31.0	43.7	51.3	53.3	51.1

Figure 4.2 graphs the change of texture index as a function of polishing time in the Micro-Deval for all nine aggregate types. For eight of the nine aggregates, texture index decreased as polishing time in Micro-Deval increased. The only exception, GA553, showed an initial increase followed by a decline in texture index. Other than this initial difference, GA553 and GA383 (both Georgia granites) exhibited similar magnitude and texture index trends as a function of polishing time in Micro-Deval. The different production processes for the two aggregates possibly caused the difference in initial texture index values. The initial increase in texture index for GA553 may have been caused by breakage early in the Micro-Deval conditioning process, which exposed rougher surfaces that were initially present in the GA383 aggregate immediately

after production. It should be noted that after this initial adjustment in texture index in Micro-Deval, the two granites subsequently polished at the same rate.

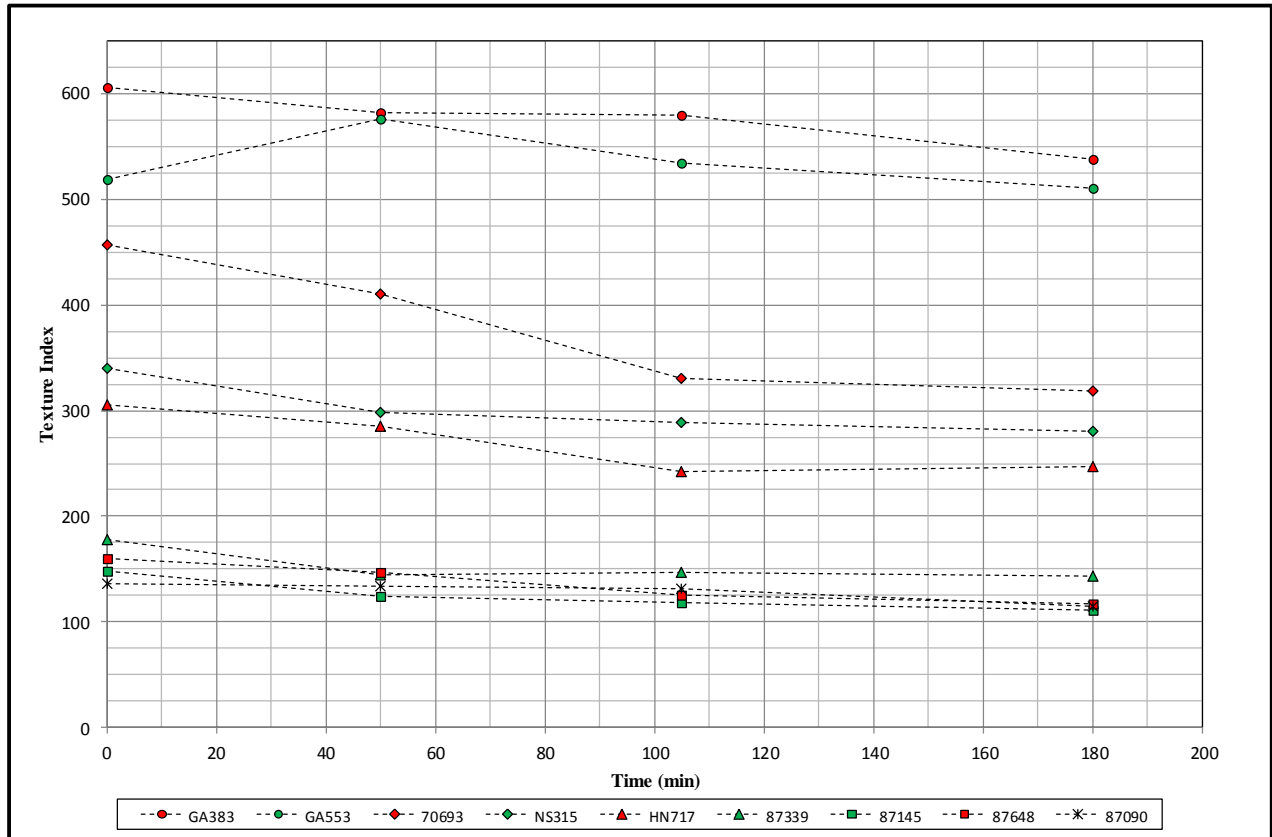


Figure 4.2 Change of texture index as a function of polishing time in the Micro-Deval

It is clear from Figure 4.3 that the three granite aggregates (GA383, GA553, NS315) and the wackestone aggregate type (70693), exhibited higher texture index as measured by AIMS (both initially and after Micro-Deval conditioning), than the four limestone aggregates (87339, 87648, 87090, and 87145). The Honduran aggregate had a similar AIMS texture index, as the granite with the lowest texture index. All aggregates, with the exception of granite 70693, exhibited relatively modest reductions in texture index after conditioning with Micro-Deval.

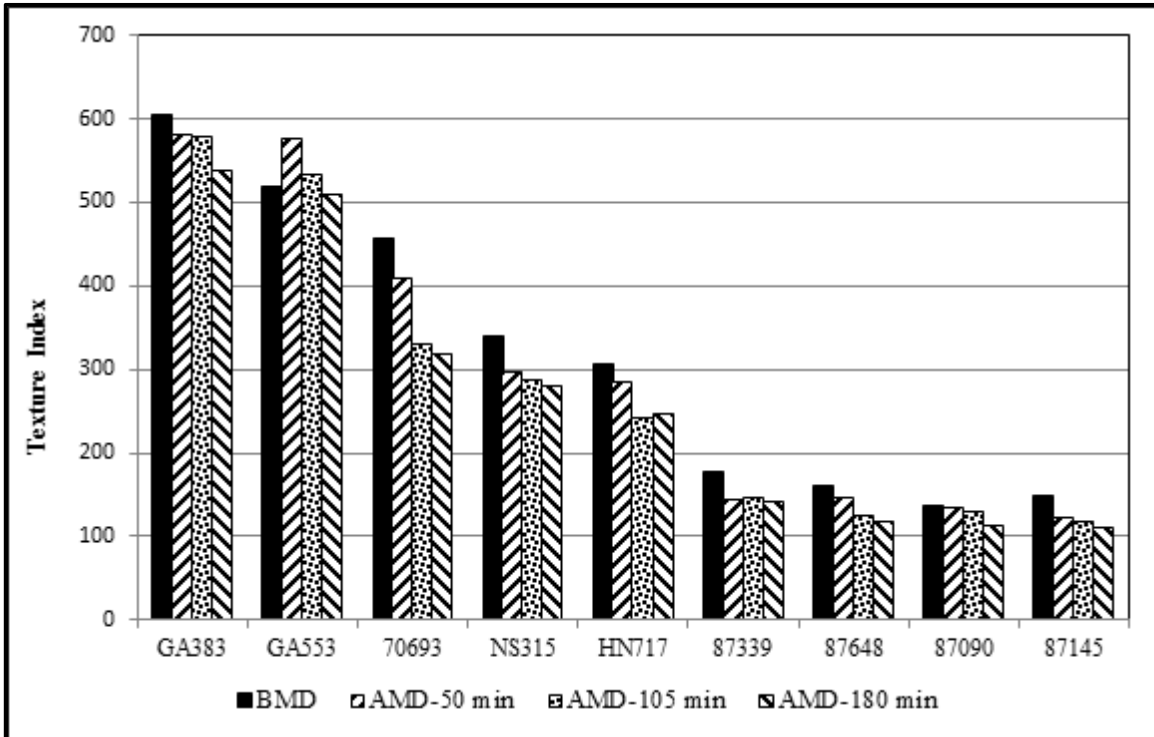


Figure 4.3 Comparison of aggregate types based on their texture index before polishing in Micro-Deval (BMD), and after polishing in Micro-Deval (AMD) at different polishing time

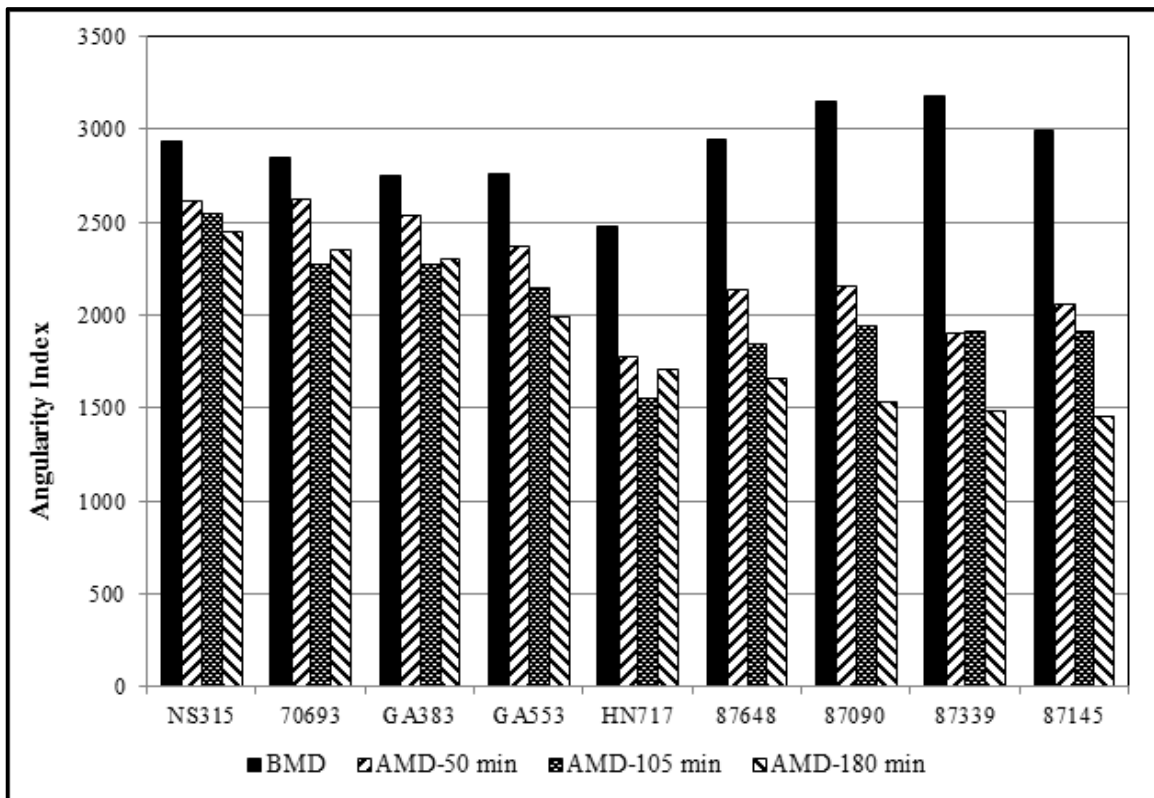


Figure 4.4 Comparison of aggregate types based on their angularity index before polishing in Micro-Deval (BMD), and after polishing in Micro-Deval (AMD) at different polishing time

Granite aggregates had slightly lower angularity than the limestone aggregates prior to conditioning with Micro-Deval, while the Honduran aggregate exhibited the lowest initial angularity (Figure 4.4). Micro-Deval conditioning resulted in a much greater reduction in angularity for limestone aggregates than for granite aggregates, while the Honduran aggregate fell somewhere between. These results were consistent with expectations, as limestone has lower resistance to breakdown than granite.

In any case, it seems that AIMS is capable of quantifying the change in texture due to polishing in the Micro-Deval test; however, reduction in angularity appeared to more clearly distinguish between aggregates resistance to Micro-Deval conditioning than reduction in texture index. The researchers analyzed field cores and aggregates recovered from field cores in attempts to interpret the meaning of the AIMS texture index measurements as related to microtexture and friction.

### **4.3 Core Analysis**

As outlined in Chapter 3, this study used five cores taken from each road section, three of which were used for AIMS testing, while the other two were saved for additional testing if needed. Each core was scanned by AIMS in four intersecting directions to determine macrottexture and microtexture. In addition, aggregates in the range of representative sizes were removed from cores and scanned individually for microtexture analysis. A total of 120 core surface scans were obtained from 30 core samples, and more than 500 individual aggregates were scanned.

#### **4.3.1 Macrottexture Measurement**

Chapter 3 explained the procedure used to level the surface for scanning. In addition, AIMS software applies a height normalization technique to measured data using a simple linear

regression to find a zero mean profile in which the area above the reference height is equal to the area below it (Rezaei et al., 2011). Figure 4.5 graphs the measured (M) and normalized (N) profile for sample 2 taken from Site No. 10 at four directions. The consistency of the profiles means that the measurements were taken on a level surface, indicating that the procedure designed to remove the scanning line slope was successful. However, the normalized heights were used in macrotexture analysis to ensure zero surface slope. Figures B.1 to B.10 in Appendix B depict the measured profiles of all samples from the ten road sections.

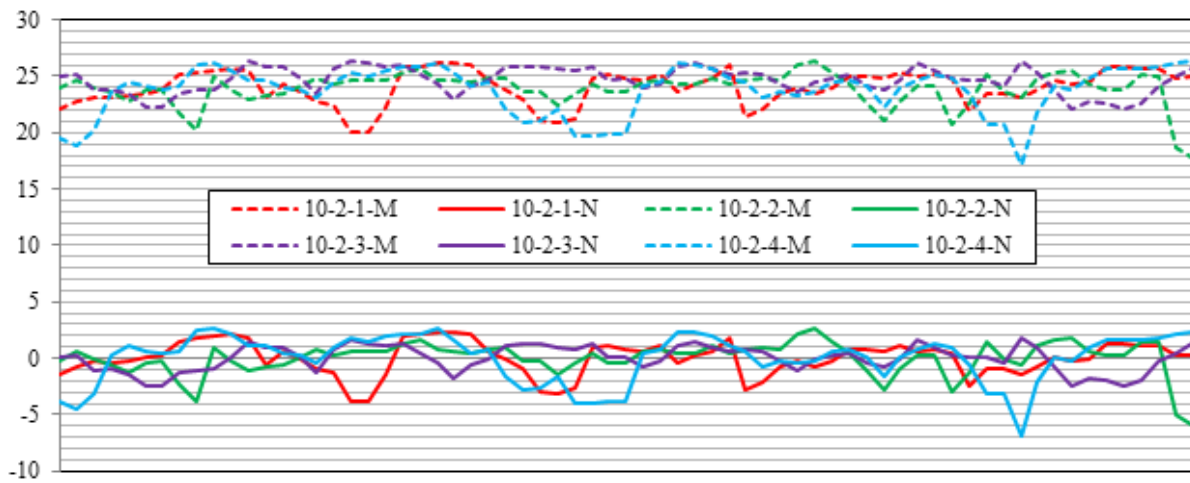


Figure 4.5 Measured and normalized core surface profiles for Sample 2

The height measurements along the scan line produce the profile that was analyzed to determine statistical parameters such as Mean Profile Depth (MPD) and Root Mean Square (RMS). MPD was calculated based on ASTM E 1845-09. The scan line profiles were analyzed at three segment lengths: 50 mm, 100 mm, and 134 mm. The highest peak in each half-segment was determined, and the average of those two heights equals the mean segment depth (Figure 4.6). The average of the mean segment depths for all cores of a road section was reported as the MPD for that road section.

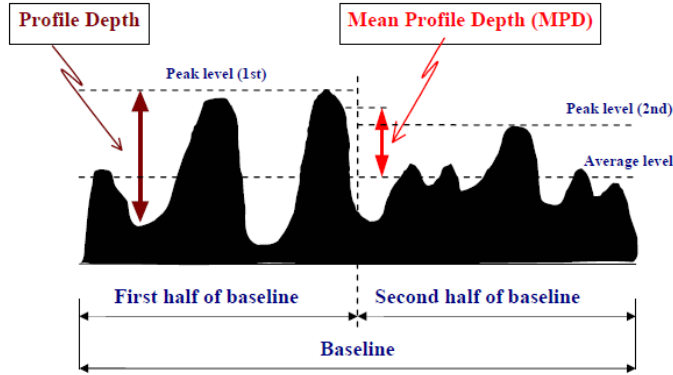


Figure 4.6 Mean profile depth calculations (ASTM E 1845-09)

Table 4.2 summarizes MPD for all road sections based on the three segment lengths. As expected, MPD decreased as analysis length decreased (Figure 4.7). No absolute MPD value for pavement surfaces is available for use as a reference to evaluate the performance of a laboratory test such as AIMS. Statistical parameters such as MPD are highly dependent on analysis length and testing equipment.

Table 4.2 Average MPD values measured by AIMS

Site #	Aggregate ID	Pavement Age	MPD		
			AIMS-134 mm	AIMS-100 mm	AIMS-50 mm
1	87145	11	1.352	1.255	1.087
2	GA553	7	1.678	1.663	1.435
3	GA553	7	2.164	2.086	1.695
4	87339	8	1.813	1.702	1.399
5	GA383	4	1.393	1.290	1.073
6	87339	7	2.405	2.401	1.903
7	87090	5	1.855	1.677	1.432
8	70693	<2	1.582	1.526	1.221
9	87090	9	1.167	1.165	1.007
10	NS315	9	2.171	1.772	1.587

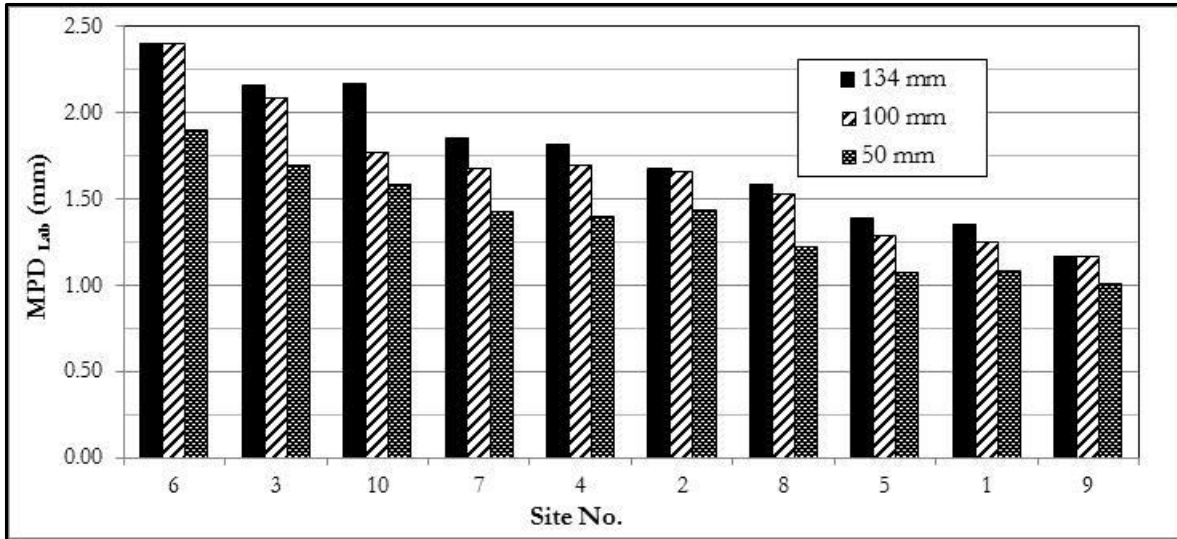


Figure 4.7 AIMS MPD for different road sections at different segment lengths

CTMeter MPD values measured in the field were available in the FDOT database for five of the selected road sections. Although these measurements were conducted one year before coring, the data was useful for comparing CTMeter MPD with AIMS MPD at different segment lengths. The analysis revealed that, for very smooth surfaces with low macrotexture (MPD around 1.0 mm), there was a relatively good correlation between average CTMeter and AIMS MPD values at a 100 mm segment length; however, as macrotexture increased, this correlation decreased (Figure 4.8).

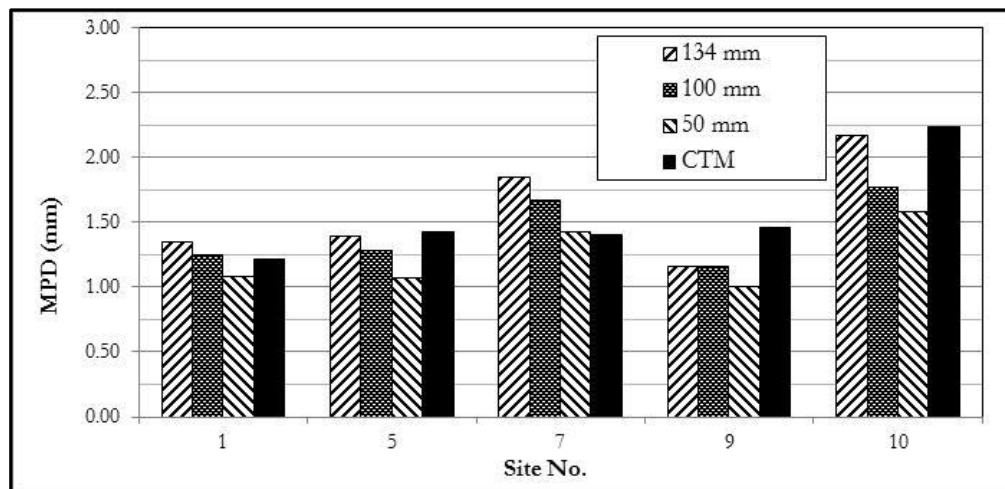


Figure 4.8 AIMS and CTMeter MPD values for five sections

In addition to MPD, RMS is another statistical parameter that represents the dispersion of measured data points from a reference line. The RMS equation is as follows, where  $h_i$  is the height of each measurement after slope adjustment and  $n$  is the total number of measurements ( $n=68$  in this study) (Rezaei, 2012):

$$RMS = \sqrt{\frac{\sum_{i=1}^n h_i^2}{n}}$$

Table 4.3 lists the average RMS for measured cores, and Figure 4.9 sorts analyzed surfaces based on this parameter, which are consistent with the AIMS MPD rankings depicted in Figure 4.7.

Table 4.3 Average RMS values measured by AIMS

Site #	Aggregate ID	Pavement Age	RMS
1	87145	11	0.958
2	GA553	7	1.163
3	GA553	7	1.606
4	87339	8	1.311
5	GA383	4	1.025
6	87339	7	1.789
7	87090	5	1.372
8	70693	<2	1.155
9	87090	9	0.965
10	NS315	9	1.428

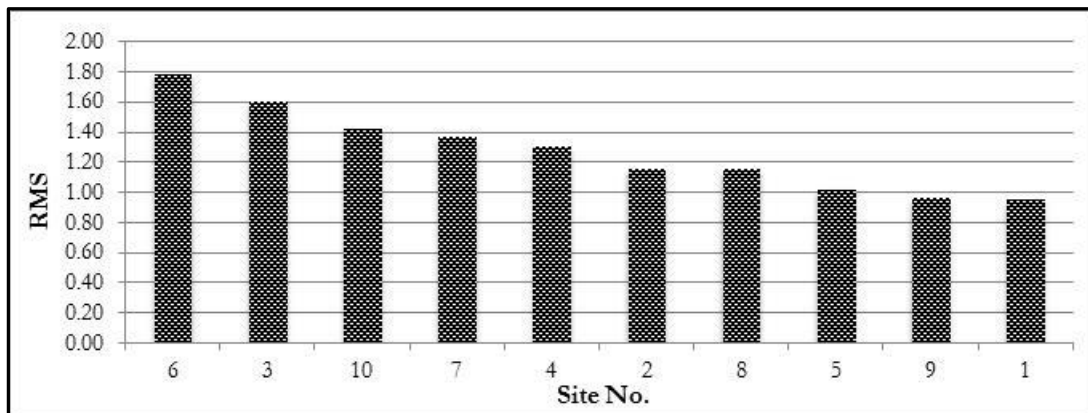


Figure 4.9 Studying road sections sorted based on AIMS RMS value

It should be noted that increase in macrotexture may result from negative texture and cavities caused by loss of surface aggregate or binder. This occurred in sections 3 and 6, which were located on I-75.

### 4.3.2 Microtexture Measurement

**Core surface scan:** As discussed earlier in this report, AIMS captures digital images from core surfaces at five magnification levels (Figure 4.10).

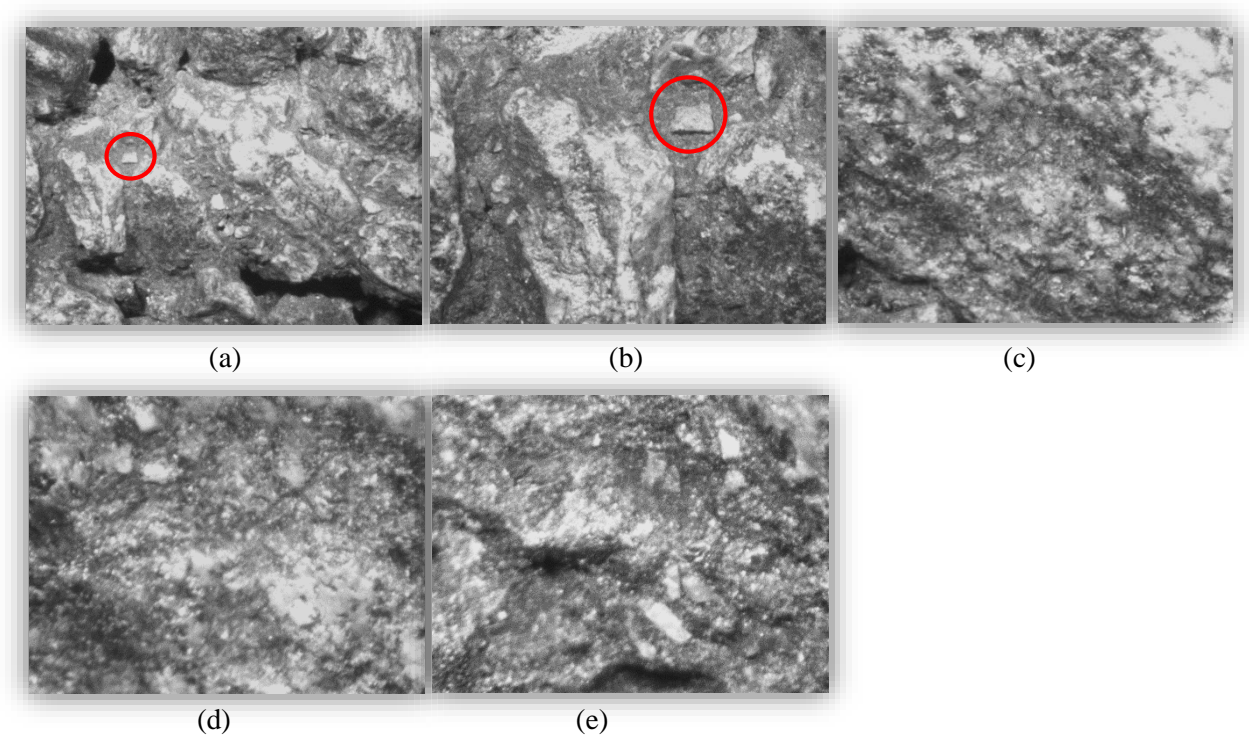


Figure 4.10 Captured images from a core at five magnification levels: a) minimum magnification level (1.2X), b) 3.13X corresponding to 19 mm particle scan, c) 6.27X corresponding to 9.5 mm particle scan, d) 12.6X corresponding to 4.75 mm particle scan, and e) maximum magnification level (15.8X)

Each magnification used has a progressively larger field of view. Consequently, for each complete diameter scan, fewer images are acquired than for the previous scan (Pine manual, 2010). Magnification levels 12.6X and 15.8X were selected for analysis, as adequate amounts of images (55 and 68, respectively) were available at these levels to be statistically representative.

In addition, core surfaces were non-uniform when compared to individual aggregate surfaces and the probability that texture index would be affected increased at lower magnification levels. Table 4.5 summarizes the average texture index values obtained from core surface scans of all road sections.

Table 4.4 Average texture index values obtained from core surface analysis

Site #	Aggregate ID	Pavement Age	Texture Index	
			12.6X	15.8X
1	87145	11	525.9	438.2
2	GA553	7	570.0	516.3
3	GA553	7	510.2	464.3
4	87339	8	498.4	423.5
5	GA383	4	481.5	417.3
6	87339	7	491.6	419.1
7	87090	5	490.1	409.6
8	70693	<2	453.2	423.7
9	87090	9	563.2	478.9
10	NS315	9	532.3	479.1

These texture index values were unexpected, as virgin aggregate scan values indicated that microtexture would decrease after polishing within several years of service. Computer software was developed to identify images that corresponded to each measurement in order to visually check the distribution of texture index and images. Figure 4.11 illustrates the distribution of texture index along a single scan line of a core at 12.6X magnification level, plotted from highest to lowest value. The figure includes corresponding images of the locations from which the highest and lowest reasonable texture index values were obtained.

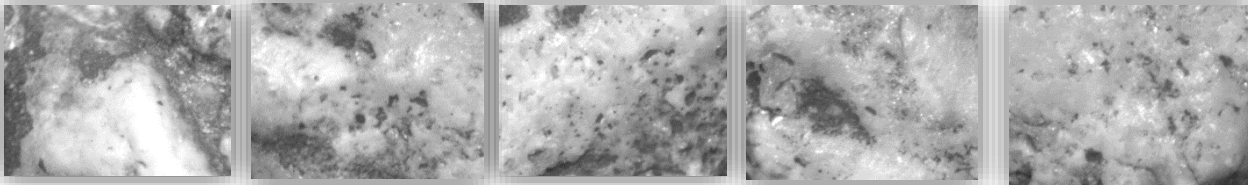
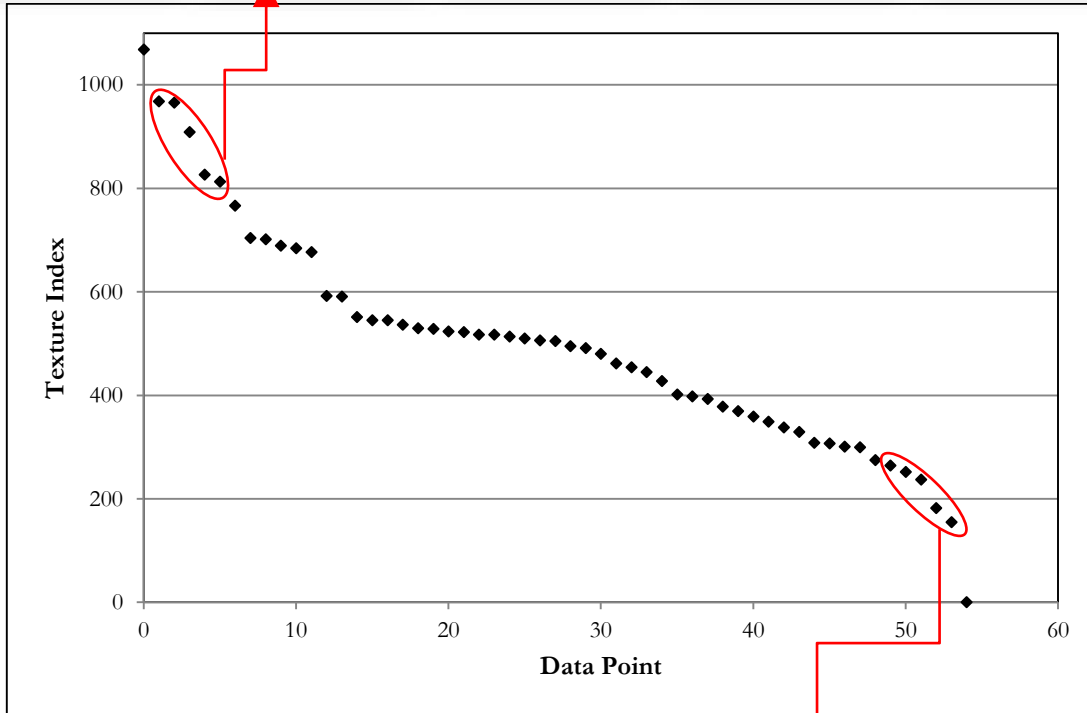
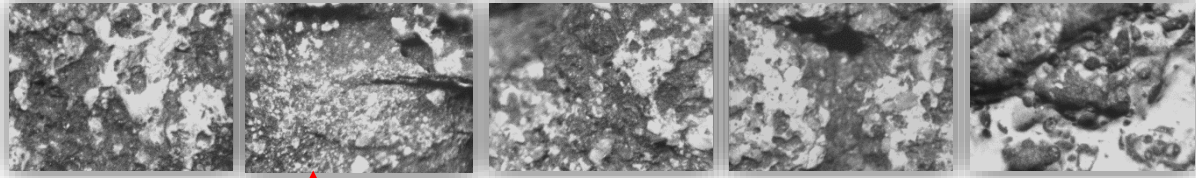


Figure 4.11 Distribution of texture index for core 5-4-A (Site No. 5, sample 4, and direction A)

The researchers performed this procedure on all cores, visually evaluated all images several times, and compared the texture index of these images with each other. The images reveal that the highest values were obtained from areas with greater color variations, while the lower values were obtained from areas with only polished aggregate surfaces and were in the range of texture index values obtained from aggregates alone. These observations indicate that color variation may affect texture index, even in the evaluation of virgin aggregates.

**Removed aggregates:** As described in Chapter 3, the researchers used Machine Interface Window to manually capture the image of aggregates and texture index parameter individually calculated for all removed aggregates. Table 4.5 presents the average measured texture index of removed aggregates at two magnification levels (12.6X and 15.8X). Lower magnification levels were not selected, as the field of view was usually larger than the aggregate polished area.

Table 4.5 Average texture index values of individual aggregates obtained from cores

Site #	Aggregate ID	Pavement Age	Texture Index	
			12.6X	15.8X
1	87145	11	339.2	265.1
2	GA553	7	441.8	394.9
3	GA553	7	382.6	338.9
4	87339	8	310.6	257.7
5	GA383	4	290.2	242.5
6	87339	7	307.0	247.2
7	87090	5	316.4	252.6
8	70693	<2	298.2	288.8
9	87090	9	347.3	286.7
10	NS315	9	575.1	534.8

Except for NS315, average texture index measured on individual aggregates was less than texture index obtained from core surface analysis. This can be attributed to the fact that, instead of scanning of the core surface with a random variability, measurements were conducted on the polished area of removed aggregates.

Figure 4.12 compares the average texture index values obtained at 12.6X magnification from 1) virgin aggregates before polishing (BMD), 2) core surfaces, 3) removed aggregates from cores, and 4) 180 minute Micro-Deval polished virgin aggregates (AMD-180min). It was expected that average texture index values obtained from scanning core surfaces and removed aggregates from cores lay somewhere between unpolished and highly polished virgin aggregates, but the results

were not consistent with this expectation. The relative average texture index of these four types of measurement was highly dependent on aggregate type. Analysis of this inconsistency resulted in important findings that can affect general acceptance of AIMS application in aggregate classification based on microtexture analysis.

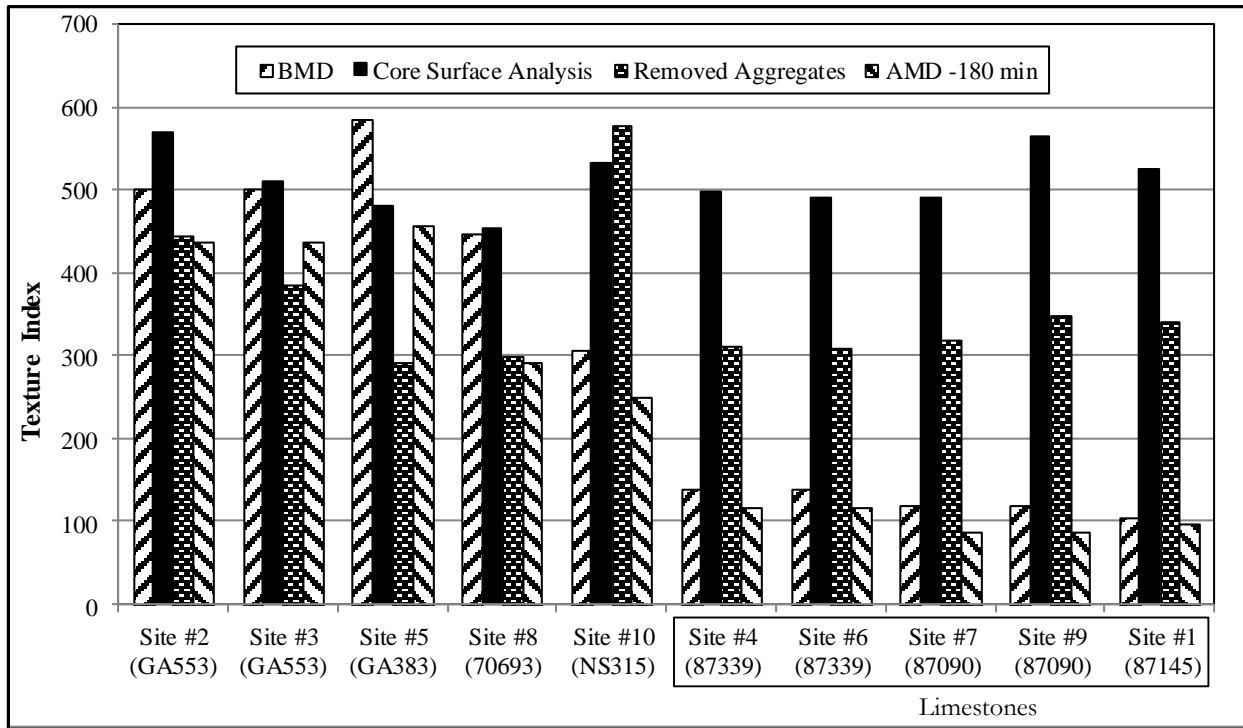


Figure 4.12 Average texture index values obtained from virgin aggregates and field cores at 12.6X magnification level

Figures C.1 to C.7 in Appendix C show the texture index distributions of polished aggregate, core surfaces, and removed aggregates for all road sections. The texture index distribution of removed aggregates and the corresponding images were used in this analysis to visually evaluate the relationship between texture index and actual microtexture. The researchers in this study found that high color variation of the granitic aggregates was responsible for the high texture index, which did not necessarily mean high levels of microtexture. The images in Figure 4.13 depict GA553 aggregates after 180 minutes polishing in Micro-Deval. This large range of texture index was unexpected—despite the fact that all aggregates were highly polished and even

considering non-uniform polishing effect—and could most likely be attributed to the effect of color variation in aggregate surface.

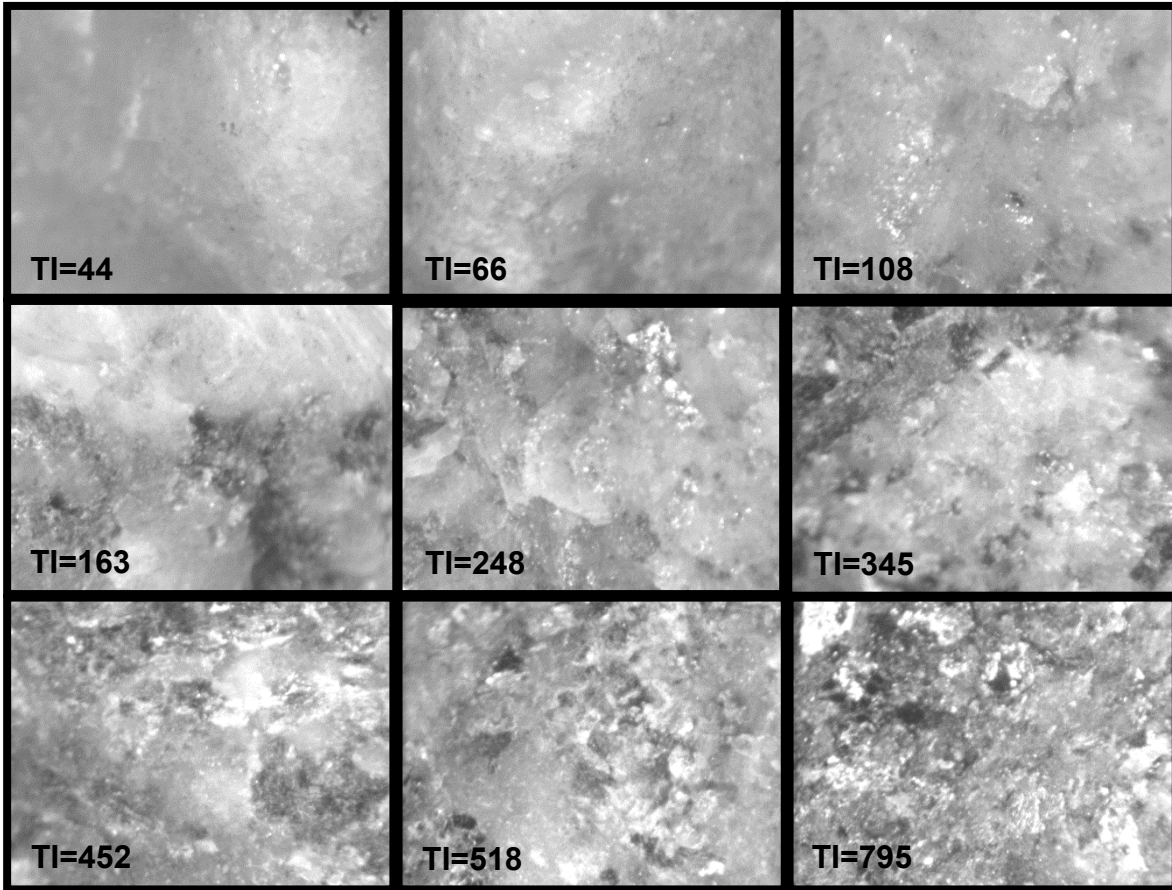


Figure 4.13 granitic aggregate (GA553) images and corresponding texture index values after 180 minutes polishing

Conversely, the low color variation in limestone aggregates resulted in lower texture index values. Figure 4.14 comprises limestone aggregate (87339) images and corresponding texture index values after 180 minutes polishing in Micro-Deval. Clearly, the range of texture index values in these images with relatively uniform color is significantly less than this range in granitic aggregates.

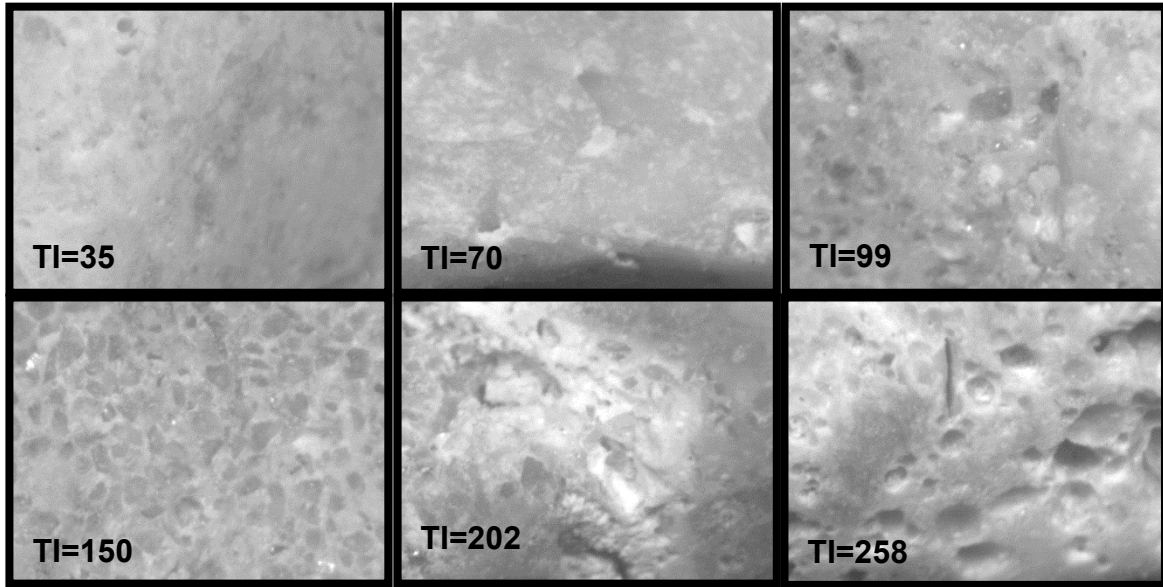


Figure 4.14 Limestone aggregate (87339) images and corresponding texture index values after 180 minutes polishing

Furthermore, in the case of aggregates removed from cores, the residual asphalt binder spotting on the surface of the aggregates resulted in increased texture index, which was more apparent in light limestone aggregates (Figure 4.15).

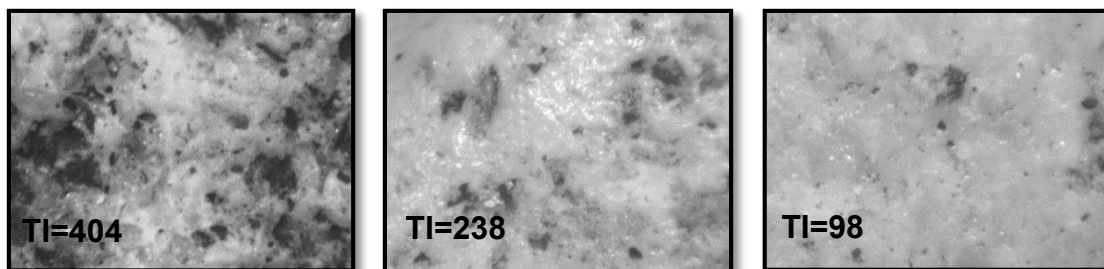


Figure 4.15 Texture index values of three individual aggregates obtained from Site No. 6 constructed using limestone aggregate (87339)

#### 4.4 Skid Resistance and its Relationship to Aggregate and Pavement Texture

FDOT runs friction testing on all newly constructed pavement surfaces, overlays, hazard location spots, re-test locations where the initial FN40R is found to be less than 34, and special requests, including research test sections, milled surfaces, or bridge decks (Jackson et al., 2002). Regular friction testing of pavements is performed every three years. In four-lane and multi-lane

roadways, the center of the left wheel path of the traffic lane is tested in both directions, while testing is conducted only on one lane for two-lane roadways, unless otherwise requested (Jackson et al., 2002).

Friction test data and traffic information was extracted from the FDOT database for the road sections selected for this study. Figure 4.16 illustrates the variation of friction numbers over time for all road sections. In general, the measured skid number progressively decreased as traffic increased. Less variation occurred after several years of traffic loading in pavement approaching terminal skid condition, which was attributed to the terminal state of aggregate texture. Table 4.6 presents traffic data for the studied roads. In traffic calculations, it was assumed that the number of vehicles in both directions was the same and all vehicle types induced the same polishing effect.

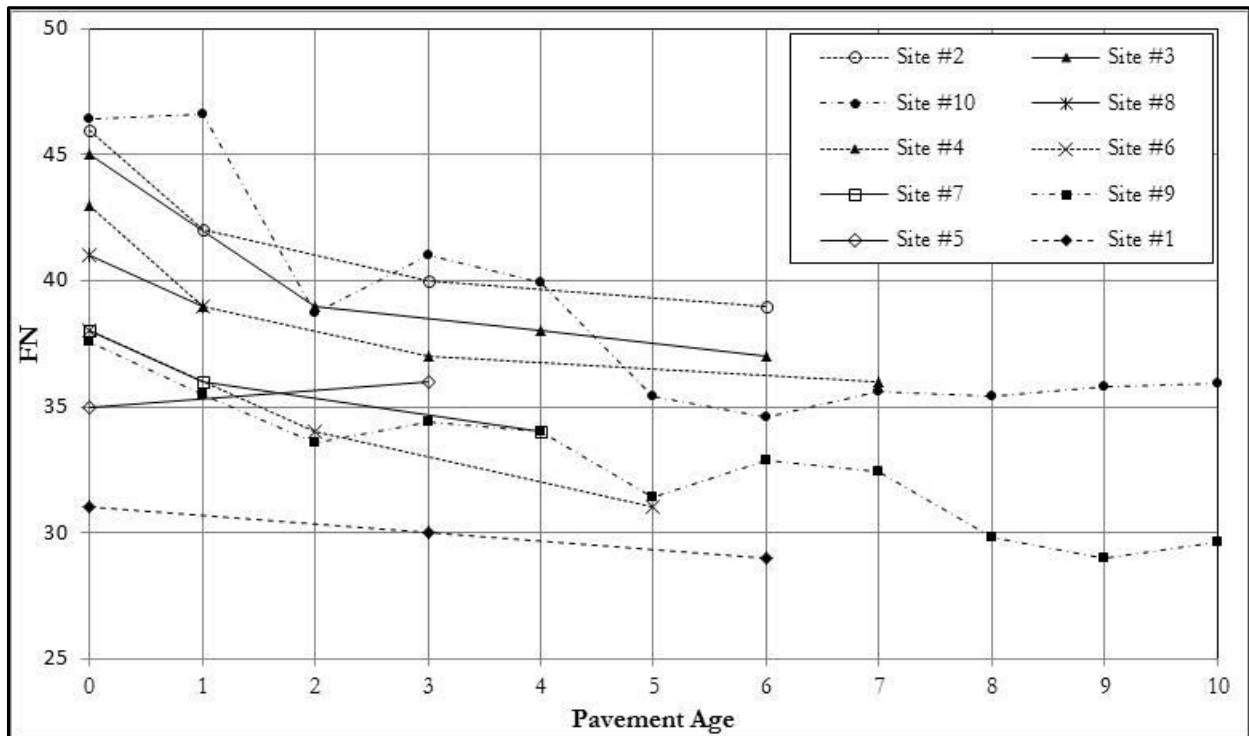


Figure 4.16 Friction number variations for all road sections

Table 4.6 Traffic data for all road sections

Site #	Aggregate ID	Pavement Age	AADT	Cumulative One-way Traffic (till 2010)
1	87145	11	14,778	48,545,000
2	GA553	7	5,050	11,059,500
3	GA553	7	22,956	50,272,545
4	87339	8	6,429	16,425,000
5	GA383	4	15,375	22,447,500
6	87339	7	28,667	62,870,000
7	87090	5	8,240	15,038,000
8	70693	<2	5,000	2,791,800
9	87090	9	5,032	16,640,864
10	NS315	9	5,032	16,640,864

This study limited mix type to open-graded friction course to isolate the effects of aggregate type and traffic level. To evaluate the effect of traffic and field polishing on friction, the researchers selected two road sections of the same age and with the same aggregate type (4 and 6 for limestone, 2 and 3 for granitic), but significantly different traffic volumes. The rate of loss in skid resistance clearly reflected the effect of polishing rate in these sections (Figure 4.16). As the polishing rate increased, friction numbers decreased.

Sections 7 and 9 were both constructed using limestone. In this case, the traffic level was low, the difference in polishing rate was not significant, and both had very similar friction performance. These results indicate that pavements with the same aggregate type and low polishing rates have relatively similar friction numbers.

Annual measurements from Sections 9 and 10 have revealed reasonable friction trends. Measured friction data for Sections 5 and 8 were insufficient, but they were the best available for field evaluation of these aggregate types.

In order to study the effect of aggregate type, the researchers recorded friction numbers at a specific high traffic level. This level was selected to ensure aggregates were in their terminal state of texture, and predicted using curves applied to friction numbers versus time data. Figure 4.17 presents the friction numbers, plotted from high to low, of all road sections, excluding sections 5 and 8.

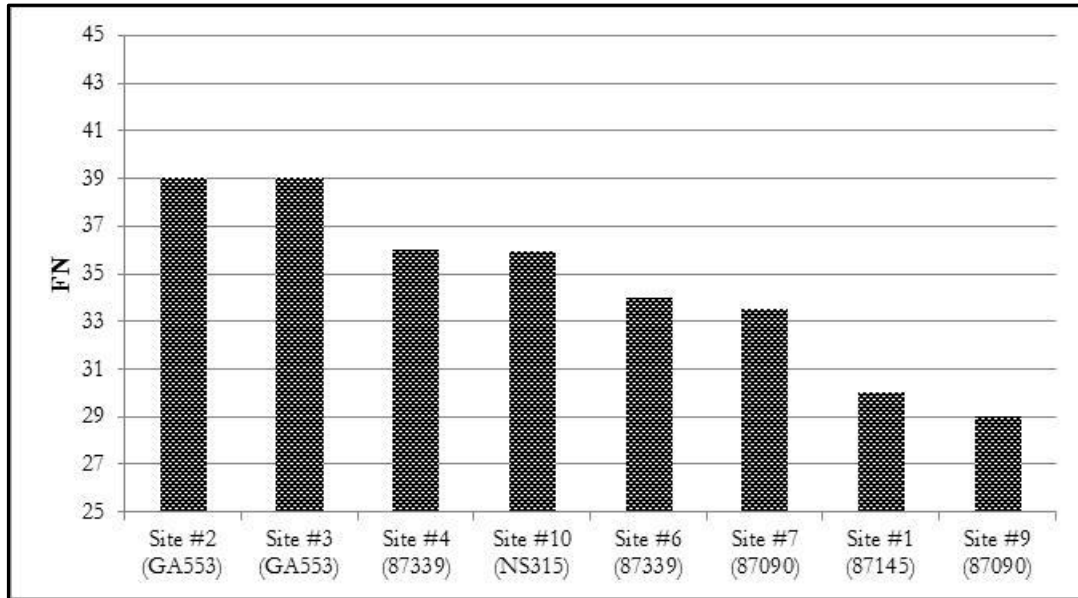


Figure 4.17 Friction number at a specific traffic level

In general, granitic aggregates have higher friction numbers than limestone aggregates. Site No. 4 was an exception to this rule, as it used limestone aggregate, yet had better friction performance than NS315, which used granitic aggregate. These results verify that the same aggregate type does not always yield consistent skid resistance.

As expected, research indicates no direct relationship between friction numbers and texture index obtained from virgin aggregates, surface scanning of cores, and aggregates removed from the cores. Data analysis revealed that texture index, as a representation of microtexture, is not a reliable parameter.

Figure 4.18 illustrates the relationship between measured skid numbers and macrotexture statistical parameters, MPD and RMS, as measured by AIMS. The high scatter of the results indicates that there is no direct relationship between these parameters and friction numbers.

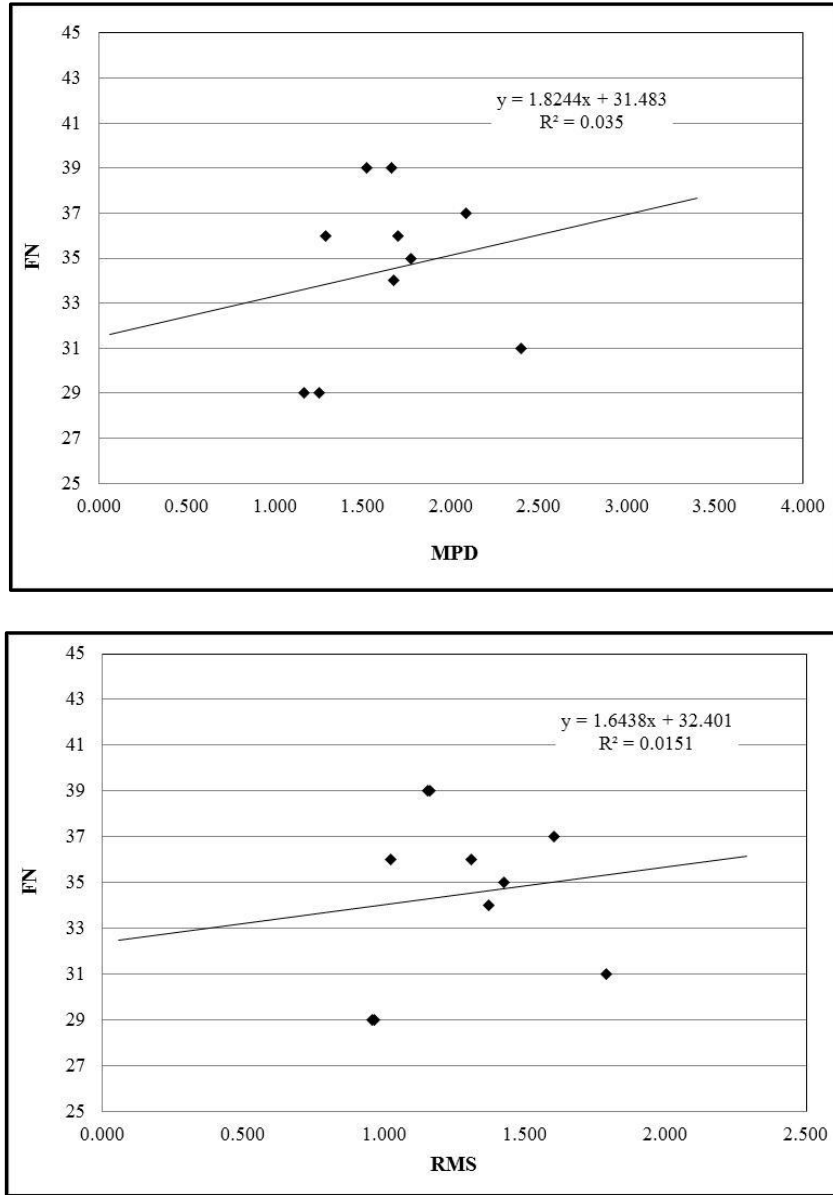


Figure 4.18 The relationship between friction number and macrotexture statistical parameters

## CHAPTER 5 CLOSURE

### 5.1 Summary and Findings

This study was conducted to identify and evaluate AIMS capability in the pre-evaluation of aggregates for use in friction course. For purposes of this study, frictional characteristics of different aggregate types were measured and analyzed. Several field sections constructed using the same aggregate types were evaluated in terms of macrotexture and microtexture. Testing results were evaluated to explore correlation with pavement friction field performance.

Findings associated with the objectives of this study are summarized as follows:

- For the range of aggregates considered in this study, it appears color variation in the aggregate surface had an overwhelming effect on the texture index measured by AIMS.
- For any particular aggregate type, the reduction in texture index measured by AIMS appears to capture the effects of conditioning with Micro-Deval for both granitic and limestone aggregates. However, regardless of which aggregate type was subjected to polishing, the percent of loss in texture index was relatively similar, and did not distinguish differences between the aggregates.
- To date, the capability of AIMS to capture true microtexture has not been evaluated using topographic data acquisition systems. In the other words, there is no evidence that texture index measured by AIMS is correlated with surface micro-roughness.

- It is well-known that skid resistance is affected by pavement texture at all length scales, ranging from micro to macro-scale. AIMS can measure texture in only a few length scales, which restricts the amount of possible information which can be collected from aggregate surface.
- There is no correlation between skid numbers observed in the field with statistical parameters including mean profile depth (MPD) and root mean square (RMS) calculated from the topographic information obtained by AIMS in macro-scale.

## **5.2 Conclusions**

The following key conclusions were drawn based on the findings of this study:

- Texture index as measured by AIMS in its current form cannot be used reliably to evaluate aggregate surface microtexture.
- Using AIMS to measure roadway macrotexture from pavement cores did not yield any usable information.
- No statistically significant mathematical relationships exist between pavement friction performance and pavement micro and macrotexture measurement using AIMS on the virgin aggregates or on the field cores.

### **5.3 Recommendations and Future Work**

Based on extensive evaluations performed in this study, recommendations for further investigations are summarized below:

- Develop roughness references using surface profilers and available topographic data analysis techniques in order to evaluate any possible physical meaning of texture index as determined by AIMS.
- Verify and estimate the color effect, and identify a method to eliminate it from AIMS measurement.
- Develop a strong correlation between the imaging technique results and topographic analytical models.
- Evaluate Micro-Deval performance as an accelerated aggregate polishing machine in the simulation of field polishing.

## LIST OF REFERENCES

- Abe, H., Henry, J.J., Tamai, A., and Wambold, J. 2000. Measurement of Pavement Macrotexture Using the CTMeter. *Transportation Research Record 1764*, Transportation Research Board, TRB, National Research Council, Washington, D.C.
- Aggregate Image Measurement System: Model AFA2A Operation Manual. *Pine Instrument Company*, Grove City, Pa., March 2010.
- Ahammed A.M. and Tighe S.L. 2007. Evaluation of Concrete Pavement's Surface Friction Using LTPP Data: Preliminary Analysis and Texture Performance Models. *Proceedings of the 86th Transportation Research Board Annual Meeting (CD)*, Washington, D.C.
- Al-Rousan, T.M. 2004. Characterization of Aggregate Shape Properties Using a Computer Automated System. *Ph.D. Dissertation*, College Station, TX.
- Al-Rousan, T., Masad, E., Tutumluer, E., and Tongyan P. 2007. Evaluation of image analysis techniques for quantifying aggregate shape characteristics. *Construction & Building Materials, Vol. 21, No. 5*.
- Bathina, M. 2005. Quality Analysis of the Aggregate Imaging System (AIMS) Measurements. *M.Sc. Dissertation*, Texas A&M University, College Station, TX.
- Bloem, D.L. 1971. Skid-Resistance: The Role of Aggregates and Other Factors. National Sand and Gravel Association Circular 109, Silver Spring, MD.
- Carbone, G., Lorenz, B., Persson, B.N.J., and Wohlers, A. 2009. Contact mechanics and rubber friction for randomly rough surfaces with anisotropic statistical properties. *European Physical Journal E, Vol. 29, No. 3*.
- Chandan, C., Sivakumar, K., Masad, E., and Fletcher, T. 2004. Application of imaging techniques to geometry analysis of aggregate particles. *Journal of Computing in Civil Engineering, Vol. 18, No. 1*.
- Chelliah, T., Stephanos P., Shah, M.G., and Smith, T. 2003. Developing a Design Policy to Improve Pavement Surface Characteristics. *Presented in Transportation Research Board 82nd Annual Meeting*, Washington, D.C.
- Choubane, B., Holzschuher, C.R., and Gokhale, S. 2004. Precision of Locked-Wheel Testers for Measurement of Roadway Surface Friction Characteristics. *Transportation Research Record 1869*, Transportation Research Board, TRB, National Research Council, Washington, D.C.
- Cooley Jr., L.A., and James, R.S. 2003. *Micro-Deval Testing of Aggregates in the Southeast. Transportation Research Record, No. 1837*, Transportation Research Board, TRB, National Research Council, Washington, D.C.

- Crouch, L.K., Shirley, G., Head, G., and Goodwin, W.A. 1996. Aggregate Polishing Resistance Pre-Evaluation. *Transportation Research Record 1530*, Transportation Research Board, TRB, National Research Council, Washington, D.C.
- Csathy, T.I., Burnett, W.C., and Armstrong, M.D. 1968. State-of-the-Art of Skid Resistance Research. *Highway Research Board Special Report 95*, Highway Research Board, National Research Council, Washington, D.C.
- Dahir, S. 1979. A Review of Aggregate Selection Criteria for Improved Wear Resistance and Skid Resistance of Bituminous Surfaces. *Journal of Testing and Evaluation, Vol. 7*.
- Davis, R.M. 2001. Comparison of Surface Characteristics of Hot-Mix Asphalt Pavement Surfaces at the Virginia Smart Road. *MSc Thesis*, Virginia Polytechnic Institute and State University.
- Davis, R.M., Flintsch, G.W., Al-Qadi, I.L.K., and McGhee, K. 2002. Effect of Wearing Surface Characteristics on Measured Pavement Skid Resistance and Texture. *Presented at 81st Transportation Research Board Annual Meeting*, Washington, D.C.
- Diringer, K. T. and Barros, R. T. 1990. Predicting the Skid Resistance of Bituminous Pavements through Accelerated Laboratory Testing of Aggregates. *Surface Characterization of Roadways: International Research and Technologies, ASTM STP 1301*, ASTM International, West Conshohocken, PA, 1990, pp. 61–76.
- Do, M.T. Zahouani, H., and Vargiolu, R. 2000. Angular Parameter for Characterizing Road Surface Microtexture. *Transportation Research Record 1723*, Transportation Research Board, TRB, National Research Council, Washington, D.C.
- Do, M.T. and Marsac, P. 2002. Assessment of the Polishing of the Aggregate Microtexture by Means of Geometric Parameters. *Presented at 81st Transportation Research Board Annual Meeting*, Washington, D.C.
- Elunai, R. and Chandran, V. 2011. Asphalt Concrete Surfaces Macrotexture Determination From Still Images. *IEEE Transactions on Intelligent Transportation Systems, Vol. 12, No. 3*.
- Ergun, M., Iyınam, S., and Iyınam, A.F. 2005. Prediction of Road Surface Friction Coefficient Using Only Macrotexture and Microtexture Measurements. *Journal of Transportation Engineering, Vol. 131, No. 4*.
- Fletcher, T., Chandan, C., Masad, E., and Sivakumar, K. 2002. Measurement of aggregate texture and its influence on hot mix asphalt (HMA) permanent deformation. *Journal of Testing and Evaluation, Vol. 30, No. 6*.
- Flintsch, G.W., De León, E.; McGhee, K.K.; and Al-Qadi, I.L. 2003. Pavement Surface Macrotexture Measurement and Applications. *Transportation Research Record 1860*, Transportation Research Board, TRB, National Research Council, Washington D.C.

- Flintsch, G.W., Luo, Y., and Al-Qadi, I.L. 2005. Analysis of the Effect of Pavement Temperature on the Frictional Properties of Flexible Pavement Surfaces. *Presented at 84th Transportation Research Board Annual Meeting*, Washington, D.C.
- Forster, S.W. 1989. Pavement Microtexture and its Relation to Skid Resistance. *Transportation Research Record 1215*, Transportation Research Board, TRB, National Research Council, Washington D.C.
- Fwa, T.F., Choo, Y.S., and Liu, Y.R. 2003. Effect of Aggregate Spacing on Skid Resistance of Asphalt Pavement. *Journal of Transportation Engineering*, Vol. 129, No. 4, American Society of Civil Engineering, ASCE.
- Gandhi, P.M., Colucci, B., and Gandhi, S.P. 1991. Polishing of Aggregates and Wet Weather Accident Rate for Flexible Pavements. *Transportation Research Record 1300*, Transportation Research Board, TRB, National Research Council, Washington, D.C.
- Gates, L., Masad, E., Pyle, R., and Bushee, D. 2011. Aggregate Imaging Measurement System 2 (AIMS2): Final Report. *FHWA Report FHWA-HIF-11-030*, Federal Highway Administration.
- Gendy, A.E., Shalaby, A. 2007. Mean profile depth of pavement surface macrotexture using photometric stereo techniques. *Journal of Transportation Engineering*, Vol. 133, No. 7.
- Gendy, A.E., Shalaby, A., Saleh, M., and Flintsch, G.W. 2011. Stereo-vision applications to reconstruct the 3D texture of pavement surface. *International Journal of Pavement Engineering*, Vol. 12, No. 3.
- Giles, C.G., Sabey, B.E., and Cardew, K.H.F. 1964. Development and Performance of the Portable Skid Resistance Tester. *Road Research Technical Paper 66*, Road Research Laboratory, Department of Scientific and Industrial Research, HMSO, London, United Kingdom.
- Goodman, S.N., Hassan, Y., and Abd El Halim, A.O. 2006. Preliminary Estimation of Asphalt Pavement Frictional Properties from Superpave Gyrotory Specimen and Mix Parameters. *Transportation Research Record 1949*, Transportation Research Board, TRB, National Research Council, Washington, D.C.
- Hall, J.W., Glover, L.T., Smith, K.L., Evans, L.D., Wambold, J.C., Yager, T.J., and Rado, Z. 2006. Guide for Pavement Friction. *Project No. 1-43*, Final Guide, National Cooperative Highway Research Program, Transportation Research Board, National Research Council, Washington, D.C.
- Hanson, D.I. and Prowell, B.D. 2004. Evaluation of Circular Texture Meter for Measuring Surface Texture of Pavements. *NCAT Report 04-05*, National Center for Asphalt Technology, Auburn, AL.
- Henry, J.J. 2000. Evaluation of Pavement Friction Characteristics. *NCHRP Synthesis: Topic 30-11*, National Cooperative Highway Research Program, Washington, D.C.

- Henry, J.J., Abe, H., Kameyama, S., Tamai, A., Kasahara, A., and Saito, K. 2000. Determination of the International Friction Index Using the Circular Track Meter and the Dynamic Friction Tester. *Proceedings of SURF 2000*, the World Road Association. Paris, France.
- Hogervorst, D. 1974. Some Properties of Crushed Stone for Road Surfaces. *Bulletin of the International Association of Engineering Geology, Vol. 10, No.1*, Springer.
- Jackson, N.M., Choubane, B., and Musselman, J.A. 2002. A Preliminary Evaluation of FC-5 and FC-6 Friction Courses in Florida. *Pavement Evaluation Conference*, Roanoke, VA
- Jayawickrama, P.W., Prasanna, R., and Senadheera, S.P. 1996. Survey of State Practices to Control Skid Resistance on Hot-Mix Asphalt Concrete Pavements. *Transportation Research Record 1536*, Transportation Research Board, TRB, National Research Council, Washington, D.C.
- Johnsen, W.A. 1997. Advances in the Design of Pavement Surfaces. *Ph.D. Dissertation*, Worcester Polytechnic Institute.
- Khoudeir, M., Brochard, J., Legeay, V., and Do M.T. 2004. Roughness Characterization Through 3D Texture Image Analysis: Contribution to the Study of Road Wear Level. *Computer-Aided Civil and Infrastructure Engineering, Vol. 19, No. 2*.
- Klüppel, M., and Heinrich, G. 2000. Rubber friction on self-affine road tracks. *Rubber Chemistry and Technology, Vol. 73, No. 4*, pp 578-606.
- Kokkalis, A.G. 1998. Prediction of skid resistance from texture measurements. *Proceedings of the Institution of Civil Engineers: Transport, Vol. 129, No. 2*.
- Kokkalis, A.G. and Panagouli, O.K. 1999. Fractal Evaluation of Pavement Skid Resistance Variations Surface Wear. *Chaos, Solutions and Fractals, Vol. 9, No. 11*.
- Kokkalis, A.G., Tsohos, G.H., and Panagouli, O.K. 2002. Consideration of Fractals in Pavement Skid Resistance Evaluation. *Journal of Transportation Engineering, Vol. 128, No. 6*, American Society of Civil Engineering: pp 591-595.
- Kowalski, K.J. 2007. Influence of Mixture Composition on the Noise and Frictional Characteristics of Flexible Pavements. *Ph.D. Dissertation*, Purdue University, West Lafayette, IN.
- Kummer, H.W. and Meyer, W.E. 1963. Penn State Road Surface Friction Tester as Adapted to Routine Measurement of Pavement Skid Resistance. *Road Surface Properties, 42nd Annual Meeting, January*.
- Kummer, H.W. 1966. *Unified Theory of Rubber and Tire Friction*. PA State University College of Engineering, University Park, PA.

- Kutay, M.E., Ozturk, H.I., Abbas, A.R., and Hu, C. 2011. Comparison of 2D and 3D image-based aggregate morphological indices. *International Journal of Pavement Engineering*, Vol. 12, No. 4.
- Lang, A.P., Range, P.H., Fowler, D.W., and Allen, J.J. 2007. Prediction of coarse aggregate performance by micro-deval and other soundness, strength, and intrinsic particle property tests. *Transportation Research Record*, No. 2026, Transportation Research Board, TRB, National Research Council, Washington D.C.
- Lee, Y.P.K., Fwa, T.F., and Choo, Y.S. 2005. Effect of Pavement Surface Texture on British Pendulum Test. *Journal of the Eastern Asia Society for Transportation Studies*, Vol. 6.
- Leu, M.C. and Henry, J.J. 1978. Prediction of Skid Resistance as a Function of Speed from Pavement Texture. *Transportation Research Record 666*, Transportation Research Board, TRB, National Research Council, Washington D.C.
- Li, S., Zhu, K., Noureldin, S., and Harris, D. 2005. Identifying Friction Variations with the Standard Smooth Tire for Network Pavement Inventory Friction Testing. *Presented in Transportation Research Board 84th Annual Meeting*, Washington D.C.
- Liang, R.Y. and Chyi L.L. 2000. Polishing and Friction Characteristics of Aggregates Produced in Ohio. *FHWA Report FHWA/OH-2000/001*, Federal Highway Administration, Columbus, OH.
- Liu, Y., Fwa, T.F., and Choo, Y.S. 2004. Effect of Surface Macrotecture on Skid Resistance Measurements by the British Pendulum Test. *Journal of Testing and Evaluation*, Vol. 32, No. 4, American Society of Civil Engineering, ASCE.
- Luce, A.D. 2006. Analysis of Aggregate Imaging System (AIMS) Measurements and Their Relationship to Asphalt Pavement Skid Resistance. *M.S.C.E Thesis*, Texas A&M University, College Station, TX.
- Luo, Y. 2003. Effect of Pavement Temperature on Frictional Properties of Hot-Mix-Asphalt Pavement Surfaces at the Virginia Smart Road. *MSc Thesis*, Virginia Polytechnic Institute and State University.
- Mahmoud, E.M., Masad, E. 2007. Experimental Method for the Evaluation of Aggregate Resistance to Polishing, Abrasion, and Breakage. *Journal of Materials in Civil Engineering*, Vol. 19, No. 11.
- Masad, E., Olcott, D., White, T., and Tashman, L. 2001. Correlation of fine aggregate imaging shape indices with asphalt mixture performance. *Transportation Research Record*, No. 1757. Transportation Research Board, TRB, National Research Council, Washington, D.C.
- Masad, E., Little, D. N., Tashman, L., Saadeh, S., Al-Rousan, T., and Sukhwani R. 2003. Evaluation of Aggregate Characteristics Affecting HMA Concrete Performance. *Research Report ICAR 203-1*. Texas Transportation Institute, College Station.

- Masad, E. 2003. NCHRP-IDEA Project 77: The Development of a Computer Controlled Image Analysis System for Measuring Aggregate Shape Properties. *Final Report*. Transportation Research Board of the National Academies, Washington, D.C.
- Masad, E., Al-Rousan, T., Button, J., Little, D., and Tutumluer, E. 2005. Test Methods for Characterizing Aggregate Shape, Texture, and Angularity. *NCHRP Project 4-30A Final Report*, National Cooperative Highway Research Program, Washington, D.C.
- Masad, E., Luce, A., and Mahmoud, E. 2006. Implementation of AIMS in Measuring Aggregate Resistance to Polishing Abrasion and Breakage. *Texas Transportation Institute, Research Report 5-1707-03-1*, Texas A&M University, College Station, TX.
- Masad, E., Rezaei, A., Chowdhury, A., and Harris, P. 2009. Predicting Asphalt Mixture Skid Resistance Based on Aggregate Characteristics. *Texas Transportation Institute, Research Report 09/0-5627-1*, Texas A&M University, College Station, TX.
- Masad, E., Rezaei, A., and Chowdhury, A. 2011. Field Evaluation of Asphalt Mixture Skid Resistance and Its Relationship to Aggregate Characteristics. *Texas Transportation Institute, Research Report 11/0-5627-3*, Texas A&M University, College Station, TX.
- McCullough, B.V. and Hankins, K.D. 1966. Skid Resistance Guidelines for Surface Improvements on Texas Highways. *Transportation Research Record 131*, Transportation Research Board, TRB, National Research Council, Washington, D.C.
- McDaniel, R.S. and Coree B.J. 2003. Identification of Laboratory Techniques to Optimize Superpave HMA Surface Friction Characterization. *Phase I: Final Report SQDH 2003-6*, North Central Superpave Center, Purdue University, West Lafayette, IN.
- Miller, M.M. and Johnson, H.D. 1973. Effects of Resistance to Skidding on Accidents: Surface Dressing on an Elevated Section of the M4 Motorway, *Report No. LR 542*, Transport and Road Research Laboratory, Berkshire, United Kingdom.
- Moore, D.F. 1966. Prediction of Skid Resistance Gradient and Drainage Characteristics for Pavements. *Highway Research Record 131*, Highway Research Board, National Research Council, Washington, D.C.
- Moore, D.F. 1969. Recommendations for an International Minimum Skid-Resistance Standard for Pavements. *Highway Research Board Special Report 101*, Highway Research Board, National Research Council, Washington, D.C.
- Moore, D.F. 1972. *The Friction and Lubrication of Elastomers*. Pergamon Press LTD., Oxford, Great Britain.
- Moore, D.F. 1975. *The Friction of Pneumatic Tires*. Elsevier Scientific Publishing Company, Amsterdam, Netherland.
- Noyce, D.A., Bahia, H.U., Yambó, J.M., and Kim, G. 2005. Incorporating Road Safety into Pavement Management: Maximizing Asphalt Pavement Surface Friction for Road Safety

- Improvements. Midwest Regional University Transportation Center Traffic Operations and Safety (TOPS) Laboratory.
- Persson, B.N.J. 1998. On the theory of rubber friction. *Surface Science*, Vol. 401, No. 3.
- Person, B.N.J. 1998. *Sliding Friction: Physical Principles and Applications*. Springer, Berlin, Germany.
- Persson, B.N.J., Tosatti, E. 2000. Qualitative theory of rubber friction and wear. *Journal of Chemical Physics*, Vol. 112, No. 4.
- Persson, B.N.J. 2001. Theory of rubber friction and contact mechanics. *Journal of Chemical Physics*, Vol. 115, No. 8.
- PIARC Technical Committee on Surface Characteristics (C1) 1995. International PIARC Experiment to Compare and Harmonize Texture and Skid Resistance Measurements, Paris, France.
- Prowell, B.D., Zhang, J., and Brown, E.R. 2005. Aggregate Properties and the Performance of Superpave-Designed Hot Mix Asphalt. *National Cooperative Highway Research Program, NCHRP Report 539*, Transportation Research Board, National Research Council, Washington, D.C.
- Purushothaman, N., Heaton, B.S., and Moore, I.D. 1988. Experimental Verification of a Finite Element Contact Analysis. *Journal of Testing and Evaluation*, Vol. 16, No. 6.
- Rangaraju, P.R., and Edlinski, J. 2008. Comparative evaluation of micro-deval abrasion test with other toughness/ abrasion resistance and soundness tests. *Journal of Materials in Civil Engineering*, Vol. 20, No. 5.
- Rizenbergs, R.L., Burchett, J.L., and Napier, C.T. 1972. Skid Resistance of Pavements. *Report No. KYHPR-64-24, Part II*, Kentucky Department of Highways, Lexington, KY.
- Rezaei, A., Hoyt, D., and Martin, A. 2011. Simple laboratory method for measuring pavement macrotexture. *Transportation Research Record*, No. 2227, Transportation Research Board, TRB, National Research Council, Washington D.C.
- Rezaei, A., Masad, E., and Chowdhury, A. 2012. Development of a Model for Asphalt Pavement Skid Resistance Based on Aggregate Characteristics and Gradation. *Journal of Transportation Engineering*, Vol. 137, No. 12, pp 863-873.
- Rogers, C. 1991. Laboratory Tests for Predicting Coarse Aggregate Performance in Ontario. *Advances in Aggregate and Armourstone Evaluation 13*.
- Saito, K., Horiguchi, T., Kasahara, A., Abe, H., and Henry, J.J. 1996. Development of Portable Tester for Measuring Skid Resistance and Its Speed Dependency on Pavement Surfaces. *Transportation Research Record 1536*, Transportation Research Board, TRB, National Research Council, Washington D.C.

- Sandberg, U., and Ejsmont, J.A. 2002. *Tyre/Road Noise Reference Book*, ISBN 91-631-2610-9, Informex, Kisa, Sweden.
- Slimane, A.B., Khoudeir, M., Brochard, J., and Do M.T. 2008. Characterization of road microtexture by means of image analysis. *Wear*, Vol. 264, No. 5-6.
- Stroup-Gardiner, M., Studdard, J., and Wagner, C. 2004. Evaluation of Hot Mix Asphalt Macrotexture and Microtexture. *Journal of Testing and Evaluation*, Vol. 32, No.1.
- Sun, W., Wang, L.; and Tutumluer, E. 2012. Image analysis technique for aggregate morphology analysis with two-dimensional fourier transform method. *Transportation Research Record*, No. 2267, Transportation Research Board, TRB, National Research Council, Washington, D.C.
- Transit New Zealand. 2002. Specification for Skid Resistance Deficiency Investigation and Treatment Selection. TNZ T/10 Transit New Zealand, Wellington, New Zealand.
- Vilaca, J.L., Fonseca, J.C., Pinho, A.M., and Freitas, E. 2009. A new machine for acquire pavement texture. *7th International Conference on Computational Cybernetics (ICCC 2009)*, pp 97-102,
- Vilaca, J.L., Fonseca, J.C., Pinho, A.C.M., and Freitas, E. 2010. 3D surface profile equipment for the characterization of the pavement texture-*TexScan*. *Mechatronics*, Vol. 20, No. 6.
- Villani, M., Artamendi, I., Kane, M., and Scarpas, A. 2011. Contribution of hysteresis component of tire rubber friction on stone surfaces. *Transportation Research Record*, No. 2227, pp 153-162.
- Vollor, T.W. and Hanson, D.I. 2006. Development of Laboratory Procedure for Measuring Friction of HMA Mixtures-Phase 1. *NCAT Report 06-06*, National Center of Asphalt Technology, Auburn University, AL.
- Walker, R.S. and Payne, L.D. Use of Selcom Laser for Pavement Texture and Skid Resistance Measurement. *Technical Memorandum, Research Project 1290*. Transportation Instrumentation Laboratory, University of Texas, Arlington, TX, undated.
- Wallman, C.G. and Astron, H. 2001. Friction Measurement Methods and the Correlation between Road Friction and Traffic Safety. *Swedish National Road and Transport Research Institute, VTI Meddelande 911A*, Linköping, Sweden.
- Wambold, J.C., Henry, J.J., and Hegmon, R.R. 1986. Skid Resistance of Wet-Weather Accident Sites. *ASTM Special Technical Publication 929*, American Society of Testing and Materials (ASTM), Philadelphia, PA.
- Wambold, J.C., Antle, C.E., Henry J.J., and Rado, Z. 1995. PIARC (Permanent International Association of Road Congress) Report. International PIARC Experiment to Compare and Harmonize Texture and Skid Resistance Measurement, C-1 PIARC Technical Committee on Surface Characteristics, France.

- Wang, L., Wang, X., Mohammad, L., and Abadie, C. 2005. Unified method to quantify aggregate shape angularity and texture using Fourier analysis. *Journal of Materials in Civil Engineering*, Vol. 17, No. 5.
- Wang, L., Lane, D.S., Lu, Y., and Druta, C. 2009. Portable image analysis system for characterizing aggregate morphology. *Transportation Research Record*, No. 2104, Transportation Research Board, TRB, National Research Council, Washington, D.C.
- West, T.R., Choi, J.C., Bruner, D.W., Park, H.J., and Cho, K.H. 2001. Evaluation of Dolomite and Related Aggregates Used in Bituminous Overlays for Indiana Pavements. *Transportation Research Record 1757*, Transportation Research Board, TRB, National Research Council, Washington, D.C.
- Westermann, S., Petry, F., Boes, R., and Thielen, G. 2004. Experimental investigations into the predictive capabilities of current physical rubber friction theories. *KGK Kautschuk Gummi Kunststoffe*, Vol. 57, No. 12, pp 645-650.
- Williams, A.R. and Lees, G. 1970. Topographical and Petrographical Variation of Road Aggregates and the Wet Skidding Resistance of Tires. *Journal of Engineering Geology*, Vol. 2.
- Woodside, A. R., and Woodward W.D.H. 2002. Wet skid resistance. In C. O'Flaherty, *Highways: The location, design, construction and maintenance of road pavements*. Elsevier Ltd.
- Wu, Y., Parker, F., and Kandhal, K. 1998. Aggregate Toughness/Abrasion Resistance and Durability/Soundness Tests Related to Asphalt Concrete Performance in Pavements. *NCAT Report 98-04*, National Center for Asphalt Technology (NCAT), Auburn, Alabama.
- Xue, W., Druta, C., Wang, L., and Lane, D.S. 2010. Assessing the polishing characteristics of coarse aggregates using Micro-Deval and imaging system. *Geotechnical Special Publication, No. 203 GSP*, Paving Materials and Pavement Analysis - Proceedings of the GeoShanghai International Conference, pp 288-295.
- Yandell, W.O. 1971. A New Theory of Hysteretic Sliding Friction. *Wear*, Vol. 17.
- Yandell, W.O., Taneerananon, P., and Zankin, V. 1983. Prediction of Tire-Road Friction from Surface Texture and Tread Rubber Properties. *Frictional Interaction of Tire and Pavement*, *ASTM Special Technical Publication 793*, W.E Meyer and J.D. Walter, Ed., American Society of Civil Engineering, Washington, D.C.
- Yandell, W.O. and Sawyer, S. 1994. Prediction of Tire-Road Friction from Texture Measurements. *Transportation Research Record 1435*, Transportation Research Board, TRB, National Research Council, Washington, D.C.

APPENDIX A  
TEXTURE INDEX DISTRIBUTION OF VIRGIN AGGREGATES BEFORE AND AFTER  
POLISHING

Note: For each sample, one of every three measurements has been shown.

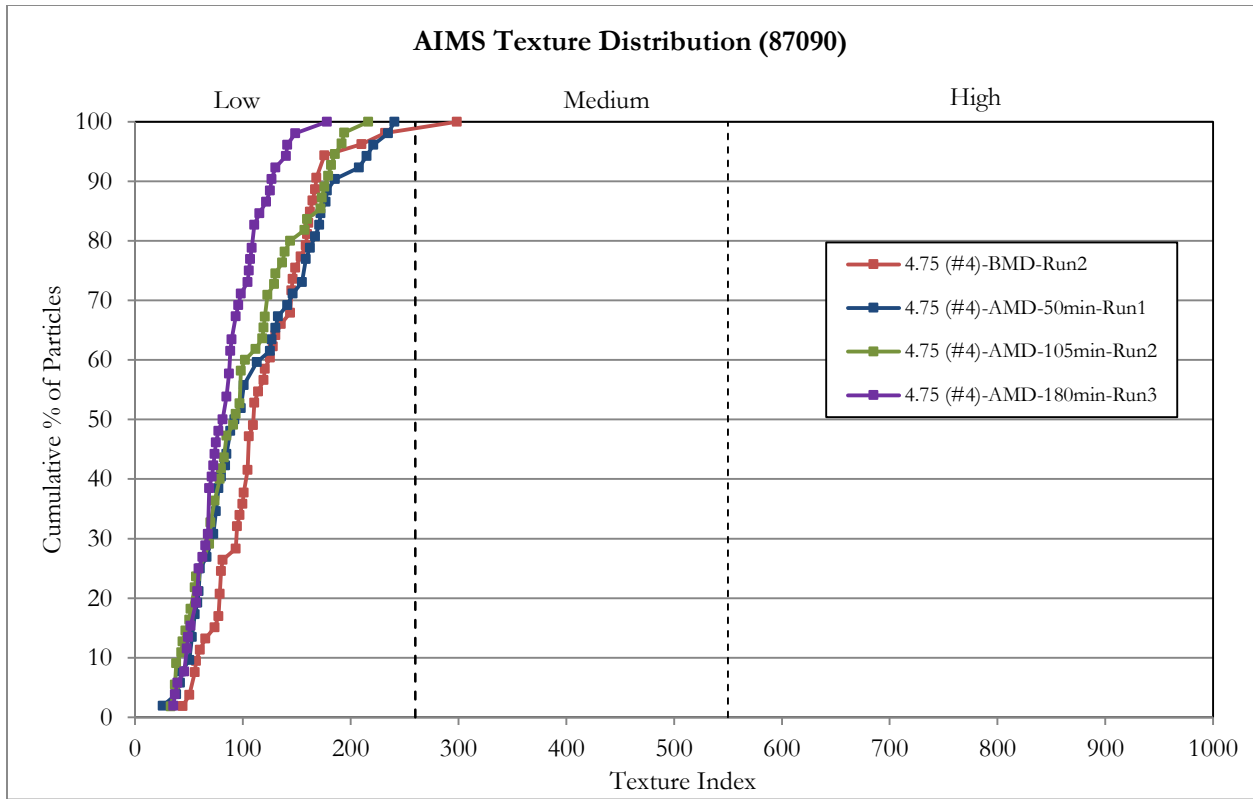


Figure A.1 Texture distribution of 87090 before and after polishing (#4)

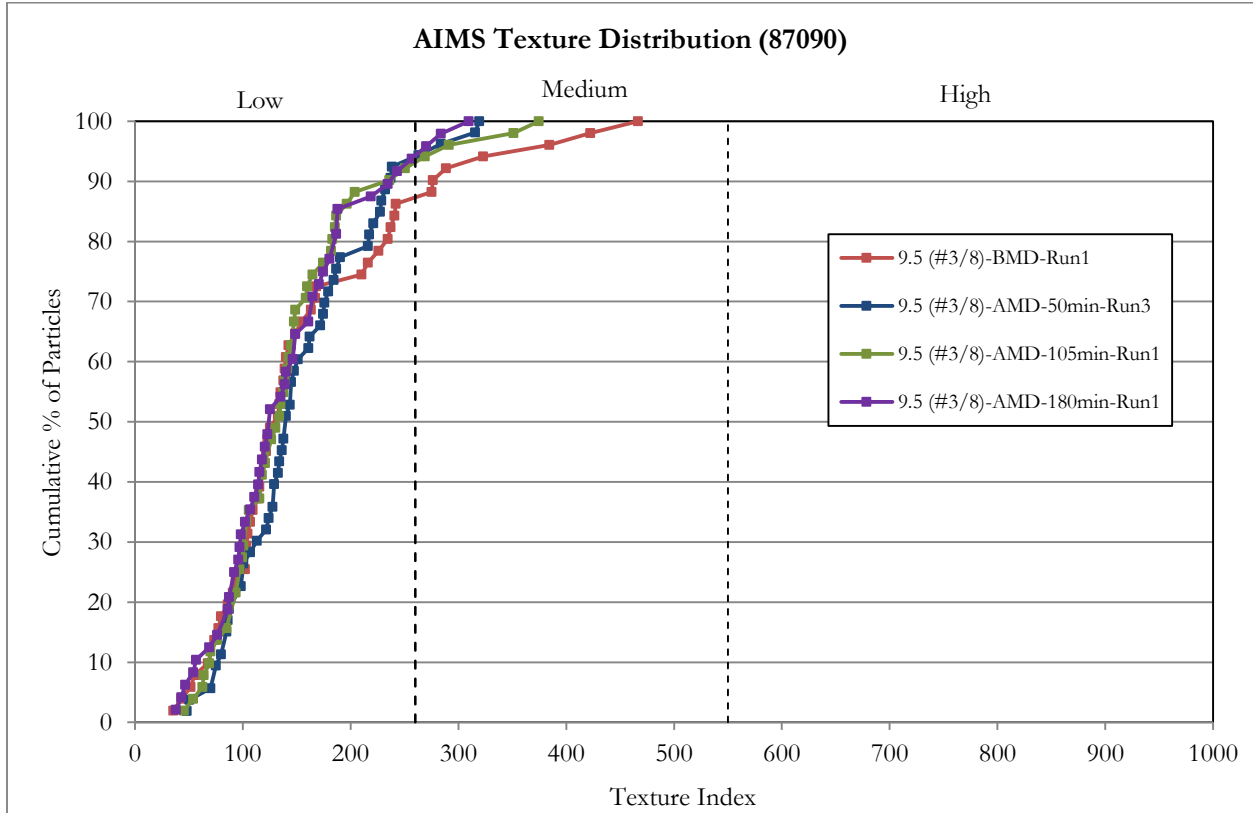


Figure A.2 Texture distribution of 87090 before and after polishing (#3/8)

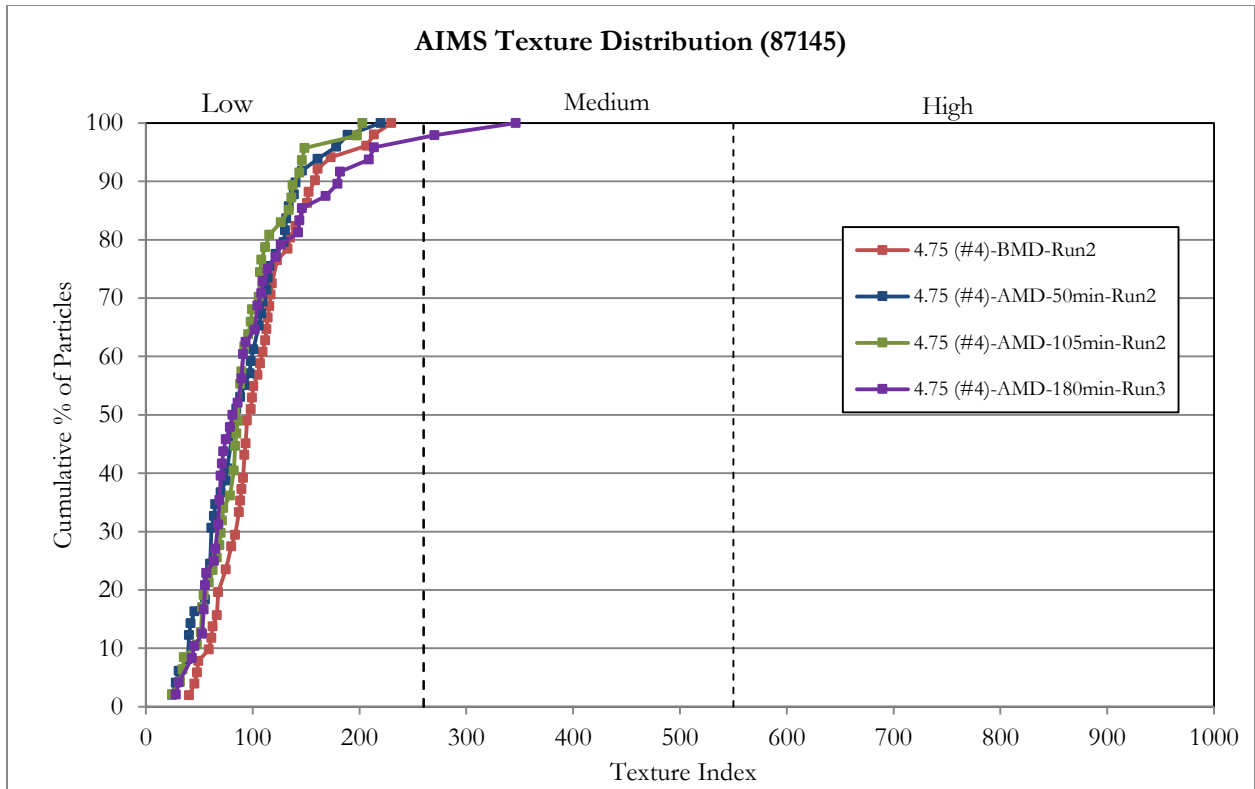


Figure A.3 Texture distribution of 87145 before and after polishing (#4)

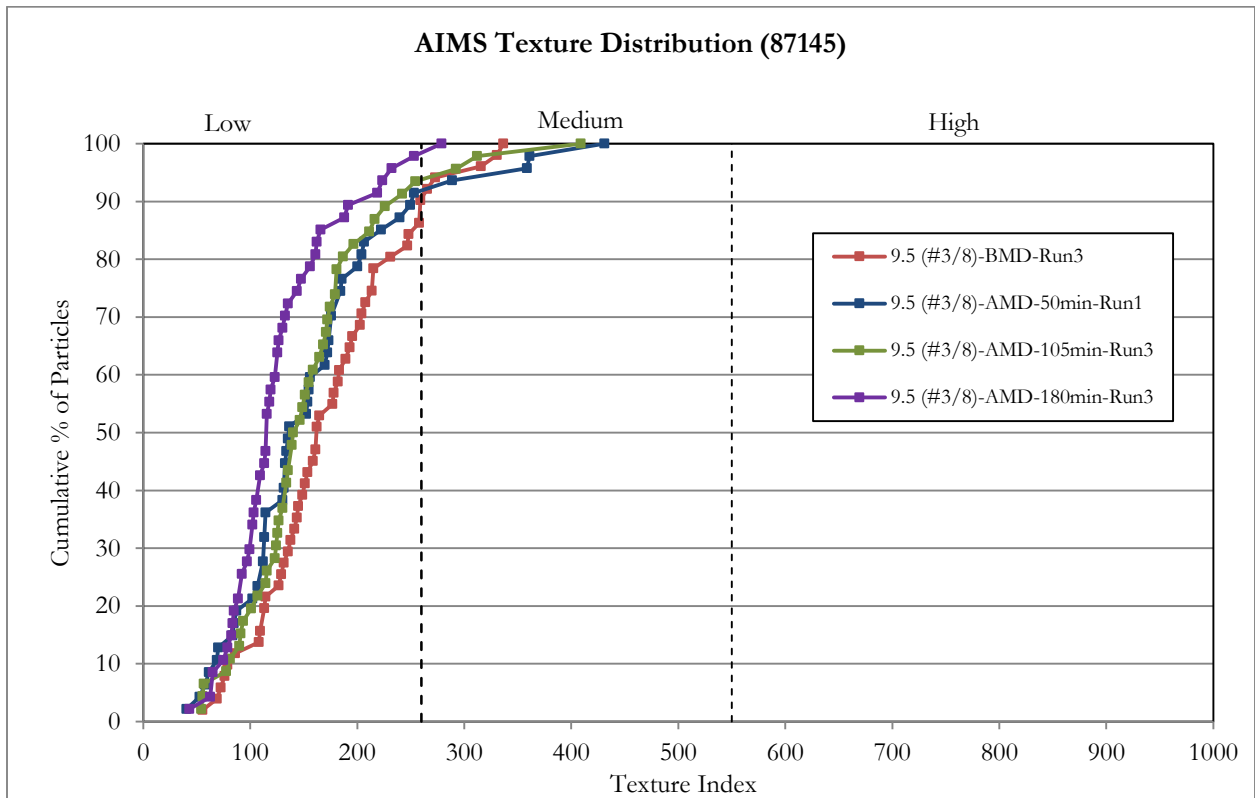


Figure A.4 Texture distribution of 87145 before and after polishing (#3/8)

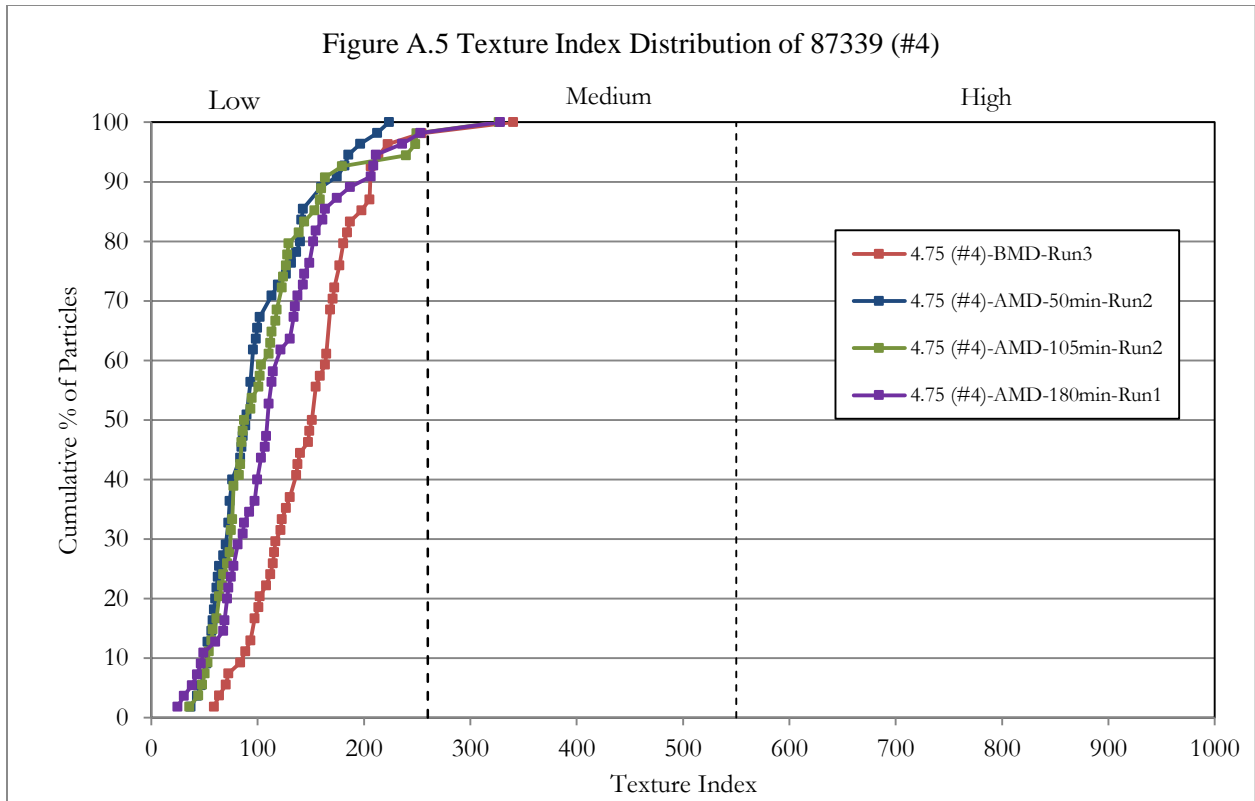


Figure A.5 Texture distribution of 87339 before and after polishing (#4)

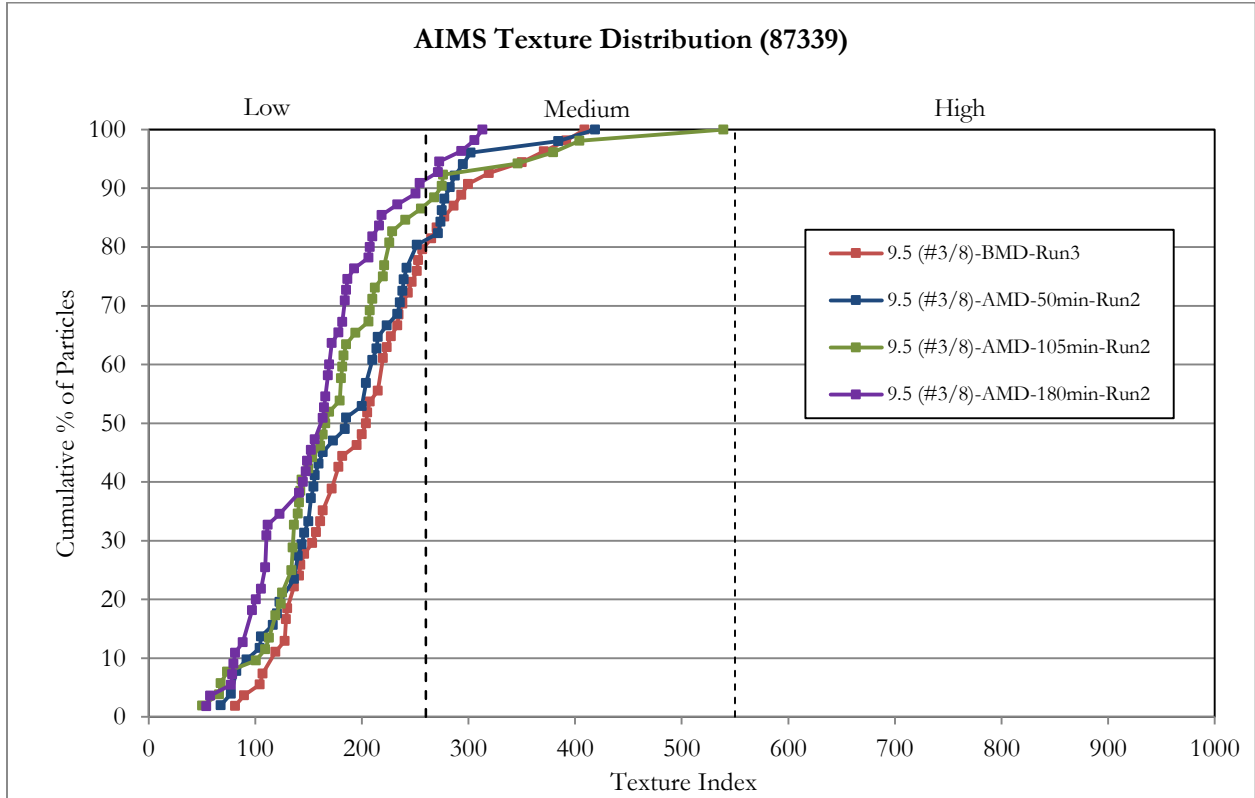


Figure A.6 Texture distribution of 87339 before and after polishing (#3/8)

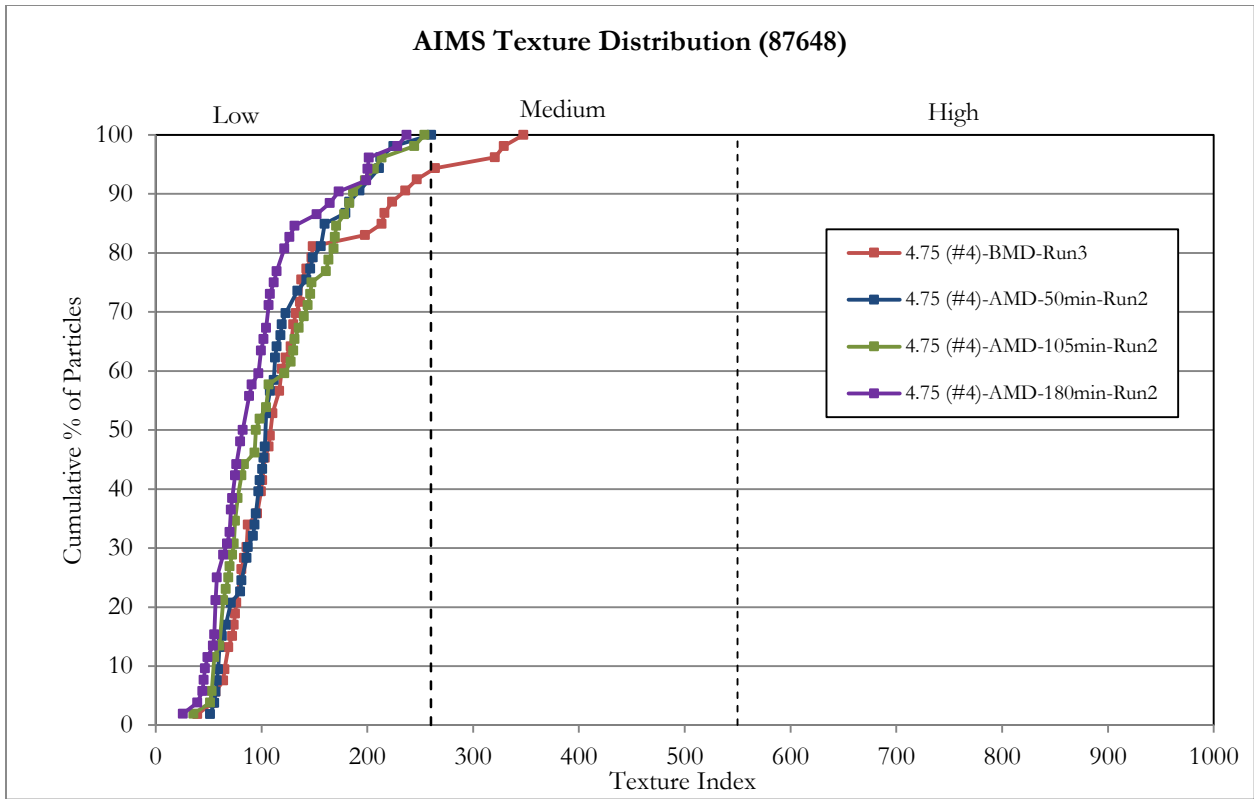


Figure A.7 Texture distribution of 87648 before and after polishing (#4)

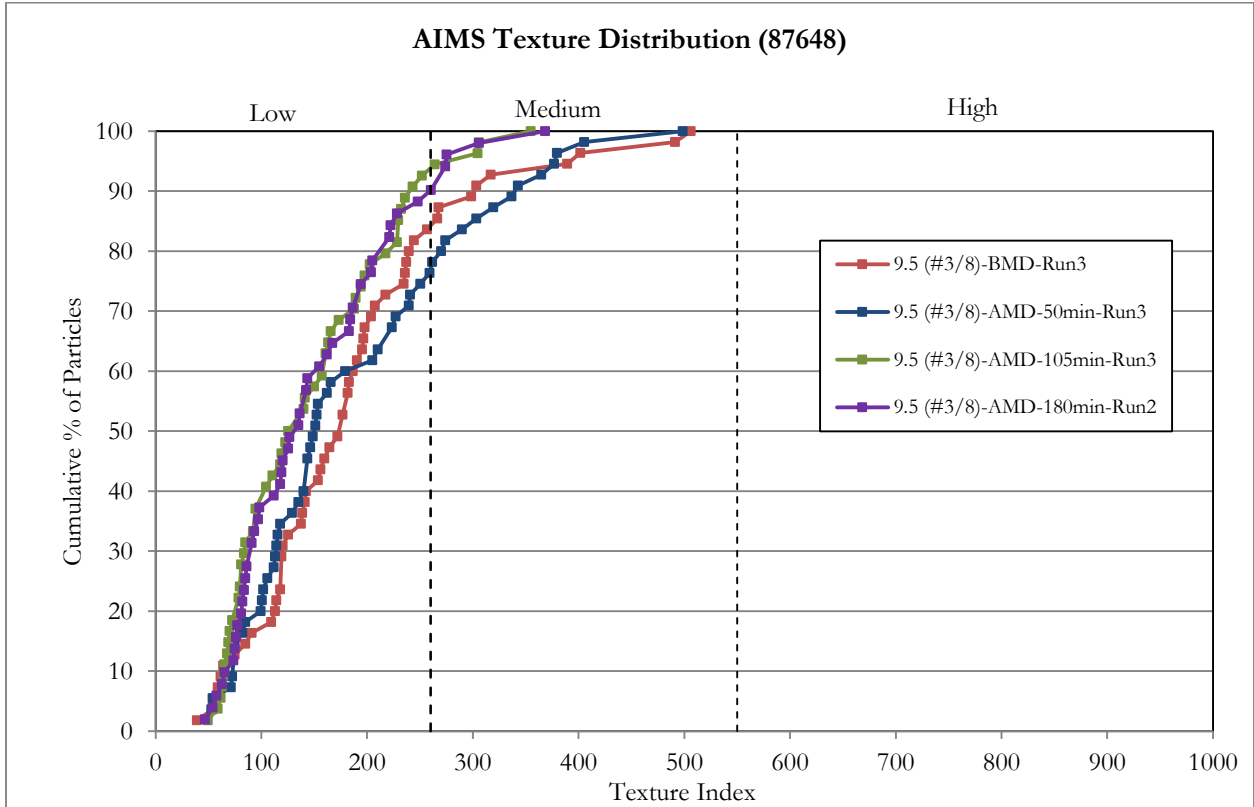


Figure A.8 Texture distribution of 87648 before and after polishing (#3/8)

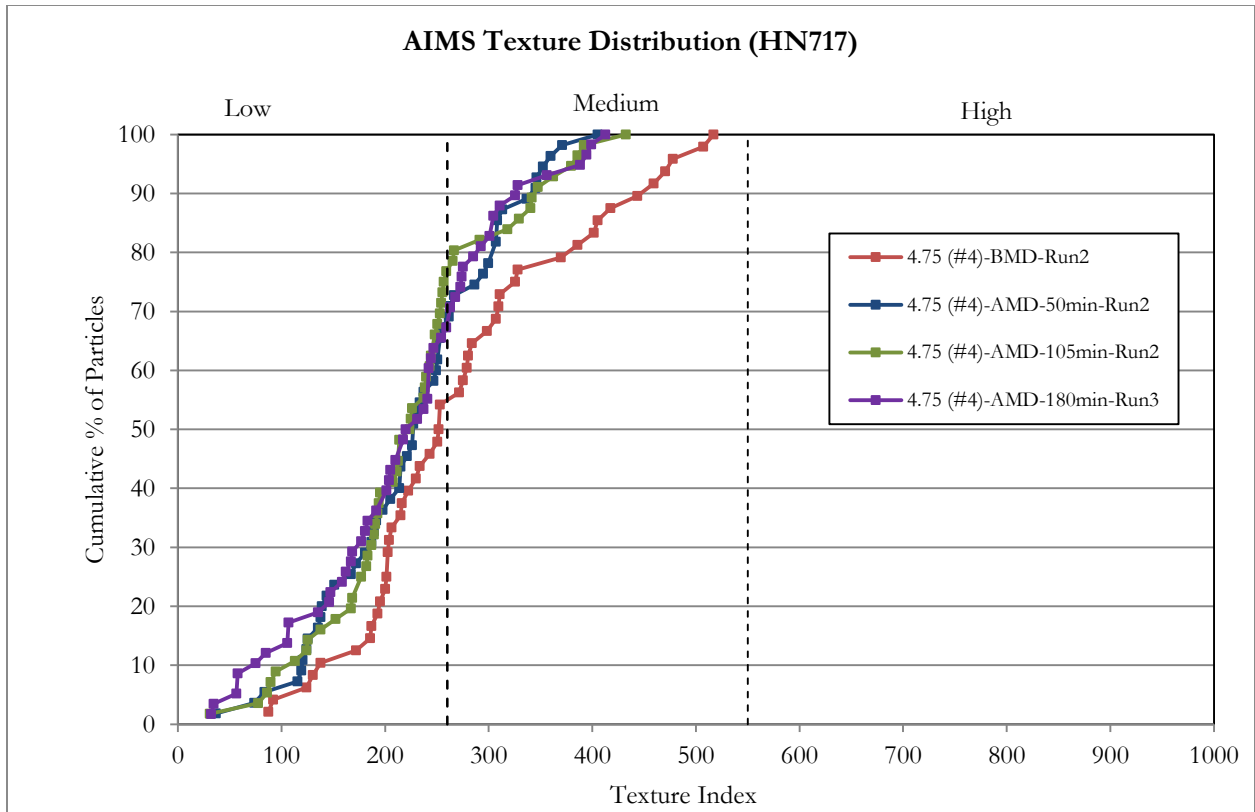


Figure A.9 Texture distribution of HN717 before and after polishing (#4)

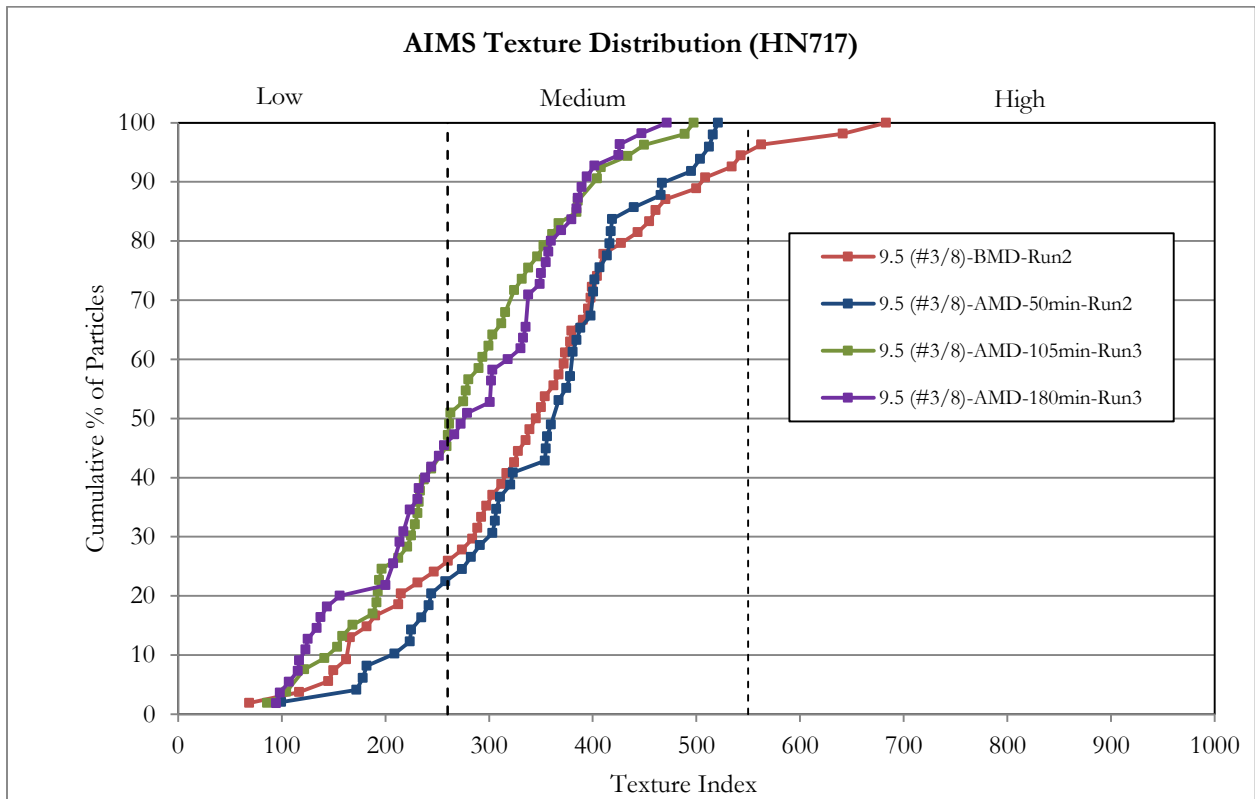


Figure A.10 Texture distribution of HN717 before and after polishing (#3/8)

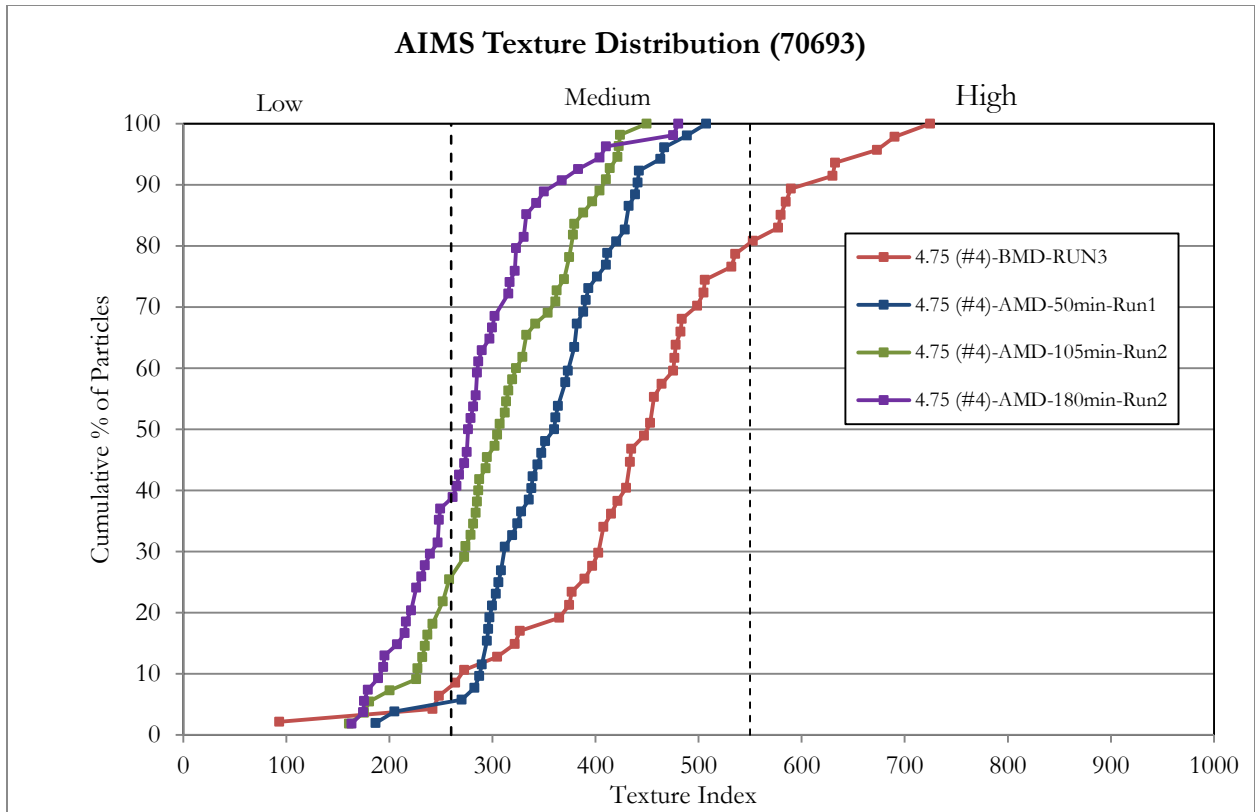


Figure A.11 Texture distribution of 70693 before and after polishing (#4)

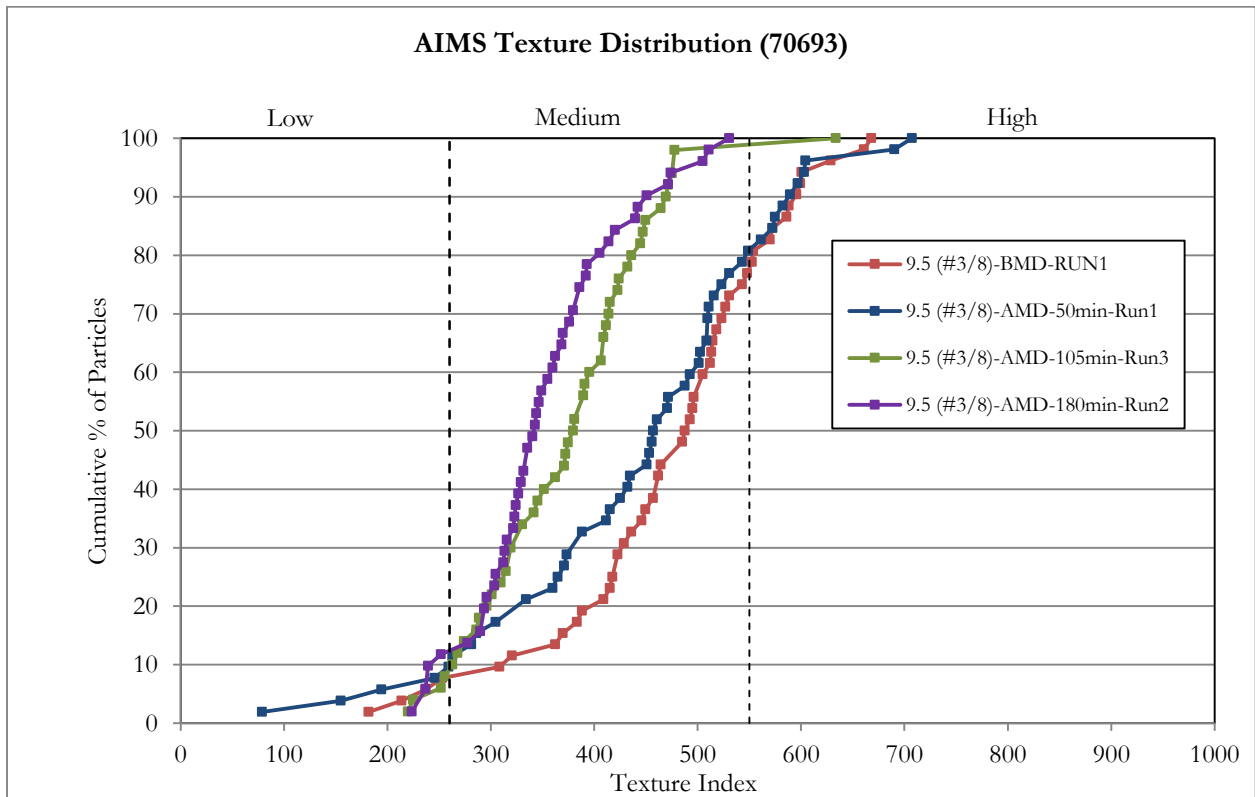


Figure A.12 Texture distribution of 70693 before and after polishing (#3/8)

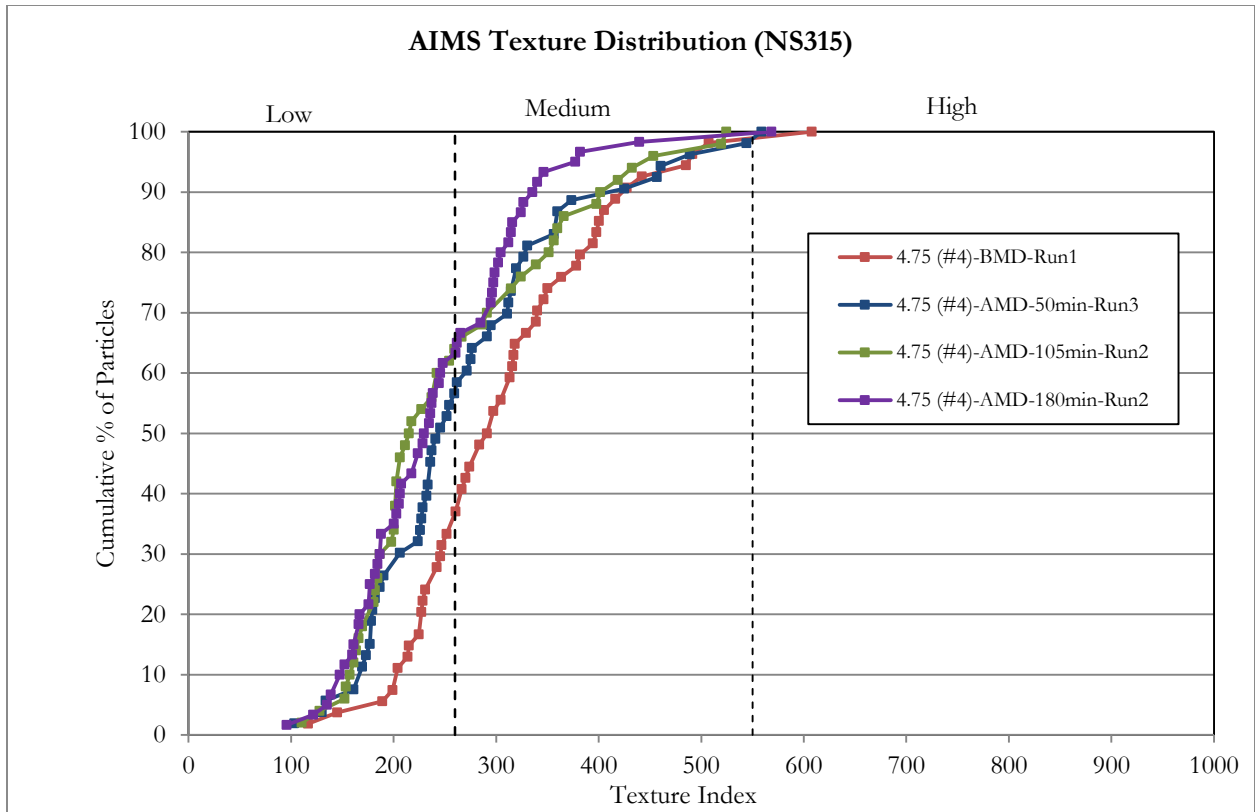


Figure A.13 Texture distribution of NS315 before and after polishing (#4)

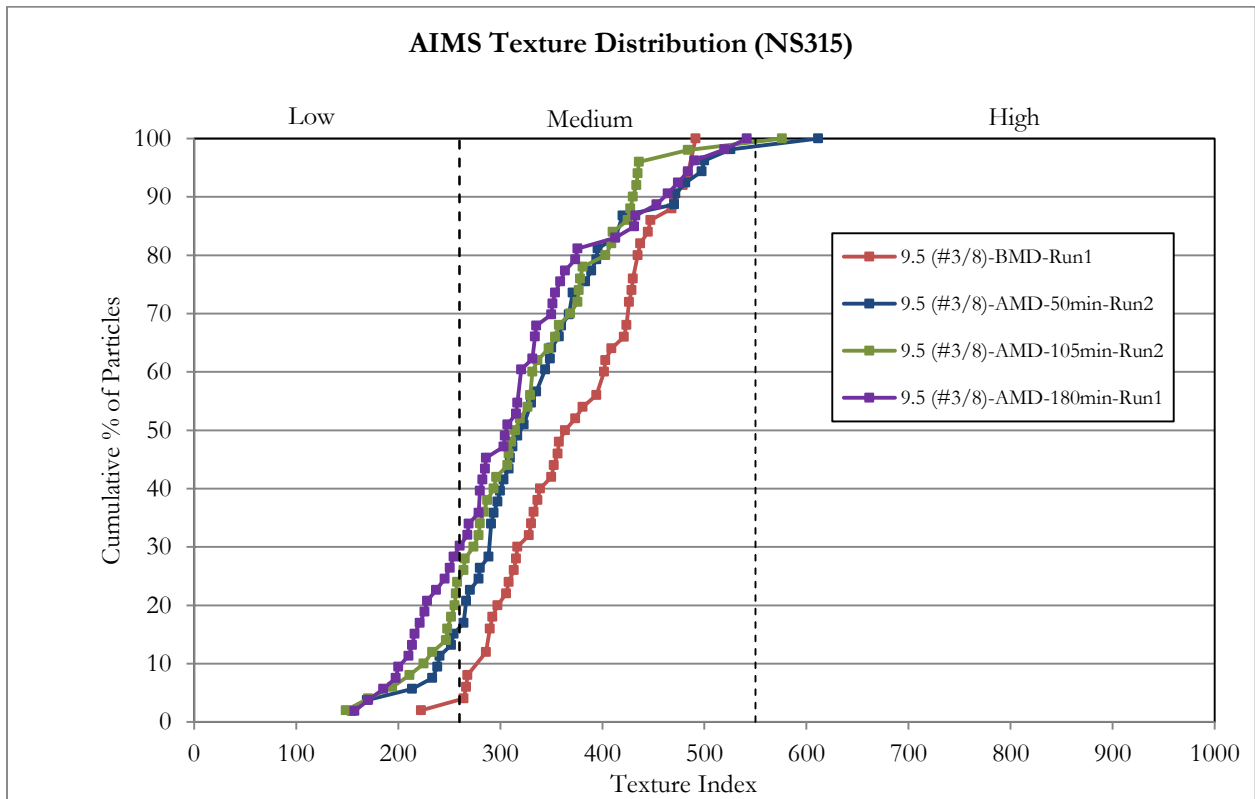


Figure A.14 Texture distribution of NS315 before and after polishing (#3/8)



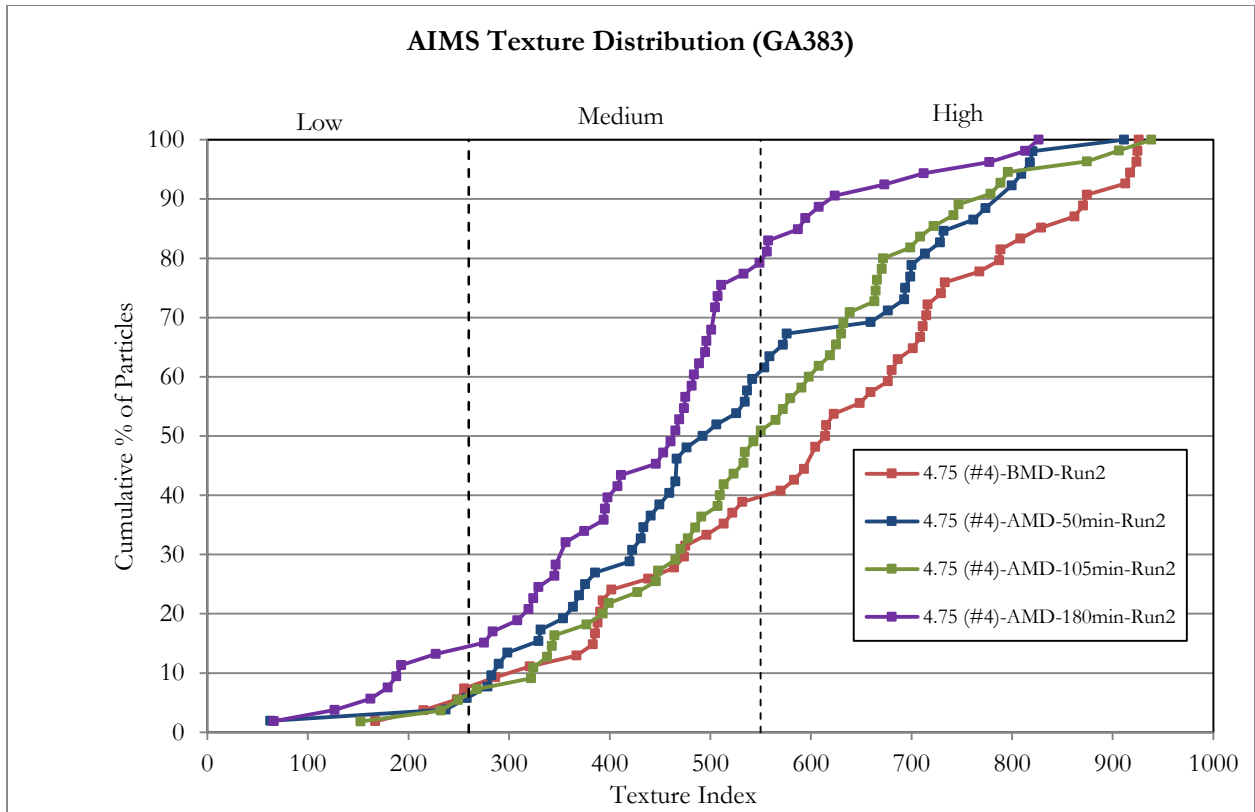


Figure A.17 Texture distribution of GA383 before and after polishing (#4)

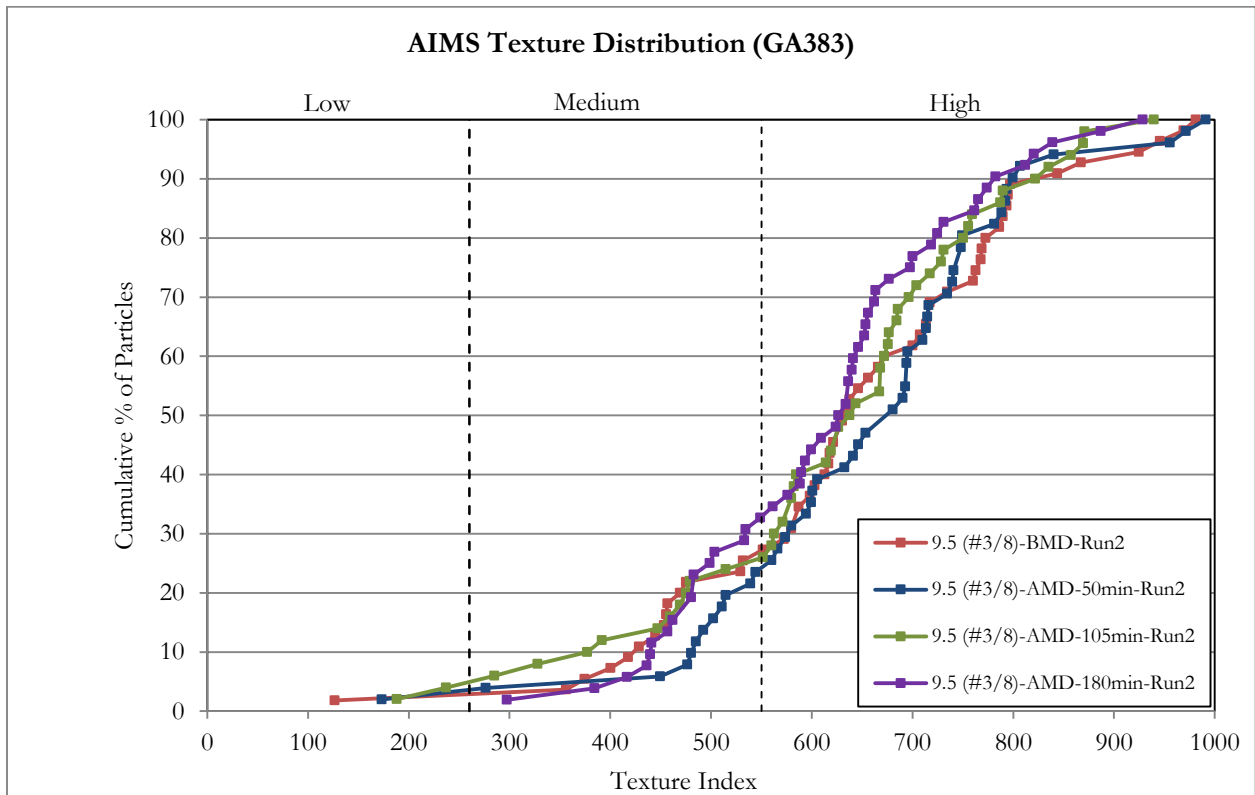


Figure A.18 Texture distribution of GA383 before and after polishing (#3/8)

APPENDIX B  
MEASURED PROFILES OF CORES

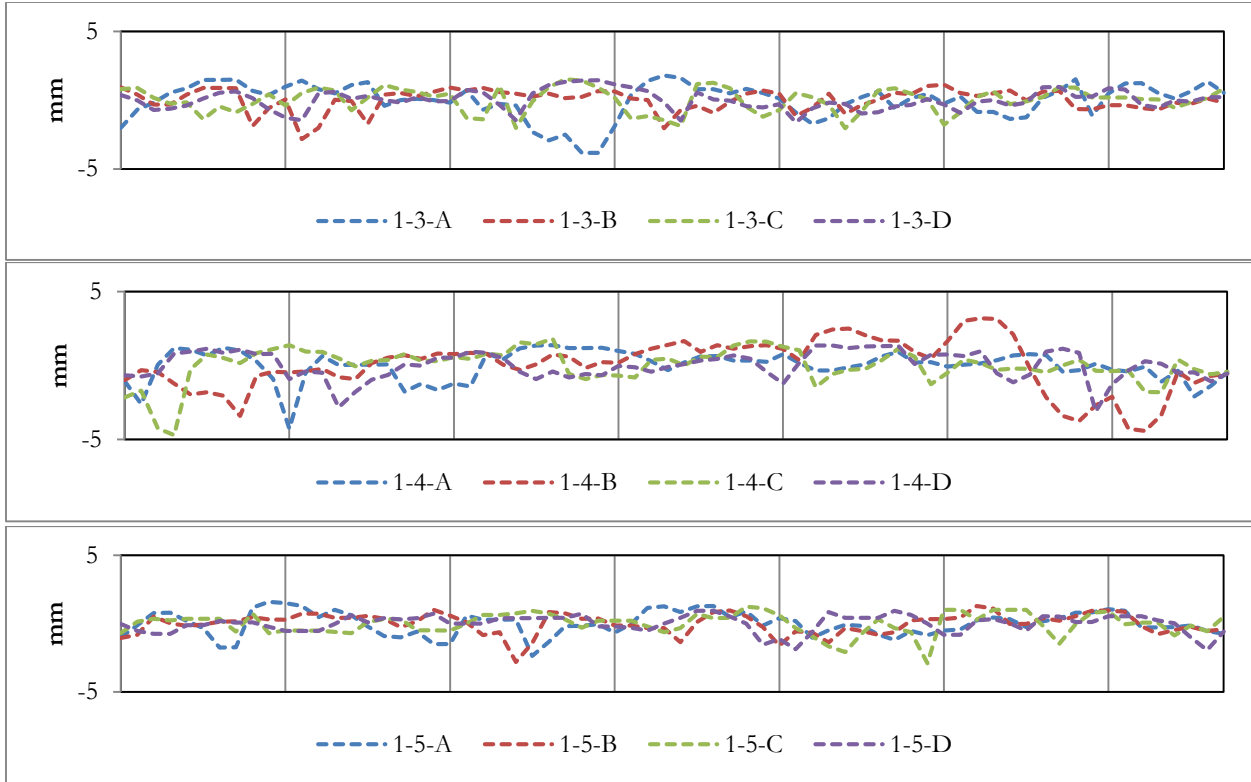


Figure B.1 Profiles measured from three cores of Site No.1 at four directions

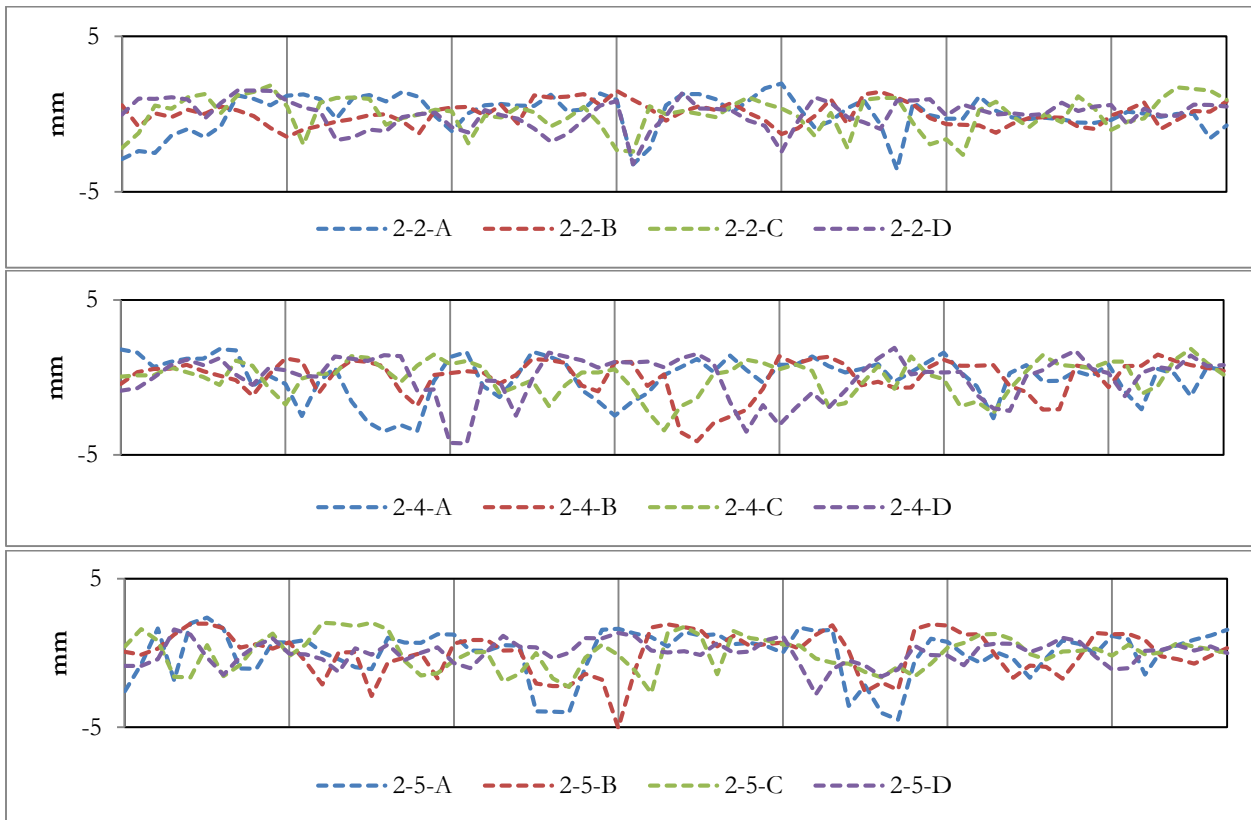


Figure B.2 Profiles measured from three cores of Site No.2 at four directions

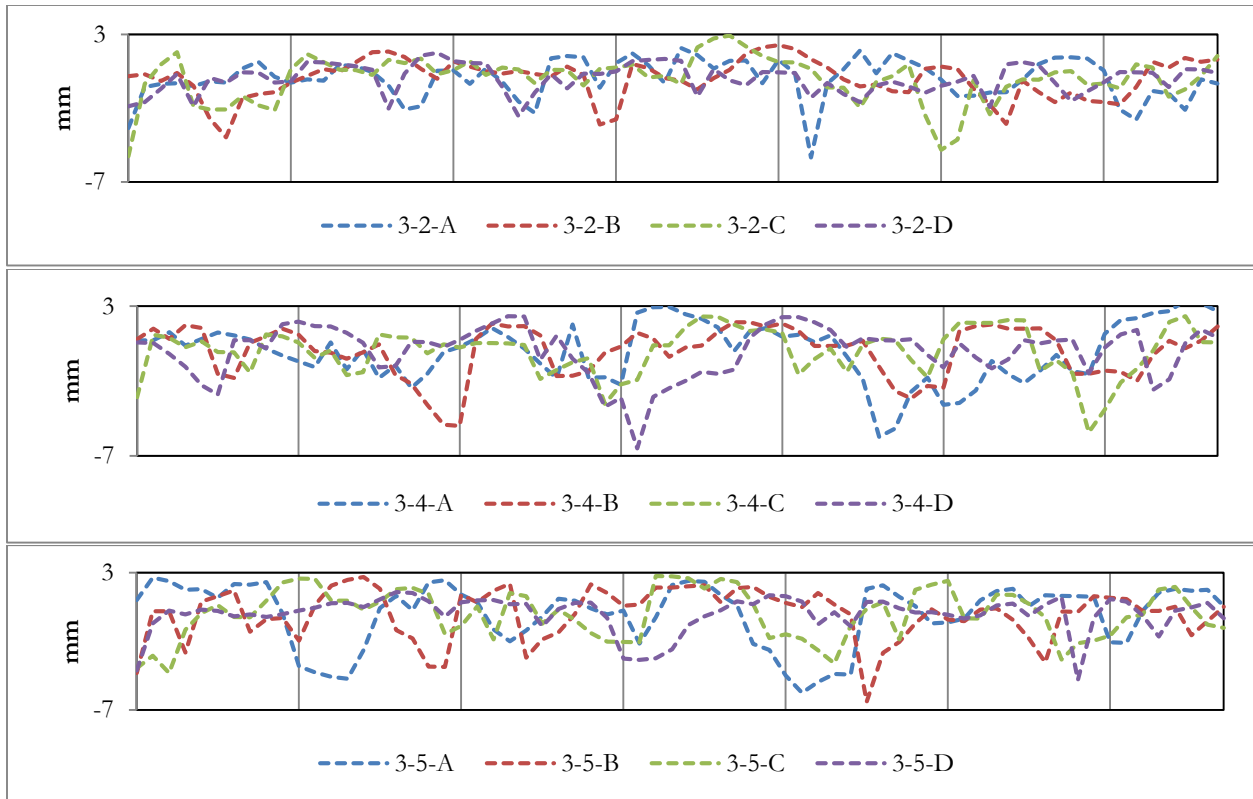


Figure B.3 Profiles measured from three cores of Site No.3 at four directions

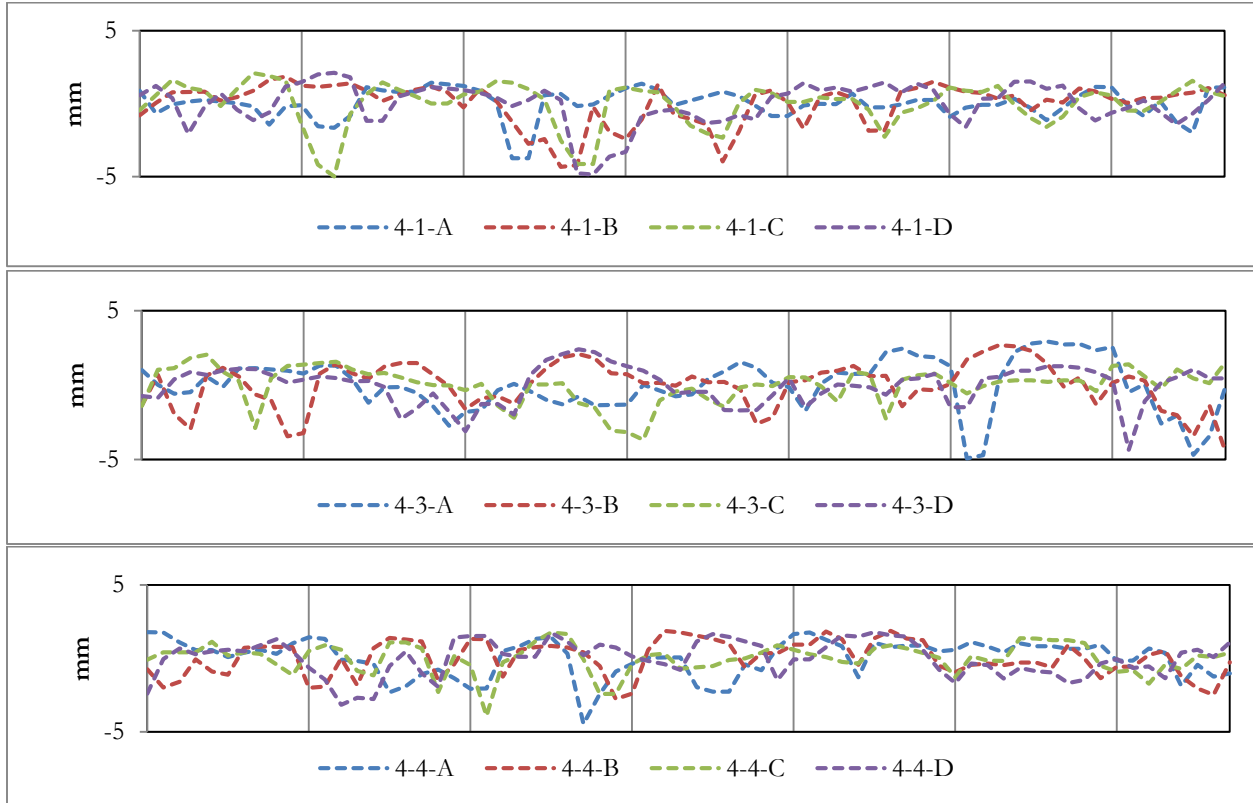


Figure B.4 Profiles measured from three cores of Site No.4 at four directions

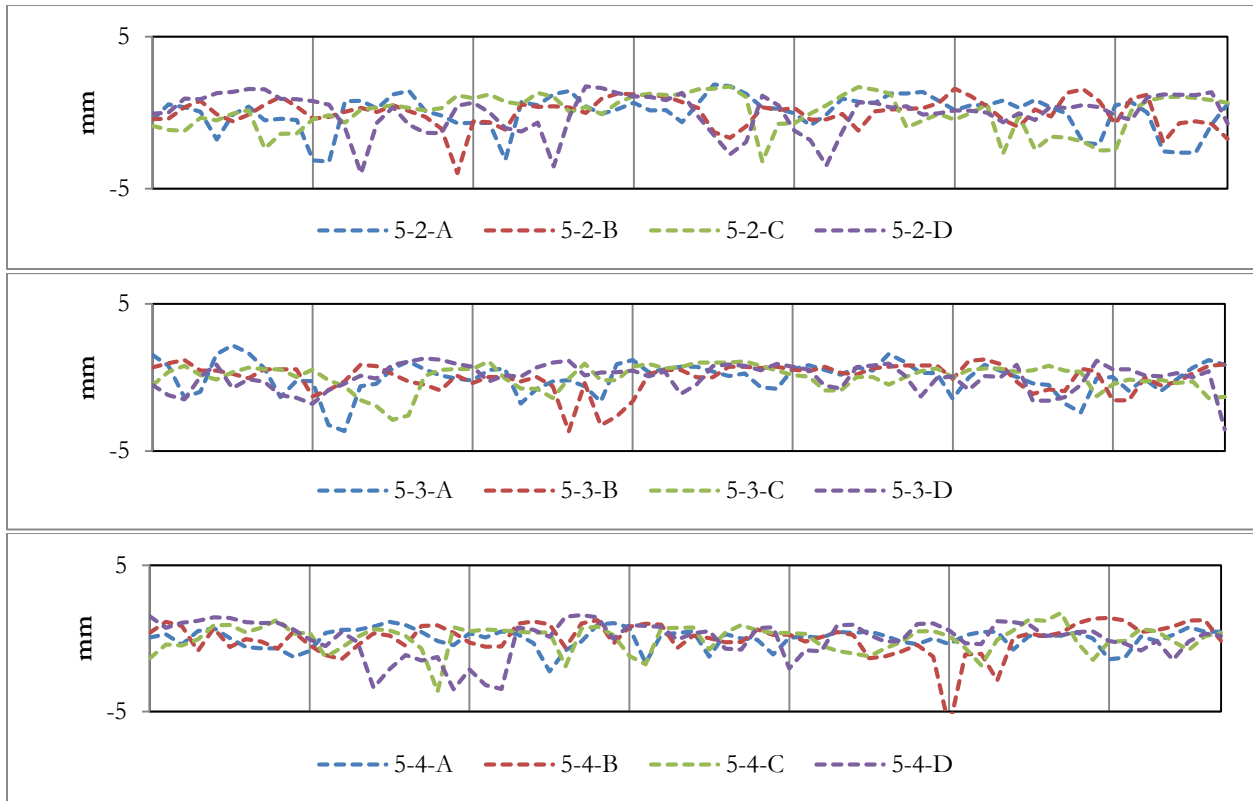


Figure B.5 Profiles measured from three cores of Site No.5 at four directions

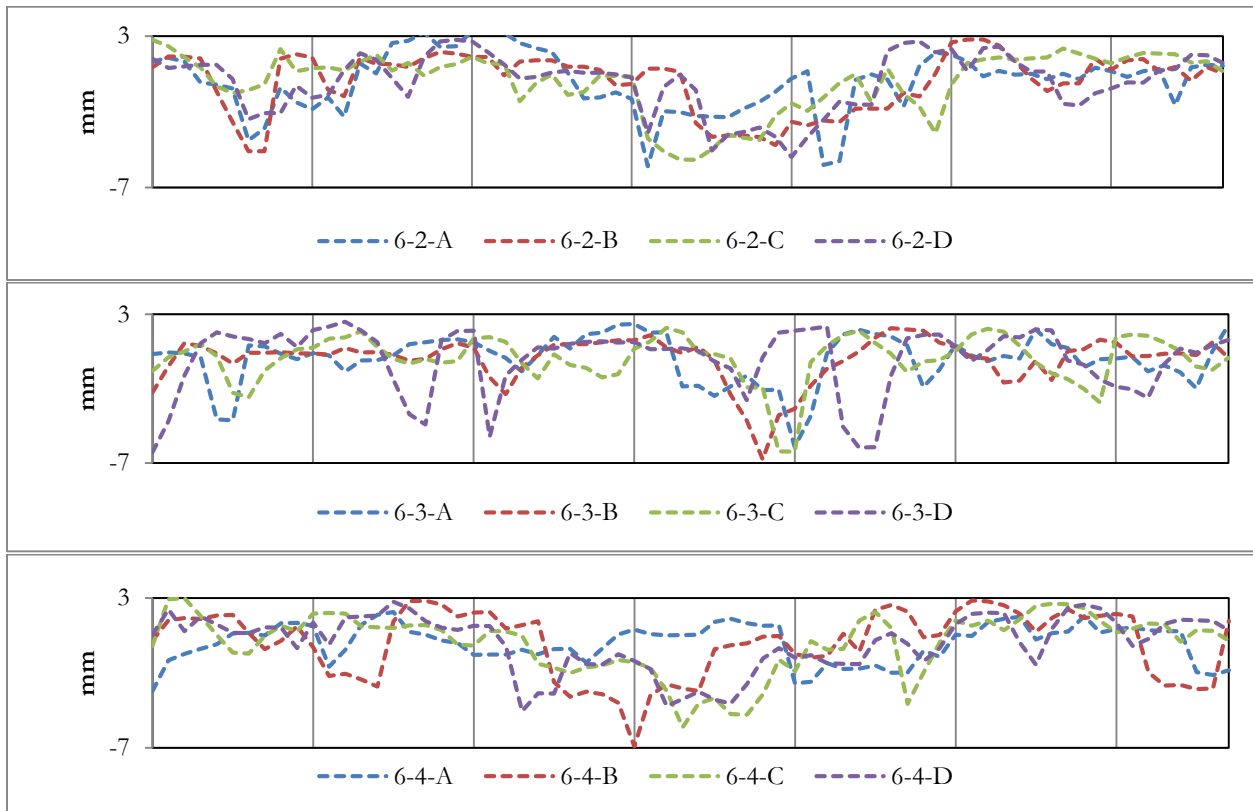


Figure B.6 Profiles measured from three cores of Site No.6 at four directions

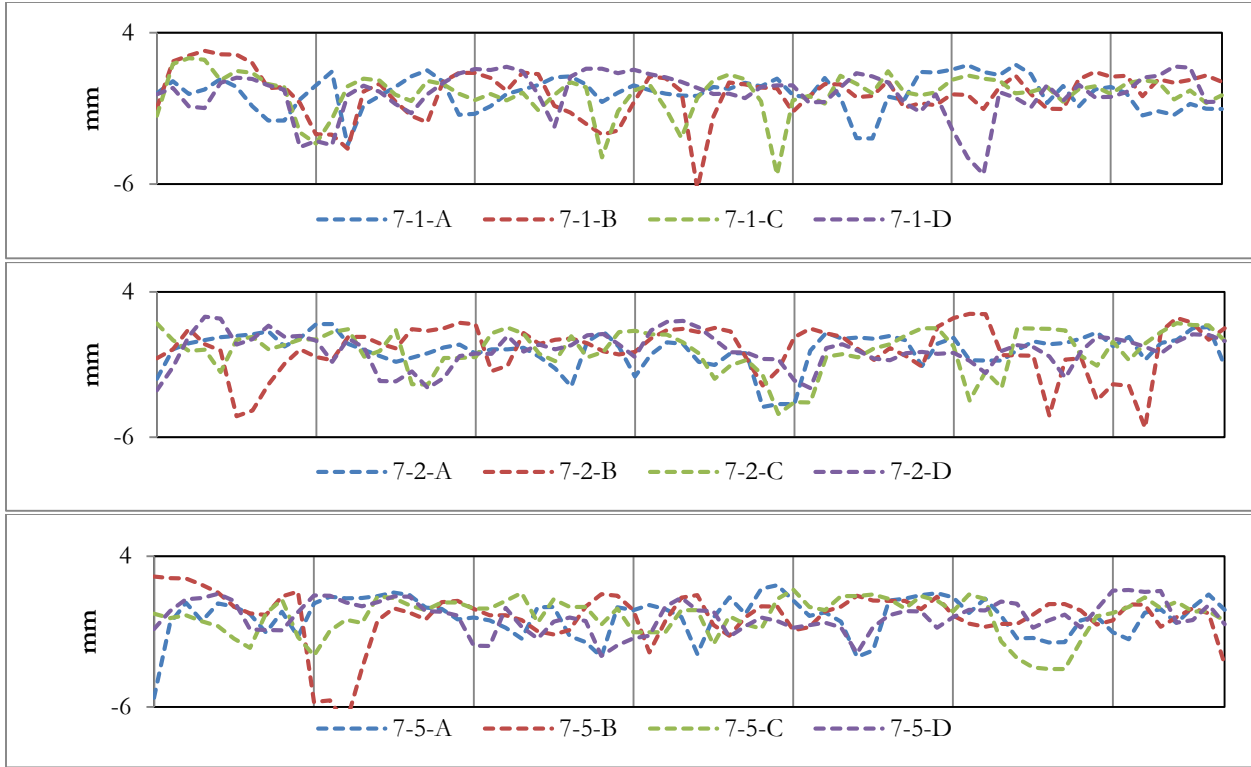


Figure B.7 Profiles measured from three cores of Site No.7 at four directions

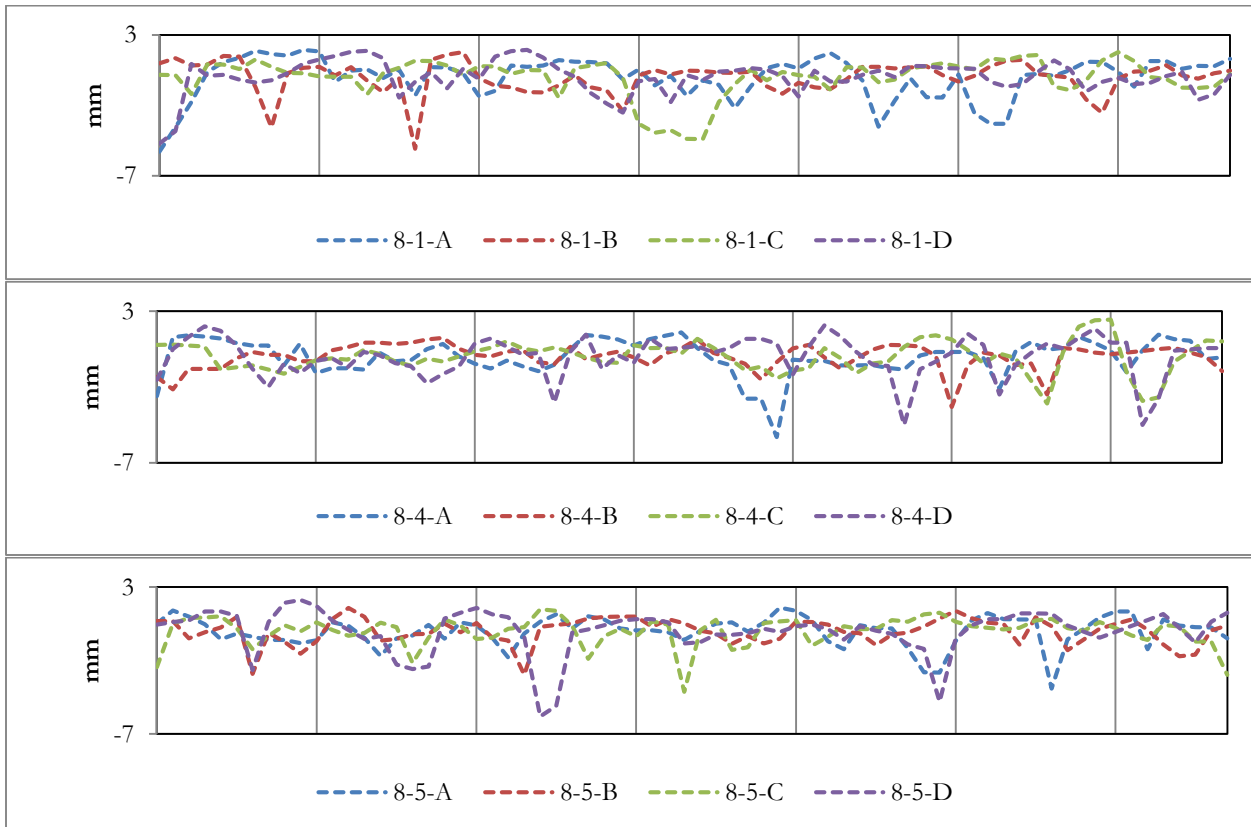


Figure B.8 Profiles measured from three cores of Site No.8 at four directions

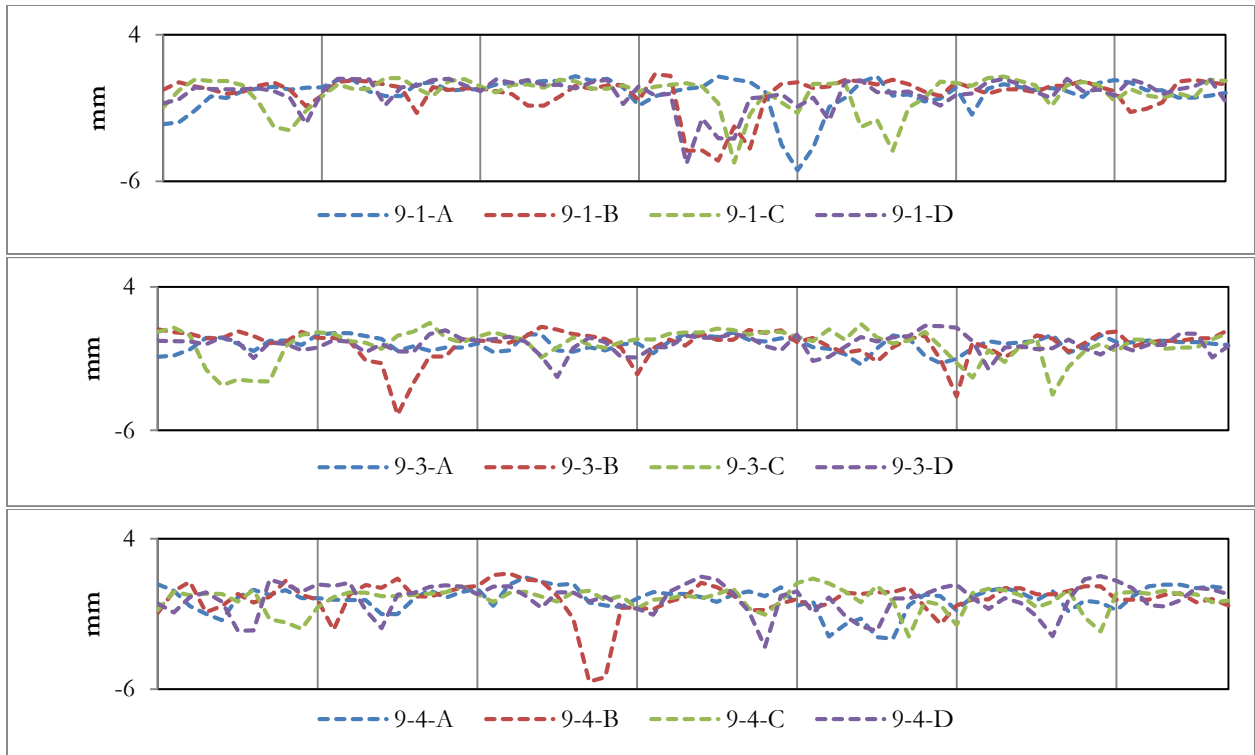


Figure B.9 Profiles measured from three cores of Site No.9 at four directions

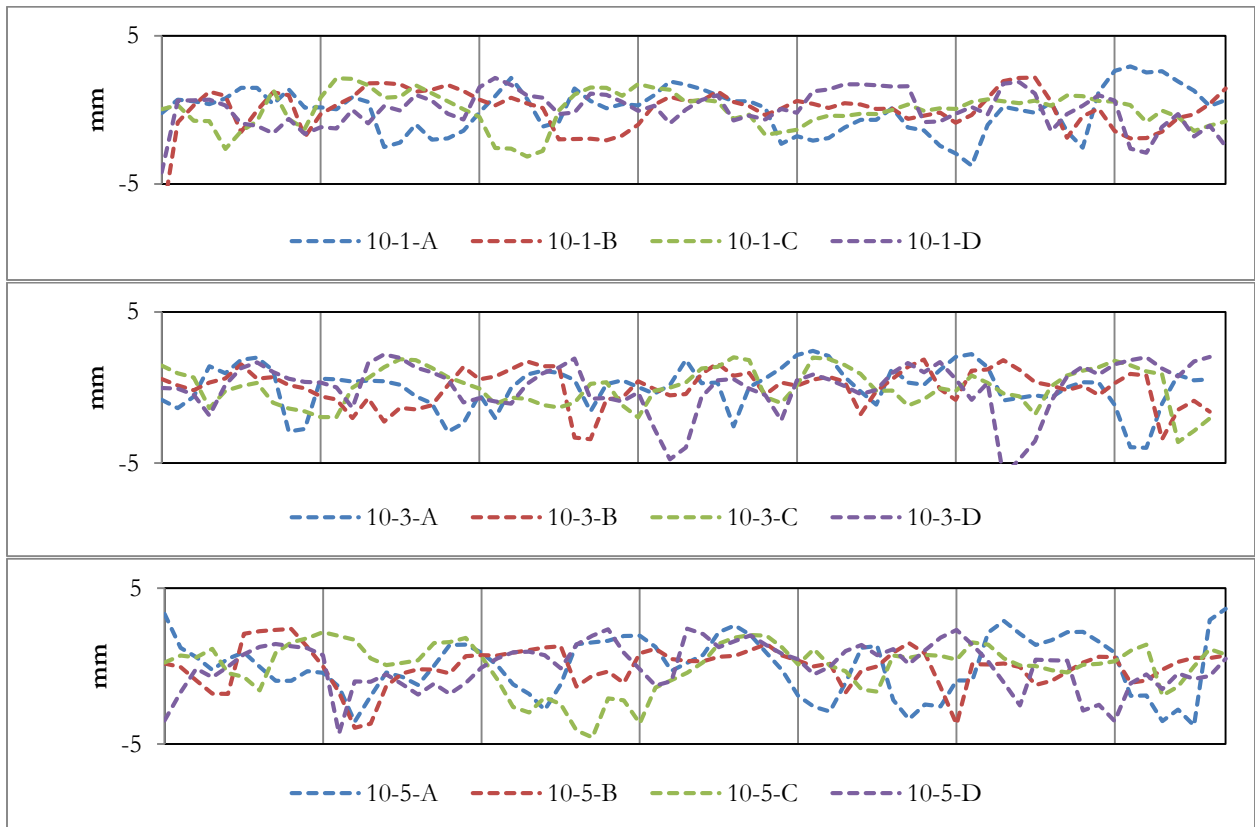


Figure B.10 Profiles measured from three cores of Site No.10 at four directions

APPENDIX C  
TEXTURE INDEX DISTRIBUTION OF LABORATORY POLISHED AGGREGATES, SCAN  
SURFACE OF CORES, AND REMOVED AGGREGATES FROM CORES

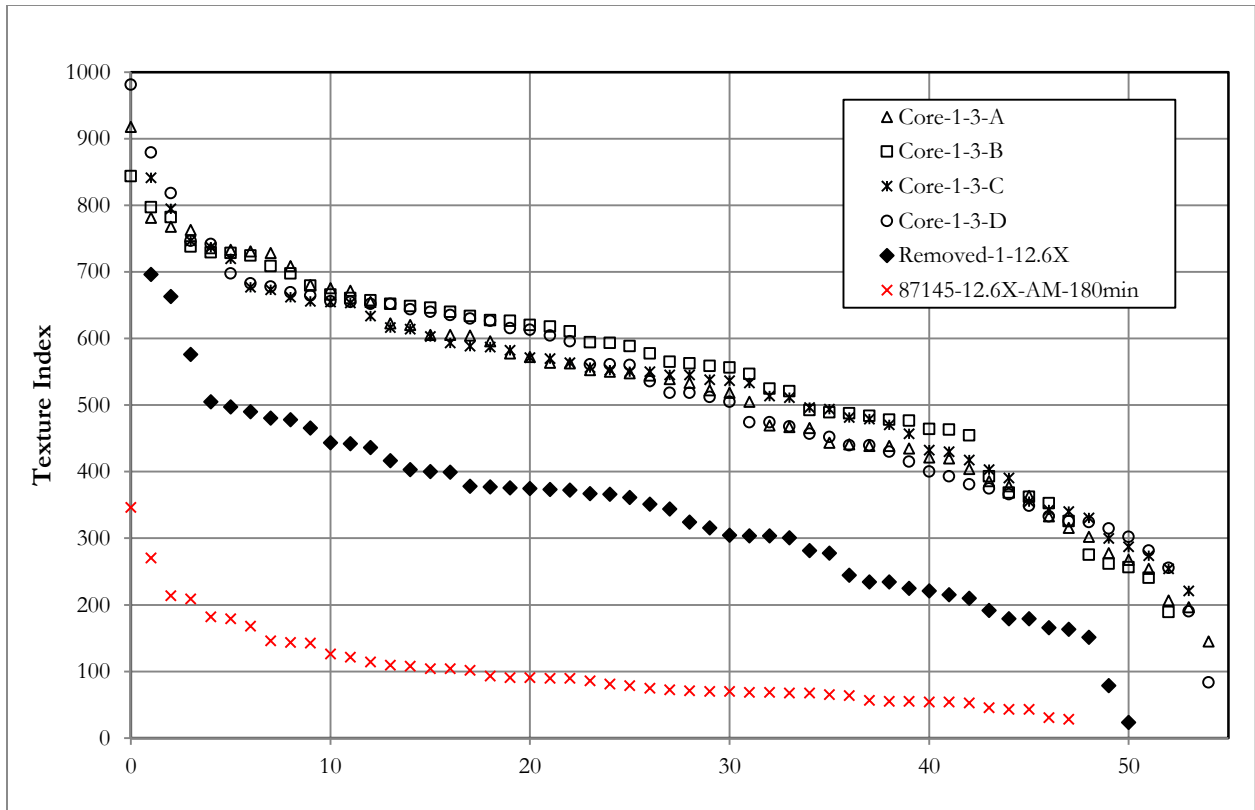


Figure C.1 Site No.1 and limestone aggregate 87145

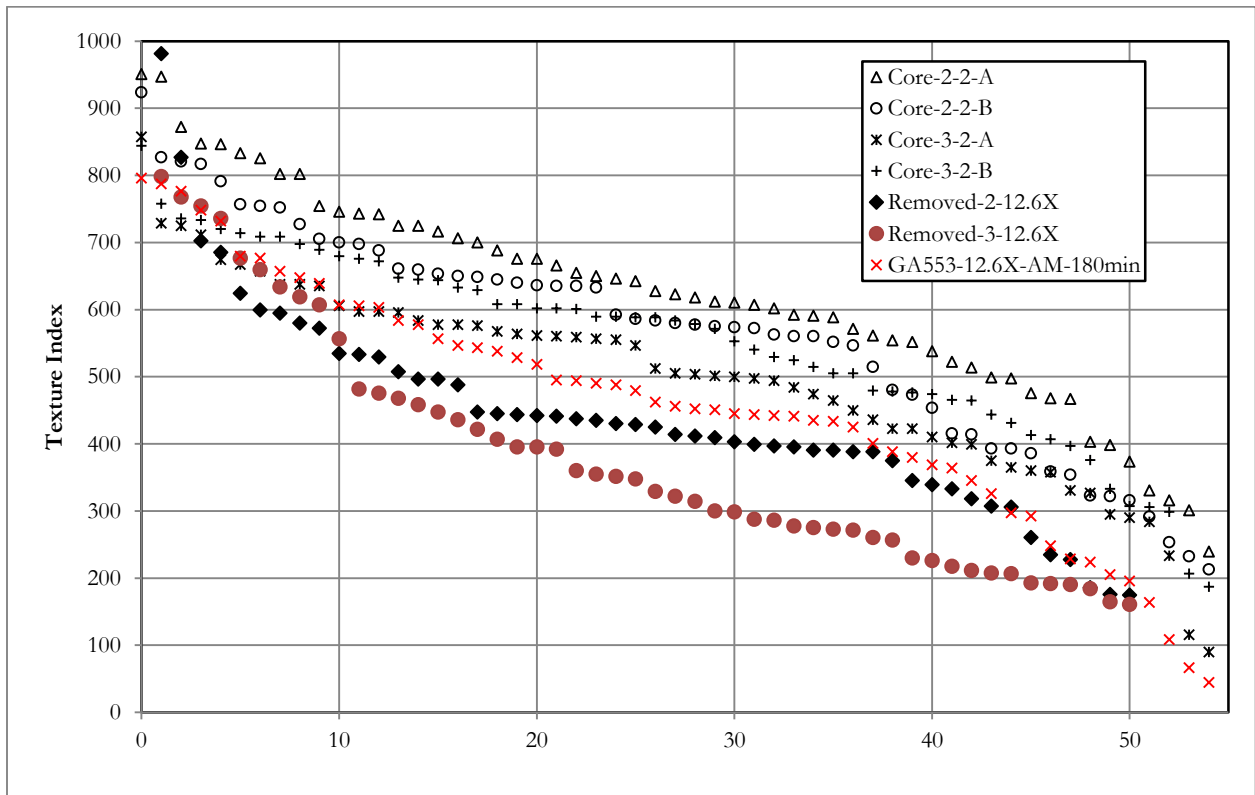


Figure C.2 Sites No.2 and No.3 and granitic aggregate GA553

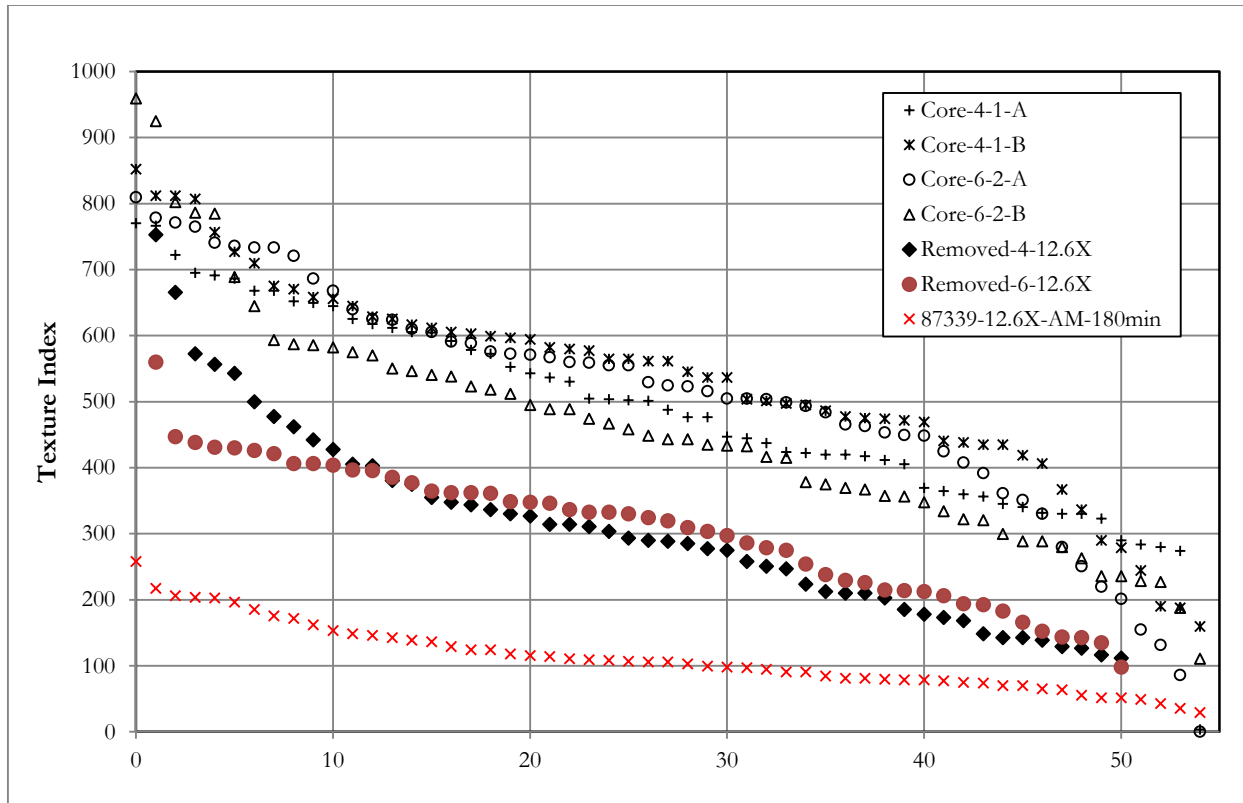


Figure C.3 Sites No.4 and No.6 and limestone aggregate 87339

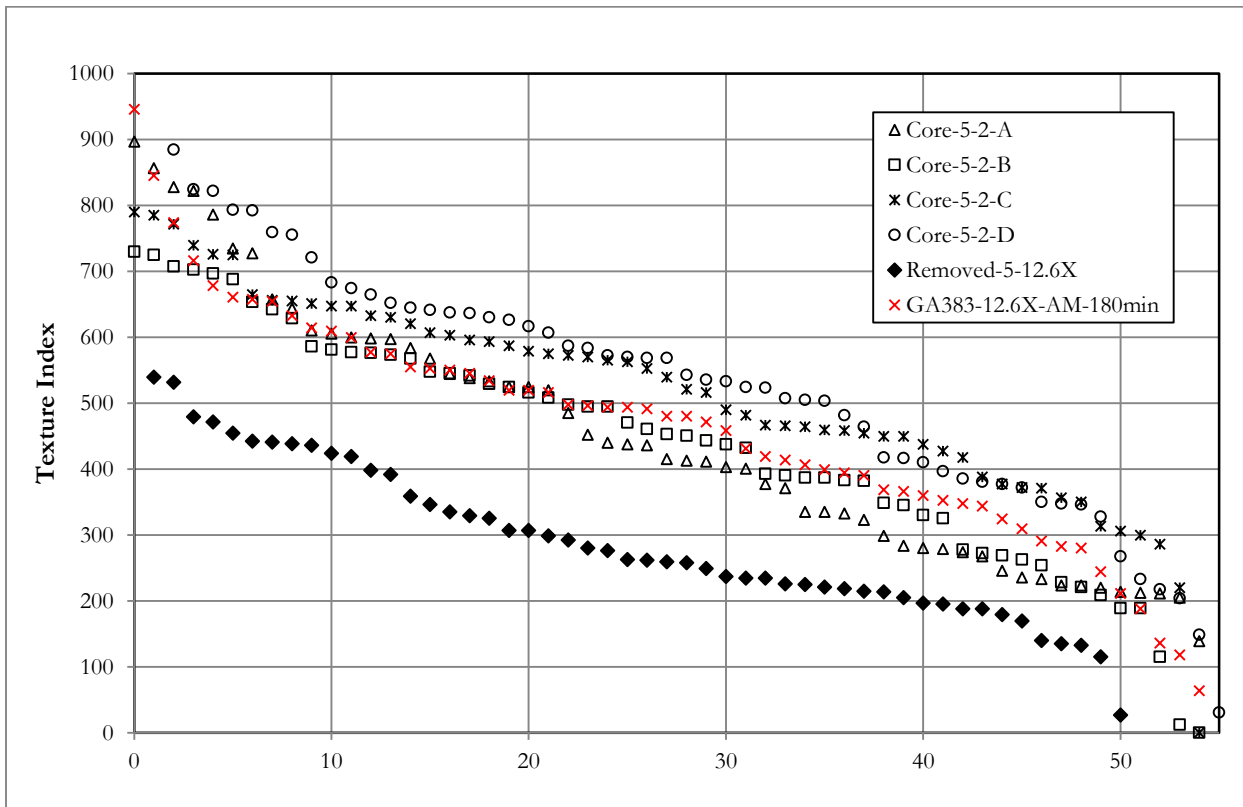


Figure C.4 Sites No.5 and granitic aggregate GA383

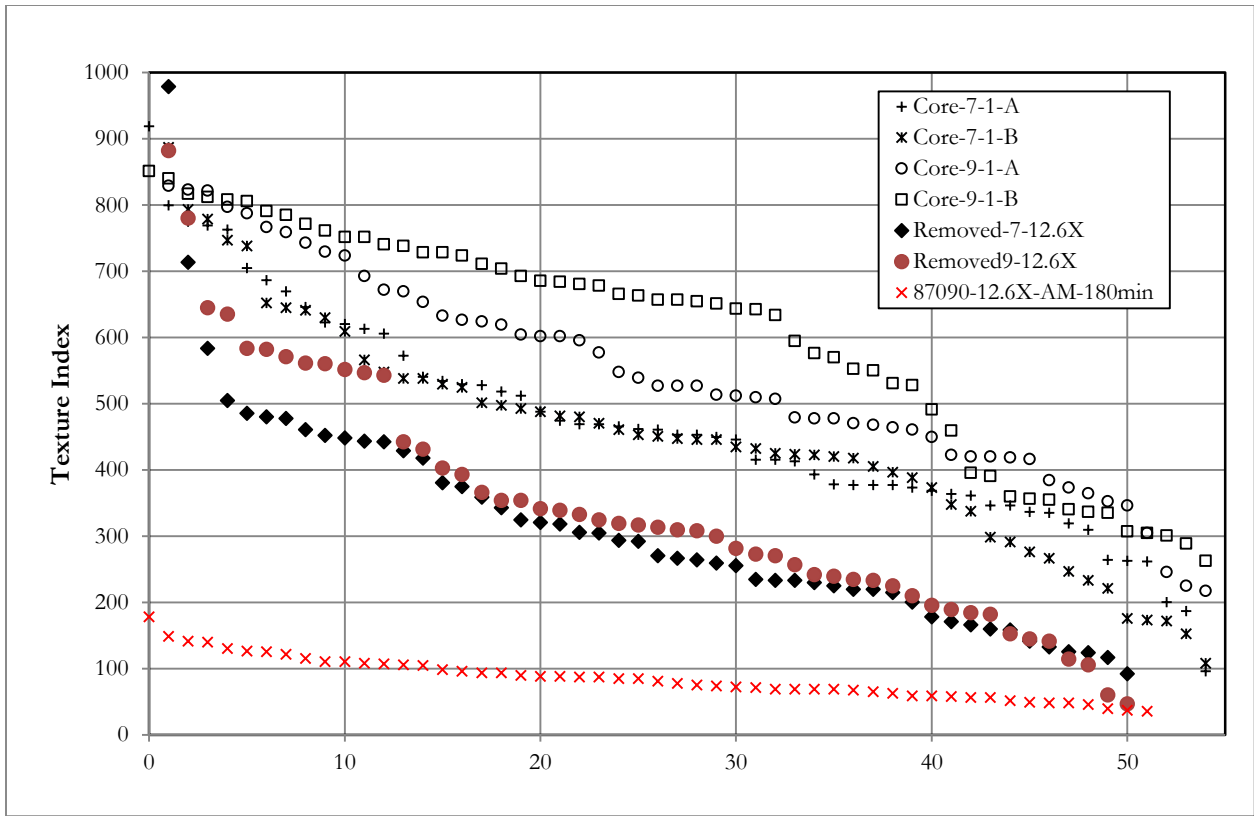


Figure C.5 Site No.7 and No.9 and limestone aggregate 87090

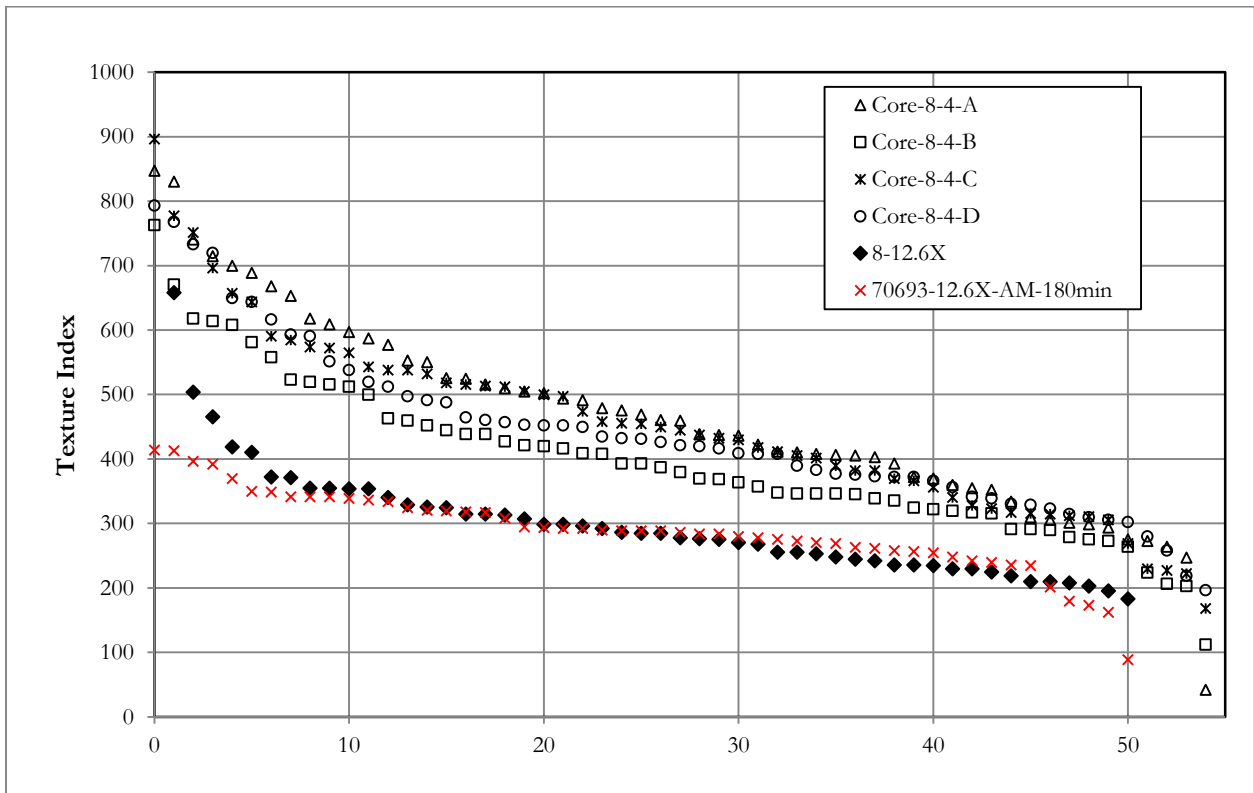


Figure C.6 Sites No.8 and Wackestone aggregate 70693

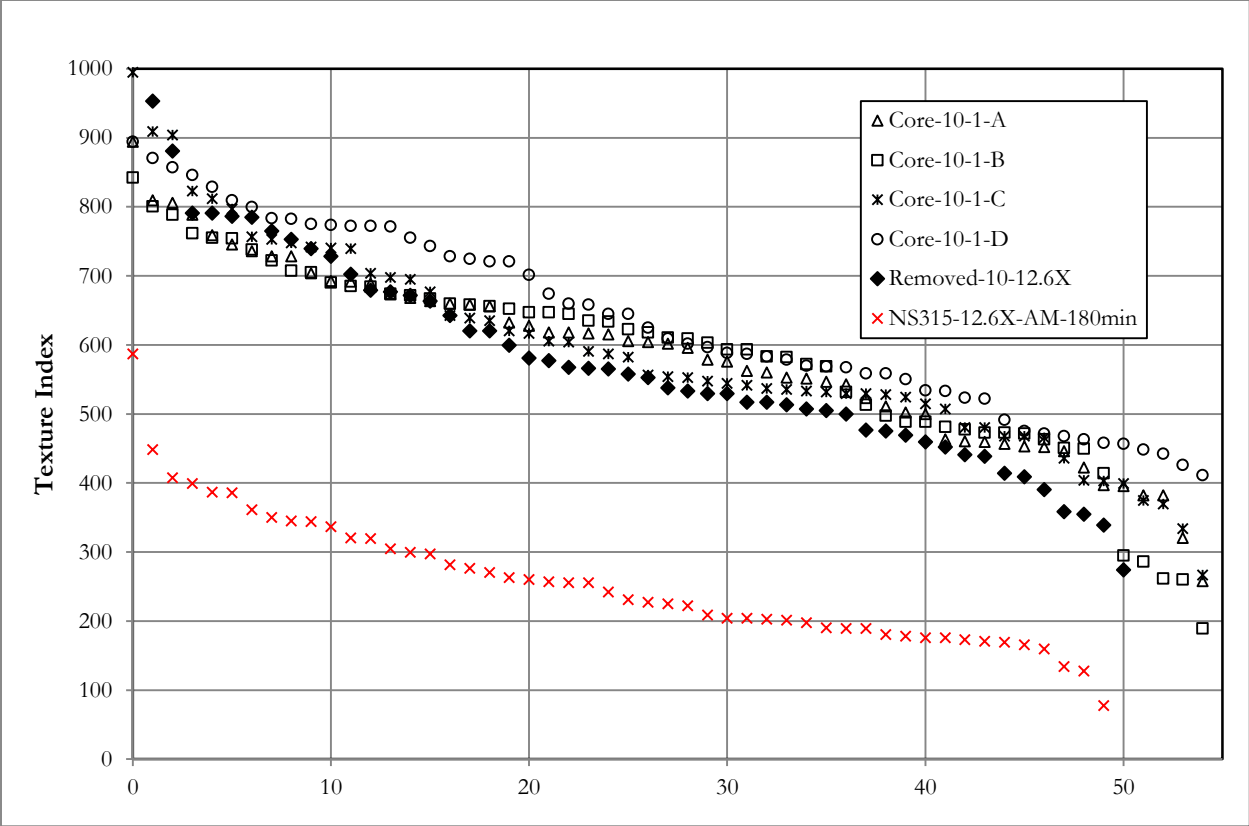


Figure C.7 Site No.10 and granitic aggregate NS315